

Supporting Information

**Reductive C–C Coupling from  $\alpha,\beta$ -Unsaturated Nitriles by Intercepting Keteniminates**

*Lillian V. A. Hale<sup>+</sup>, N. Marianne Sikes<sup>+</sup>, and Nathaniel K. Szymczak\**

ange\_201904530\_sm\_miscellaneous\_information.pdf

## Table of Contents

<b>I. General Considerations.....</b>	<b>S1</b>
<b>II. Synthesis, Isolation and Characterization of 3a .....</b>	<b>S2</b>
Figure S1. <sup>1</sup> H NMR spectrum of 3a in toluene- <i>d</i> <sub>8</sub> . .....	S3
Figure S2. Expanded <sup>1</sup> H NMR spectrum of 3a in toluene- <i>d</i> <sub>8</sub> showing the hydride region.....	S3
Figure S3. <sup>13</sup> C NMR spectrum of 3a in toluene- <i>d</i> <sub>8</sub> . .....	S3
Figure S4. <sup>1</sup> H- <sup>13</sup> C HMBC of 3a in toluene- <i>d</i> <sub>8</sub> .....	S4
Table S1. Tabulated correlations identifying the quaternary carbons of the keteniminate group based on <sup>1</sup> H- <sup>13</sup> C HMBC.....	S4
Figure S5. <sup>1</sup> H- <sup>13</sup> C HSQC of 3a formed in situ in C <sub>6</sub> D <sub>6</sub> .....	S5
Figure S6: <sup>31</sup> P NMR spectrum of isolated 3a in toluene- <i>d</i> <sub>8</sub> .....	S6
Figure S7: <sup>31</sup> P NMR spectrum of 3a formed in situ in C <sub>6</sub> D <sub>6</sub> . .....	S6
Figure S8: ATR IR of crystalline 3a. ....	S7
Figure S9: ATR IR of 3a prepared by precipitation with pentane from a solution of THF.....	S7
Figure S10: ATR IR of $\alpha$ -phenylcinnamionitrile .....	S8
Figure S11: Depiction of the HOMO (- 4.042 eV) for 3a using rb3lyp/631-G(d,p))/SDD/PCM in benzene.....	S9
Figure S12: Optimized geometry and NBO analysis for 3a using rb3lyp/631-G(d,p))/SDD level of theory. ....	S9
Solution stability of 3a in C <sub>6</sub> D <sub>6</sub> .....	S10
Figure S13. Initial <sup>1</sup> H NMR spectrum of 3a formed from 1 and 2a in C <sub>6</sub> D <sub>6</sub> . Insertion occurs quantitatively (>99% NMR yield) based on PhTMS as the internal standard. ....	S10
Figure S14. <sup>31</sup> P NMR spectra of 3a after 20 minutes at 25, 40, 60, and 75 °C.....	S11
Figure S15. <sup>1</sup> H NMR spectra of 3a after 20 minutes at 25 and 75 °C. ....	S12
Table S2. Amount (mmol) of 3a remaining after 20 minutes at indicated temperature. ....	S12
<b>III. In situ characterization of Ru-keteniminates 3b-3e .....</b>	<b>S13</b>
Figure S16: <sup>1</sup> H NMR spectrum for 3b prepared <i>in situ</i> in toluene- <i>d</i> <sub>8</sub> .....	S13
Figure S17: Aromatic region of the <sup>1</sup> H NMR spectrum of 3b in toluene- <i>d</i> <sub>8</sub> .....	S14
Figure S18: Expanded <sup>1</sup> H NMR spectrum of 3b in toluene- <i>d</i> <sub>8</sub> showing the hydride region .	S14
Figure S19: <sup>13</sup> C NMR spectrum of 3b in toluene- <i>d</i> <sub>8</sub> .....	S15
Figure S20: <sup>31</sup> P NMR spectrum of 3b in toluene- <i>d</i> <sub>8</sub> . # = PPh <sub>3</sub> ; * = unknown byproduct.....	S15

Figure S21: ATR IR spectrum of 3b precipitated with pentane from a solution of THF .....	S16
Figure S22: <sup>1</sup> H NMR spectrum of 3c prepared <i>in situ</i> in toluene- <i>d</i> <sub>8</sub> .....	S17
Figure S23: Expanded <sup>1</sup> H NMR spectrum of 3c in toluene- <i>d</i> <sub>8</sub> showing the hydride region..	S17
Figure S24: <sup>13</sup> C NMR spectrum of 3c prepared <i>in situ</i> in toluene- <i>d</i> <sub>8</sub> .....	S18
Figure S25: <sup>31</sup> P NMR spectrum of 3c prepared <i>in situ</i> in toluene- <i>d</i> <sub>8</sub> .....	S18
Figure S26: ATR IR spectrum of 3c precipitated with pentane from a solution of THF .....	S19
Figure S27: <sup>1</sup> H NMR spectrum of 3d prepared in situ in toluene- <i>d</i> <sub>8</sub> .....	S20
Figure S28: Expanded <sup>1</sup> H NMR spectrum of 3d in toluene- <i>d</i> <sub>8</sub> showing the hydride region .	S20
Figure S29: <sup>13</sup> C NMR spectrum of 3d prepared <i>in situ</i> in toluene- <i>d</i> <sub>8</sub> .....	S21
Figure S30: <sup>31</sup> P NMR spectrum of 3d in toluene- <i>d</i> <sub>8</sub> . .....	S21
Figure S31: ATR IR spectrum of 3d precipitated with pentane from a solution of THF. ....	S22
Figure S32: <sup>1</sup> H NMR spectrum of 3e prepared in situ in toluene- <i>d</i> <sub>8</sub> . .....	S23
Figure S33: Expanded <sup>1</sup> H NMR spectrum of 3e in toluene- <i>d</i> <sub>8</sub> showing the hydride region..	S23
Figure S34: <sup>13</sup> C NMR spectrum of 3e in toluene- <i>d</i> <sub>8</sub> .....	S24
Figure S35: <sup>31</sup> P NMR spectrum of 3e in toluene- <i>d</i> <sub>8</sub> .....	S24
Figure S36: ATR IR spectrum of 3e precipitated with pentane from a solution of THF .....	S25
<b>IV. General procedure for the hydrogenation and hydrogenative acylation of <math>\alpha,\beta</math>-unsaturated nitriles using 1 and H<sub>2</sub>.....</b>	<b>S26</b>
A. Hydrogenation of $\alpha,\beta$ -unsaturated nitriles.....	S26
Table S3. Hydrogenation of 2a using 1 (1 mol %) and H <sub>2</sub> (100 psi) in the presence of basic additives (10 mol %). .....	S27
Figure S37. <sup>1</sup> H NMR spectrum of the reaction mixture containing 5a, 6a, and 6a' resulting from the hydrogenation of 2a at 70 °C with 1 (1 mol %), and H <sub>2</sub> (100 psig) (Table S3, entry 5). S28	
Figure S38. <sup>1</sup> H NMR spectrum showing only the formation of 5a resulting from the hydrogenation of 2a with DBU (10 mol %), 1 (2 mol %), and H <sub>2</sub> .....	S29
B. Hydrogenative acylation of $\alpha,\beta$ -unsaturated nitriles .....	S29
C. Hydrogenative acylation of $\alpha,\beta$ -unsaturated nitriles at reduced temperature and pressure. ....	S30
Table S4. Formation of 4a versus 5a with DBU (10 mol%), 1 (2 mol%), and H <sub>2</sub> (50 psig), at 50 °C monitored by <sup>1</sup> H NMR spectroscopy .....	S30
<b>V. Isolation and characterization of <i>tert</i>-butyl 2-cyano-2,3-diphenylpropanoate derivatives 4a-4k.....</b>	<b>S30</b>

Figure S39. $^1\text{H}$ NMR spectrum of 4a in $\text{CDCl}_3$ .....	S33
Figure S40. $^{13}\text{C}$ NMR spectrum of 4a $\text{CDCl}_3$ .....	S33
Figure S41. $^1\text{H}$ NMR spectrum of 4b in $\text{CDCl}_3$ .....	S34
Figure S42. $^{13}\text{C}$ NMR spectrum of 4b in $\text{CDCl}_3$ .....	S34
Figure S43. $^1\text{H}$ NMR spectrum of 4c in $\text{CDCl}_3$ .....	S35
Figure S44. $^{13}\text{C}$ NMR spectrum of 4c in $\text{CDCl}_3$ .....	S35
Figure S45. $^1\text{H}$ NMR spectrum of 4d in $\text{CDCl}_3$ .....	S36
Figure S46. $^{13}\text{C}$ NMR spectrum of 4d in $\text{CDCl}_3$ .....	S36
Figure S47. $^1\text{H}$ NMR spectrum of 4e in $\text{CDCl}_3$ .....	S37
Figure S48. $^{13}\text{C}$ NMR spectrum of 4e in $\text{CDCl}_3$ .....	S37
Figure S49. $^1\text{H}$ NMR spectrum of 4f in $\text{CDCl}_3$ .....	S38
Figure S50. $^{13}\text{C}$ NMR spectrum of 4f in $\text{CDCl}_3$ .....	S39
Figure S51: $^1\text{H}$ NMR spectrum of 4g in $\text{CDCl}_3$ .....	S39
Figure S52: $^{13}\text{C}$ NMR spectrum of 4g in $\text{CDCl}_3$ .....	S40
Figure S53: $^1\text{H}$ NMR spectrum of 4h in $\text{CDCl}_3$ .....	S40
Figure S54: $^{13}\text{C}$ NMR spectrum of 4h in $\text{CDCl}_3$ .....	S41
<b>VI. Control Reactions for hydrogenative acylation of <math>\alpha,\beta</math>-unsaturated nitriles .....</b>	<b>S41</b>
Figure S55. Initial $^1\text{H}$ NMR spectrum of 2,3-diphenylpropanenitrile under hydrogenative acylation conditions .....	S42
Figure S56: Final $^1\text{H}$ NMR spectrum of 2,3-diphenylpropanenitrile under hydrogenative acylation conditions .....	S43
Figure S57: Stacked $^1\text{H}$ NMR spectra of initial and final timepoints for the reaction of 2,3-diphenylpropanenitrile under hydrogenative acylation conditions with 1 .....	S44
Figure S58. $^1\text{H}$ NMR spectrum obtained from the stoichiometric reaction of 3a with $\text{Boc}_2\text{O}$ and DBU showing 95% conversion to 4a .....	S45
Figure S59. $^1\text{H}$ NMR spectrum of 2,3-diphenylpropanenitrile with $\text{Boc}_2\text{O}$ and 10% DBU..	S46
<b>VII. Proposed Catalytic Cycle .....</b>	<b>S47</b>
Figure S60. Proposed catalytic cycle .....	S47
<b>VIII. Cation dependence of hydrogenation acylation in the presence of alkoxide bases ...</b>	<b>S48</b>
Table S5. Cation dependence of hydrogenative acylation in the presence of alkoxide bases	S48
<b>IX. Crystallographic Details for 3a .....</b>	<b>S48</b>
<b>X. Computational Details.....</b>	<b>S50</b>

Cartesian coordinates (Å) based on 6-31g(d,p) and SDD optimized geometry of 3a.....	S50
Summary of Natural Population Analysis for 3a: .....	S51
<b>XI. References .....</b>	<b>S54</b>

## I. General Considerations

All manipulations involving the catalyst HRubMepi(PPh<sub>3</sub>)<sub>2</sub> (**1**) and catalytic reactions were conducted under a nitrogen atmosphere using standard Schlenk technique, or in a glovebox unless otherwise stated.  $\alpha,\beta$ -Unsaturated nitriles and **1** were synthesized according to literature procedures.<sup>1-4</sup> Toluene-*d*<sub>8</sub> and C<sub>6</sub>D<sub>6</sub> were purchased from Cambridge Isotope Laboratories, and degassed immediately after opening using evacuation/refill cycles, then stored over 3 Å molecular sieves for at least 24 h in the glovebox prior to use. Degassed, anhydrous solvents were obtained using a Glass Contour, SG Waters USA solvent purification system or were distilled over CaH<sub>2</sub>, degassed, and stored over 3 Å molecular sieves for at least 24 h in the glovebox prior to use. The 3 Å molecular sieves were dried at 250 °C under dynamic vacuum for 24 h. Organic products were isolated using a Biotage Isolera One flash chromatography system with SiliaFlash P60 silica on a 10g column and hexanes/ethyl acetate as the eluent.

NMR spectra were recorded on Varian Inova 500, Varian MR400, Varian vnmrs 500 and Varian vnmrs 700 spectrometers at ambient temperature, unless otherwise stated. <sup>1</sup>H, <sup>13</sup>C, and <sup>31</sup>P chemical shifts are reported in parts per million (ppm) relative to trimethylsilane (TMS), with the residual solvent peak used as an internal reference. <sup>31</sup>P resonances are referenced on a unified scale, where the primary reference is the frequency of the residual solvent peak in the <sup>1</sup>H NMR spectrum. <sup>1</sup>H and <sup>13</sup>C NMR resonances are referenced versus TMS, and <sup>31</sup>P resonances are referenced versus phosphoric acid. Multiplicities are reported as follows: singlet (s), doublet (d), triplet (t), quartet (q), and multiplet (m). Fourier-transform infrared spectroscopy (FTIR) was performed on a Nicolet iS10 using attenuated total reflectance (ATR). Mass spectrometry was performed using an Agilent 6230 TOF HPLC-MS.

Crystal structures were solved and refined with the Olex2 software package and ShelXL.<sup>5,6</sup> Calculations were performed with the Gaussian 09 suite of programs.<sup>7</sup> All atoms underwent geometry optimization using the rb3lyp functional and 6-31G(d,p) basis set, with the exception of ruthenium, which was optimized using the SDD basis set. The polarizable continuum model (PCM) for benzene was used in all cases. Natural bonding orbital analysis was performed using NBO version 3.115 as implemented in Gaussian 09. Optimized structures and orbitals are illustrated with the Chimera11 molecular modeling program.<sup>8</sup>

## II. Synthesis, Isolation and Characterization of **3a**

A 20 mL vial was charged with **1** (75 mg, 0.079 mmol),  $\alpha$ -phenylcinnamionitrile (19.4 mg, 0.094 mmol), and 5 mL THF. After stirring for ca. 5-10 minutes at room temperature, the dark blue solution was layered with 15 mL pentane and stored at  $-35\text{ }^{\circ}\text{C}$ . After 24 h the pentane/THF solution was decanted and the remaining crystalline solid was washed with pentane (3 x 15 mL) and dried under vacuum to yield 59 mg (78% yield) dichromic blue and purple crystals of **3a**. Crystals of **3a** suitable for X-ray diffraction were grown by slow diffusion of pentane into a dilute sample of the reaction solution in THF at  $-35\text{ }^{\circ}\text{C}$ . For ATR IR characterization and comparison, a second batch of **3a** was prepared by precipitation from THF with pentane.  $^1\text{H}$  NMR (700 MHz, Toluene- $d_8$ )  $\delta$  7.90 (dd,  $^3J_{\text{HH}} = 5.0, 3.0\text{ Hz}$ , 2H), 7.57 (d,  $^2J_{\text{HH}} = 8.1\text{ Hz}$ , 2H), 7.25 (t,  $^3J_{\text{HH}} = 7.6\text{ Hz}$ , 2H), 7.03 (dd,  $^3J_{\text{HH}} = 8.6, 3.1\text{ Hz}$ , 3H), 6.89 (d,  $^3J_{\text{HH}} = 7.5\text{ Hz}$ , 2H), 6.85 – 6.78 (m, 5H), 6.76 (t,  $^3J_{\text{HH}} = 7.3\text{ Hz}$ , 3H), 6.71 (s, 6H), 6.64 (t,  $^3J_{\text{HH}} = 6.9\text{ Hz}$ , 6H), 6.57 (t,  $^3J_{\text{HH}} = 7.2\text{ Hz}$ , 1H), 6.37 (d,  $^3J_{\text{HH}} = 7.0\text{ Hz}$ , 2H), 6.34 (d,  $^3J_{\text{HH}} = 7.7\text{ Hz}$ , 2H), 3.11 (s, 2H), 1.53 (s, 6H).  $^{13}\text{C}$  NMR (176 MHz, Toluene- $d_8$ )  $\delta$  162.29, 159.08, 155.87, 153.32, 145.01, 142.88, 141.89, 134.99, 134.71, 132.87, 120.56, 120.33, 118.62, 117.23, 54.45, 34.99, 23.56.  $^{31}\text{P}$  NMR (200 MHz, Toluene- $d_8$ )  $\delta$  39.73. Purity was assessed using NMR spectroscopy with PhTMS internal standard: > 99%.

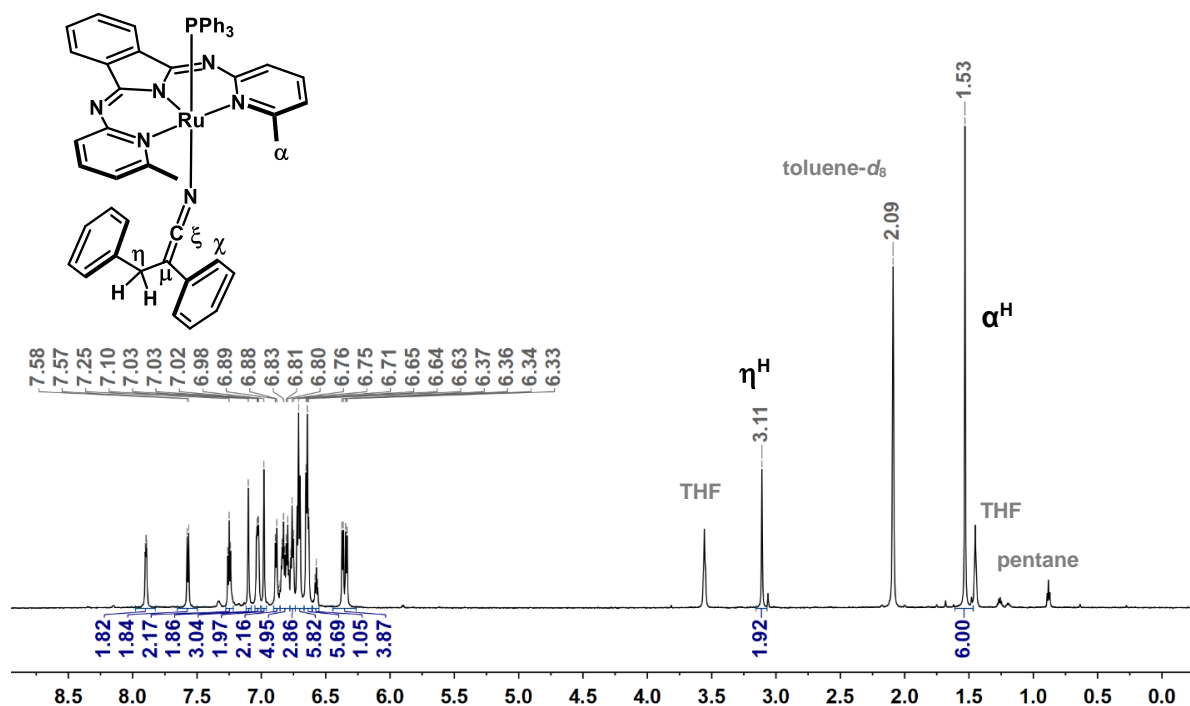


Figure S1.  $^1\text{H}$  NMR spectrum of 3a in toluene- $d_8$ .

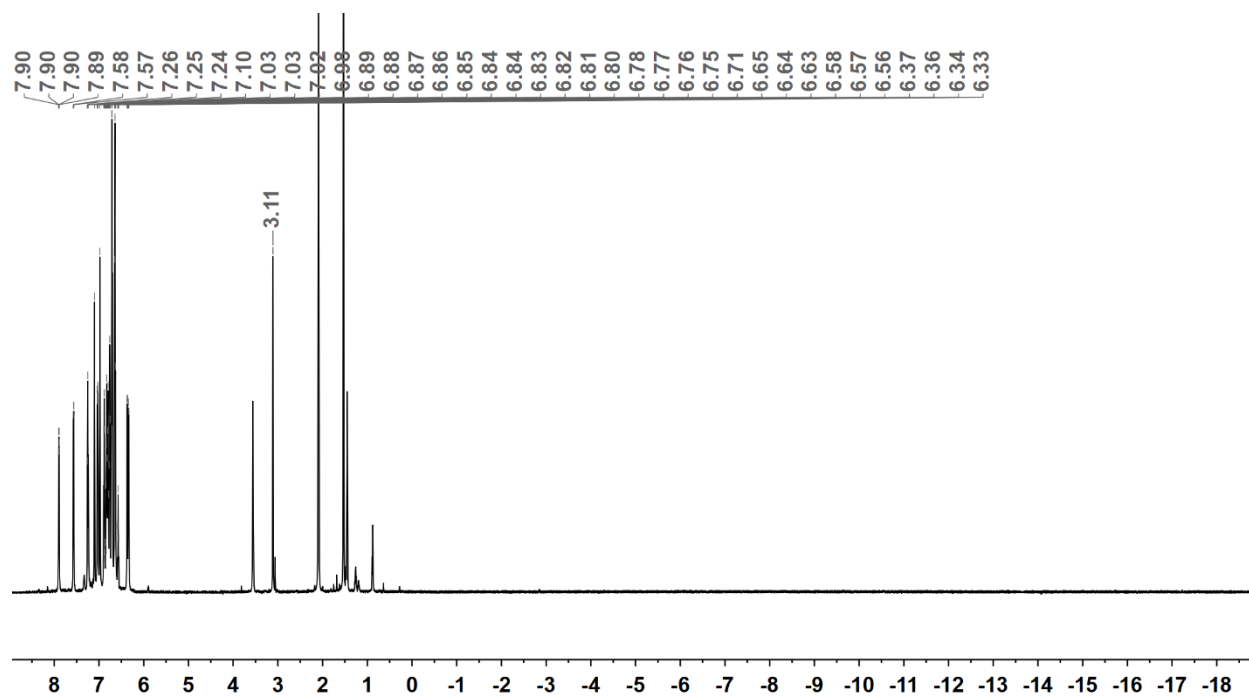


Figure S2. Expanded  $^1\text{H}$  NMR spectrum of 3a in toluene- $d_8$  showing the hydride region.

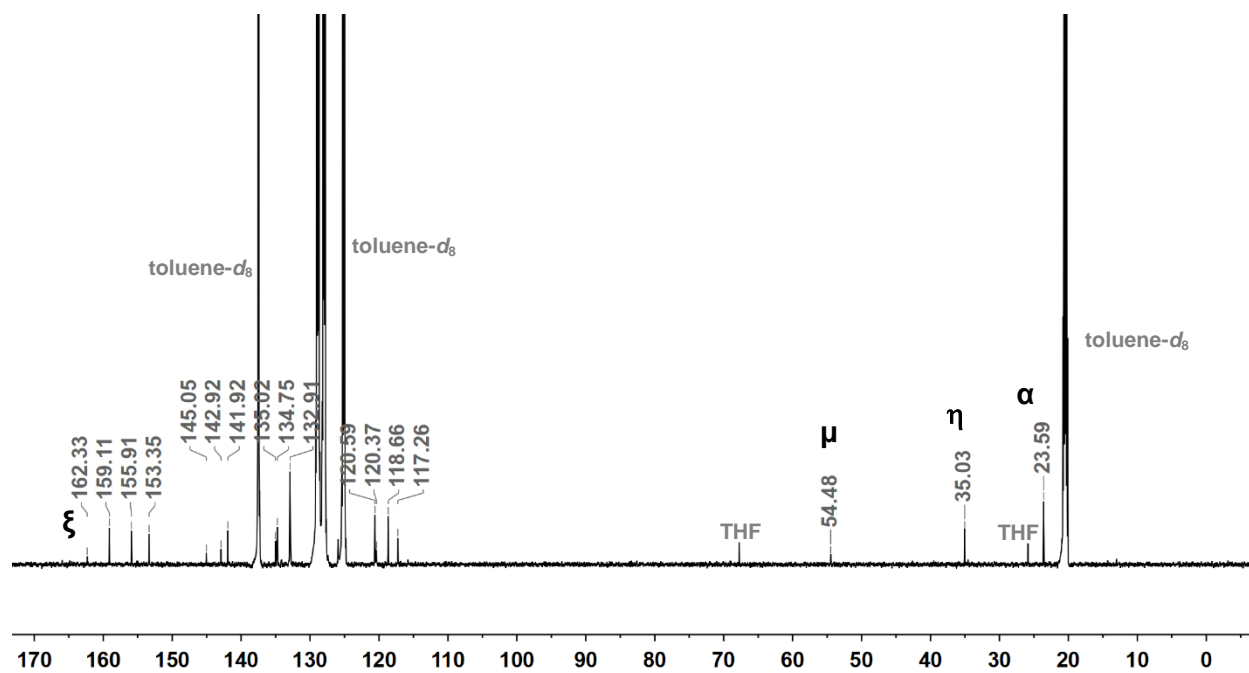
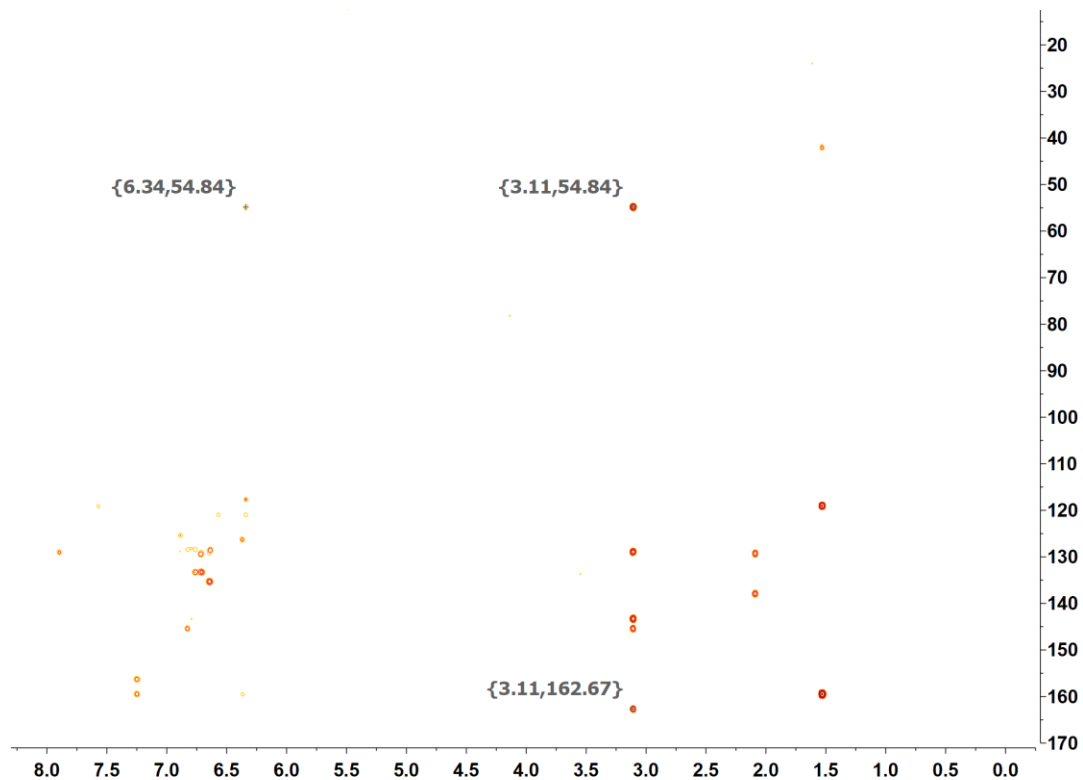


Figure S3.  $^{13}\text{C}$  NMR spectrum of 3a in toluene- $d_8$ .





**Figure S4.**  $^1\text{H}$ - $^{13}\text{C}$  HMBC of **3a** in toluene- $d_8$

The  $\delta^1\text{H}$ - $^{13}\text{C}$  HMBC of **3a** identifies the quaternary carbons of the keteniminate ligand. In toluene- $d_8$ , carbon  $\xi$  ( $^{13}\text{C}\delta$ : 162.33) shows only  $^3\text{J}_{\text{H-C}}$  long range coupling to the benzylic  $-\text{CH}_2$  protons  $\eta^{\text{H}}$  ( $^1\text{H}$   $\delta$ : 3.11). Carbon  $\mu$  ( $^{13}\text{C}$   $\delta$ : 54.84) shows  $^2\text{J}_{\text{H-C}}$  long range coupling to  $\eta^{\text{H}}$  and  $^3\text{J}_{\text{H-C}}$  coupling to aromatic proton  $\chi^{\text{H}}$  ( $^1\text{H}$   $\delta$ : 6.34).

**Table S1.** Tabulated correlations identifying the quaternary carbons of the keteniminate group based on  $^1\text{H}$ - $^{13}\text{C}$  HMBC

Carbon ( $^{13}\text{C}$ ppm)	$^2\text{J}_{\text{C-H}}$ ( $^1\text{H}$ ppm)	$^3\text{J}_{\text{C-H}}$ ( $^1\text{H}$ ppm)
$\xi$ (162.33)	—	$\eta^{\text{H}}$ (3.11)
$\mu$ (54.84)	$\eta^{\text{H}}$ (3.11)	$\chi^{\text{H}}$ (6.34)

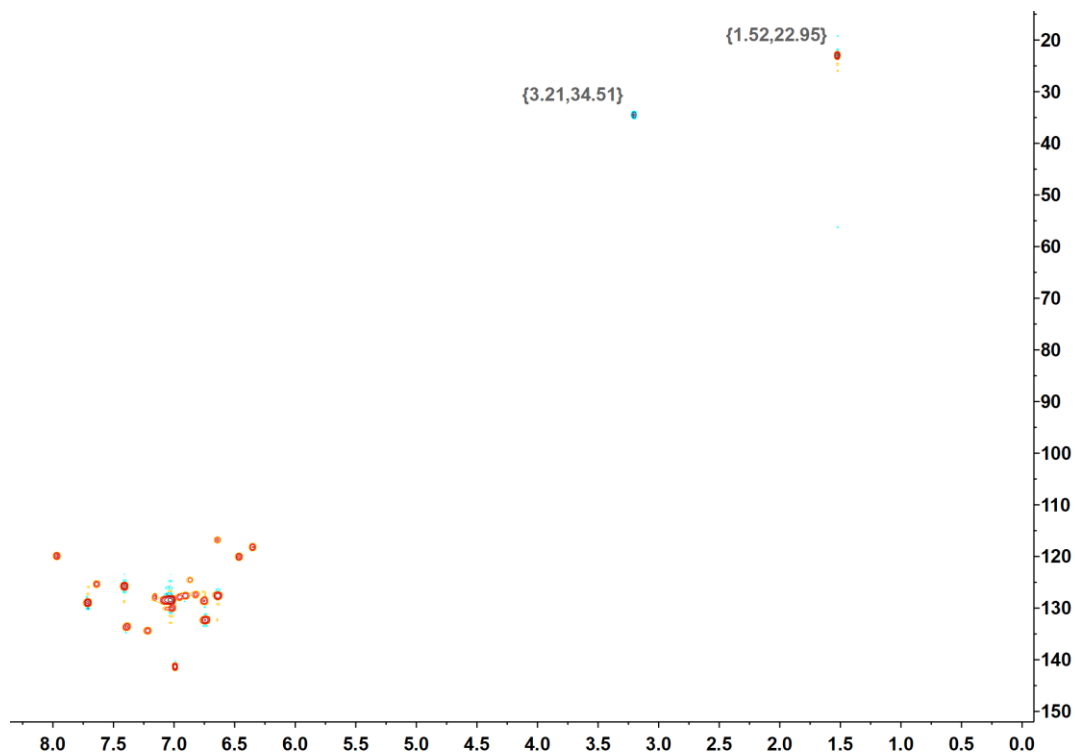


**Figure S5.**  $^1\text{H}$ - $^{13}\text{C}$  HSQC of **3a** formed in situ in  $\text{C}_6\text{D}_6$

The phase sensitive  $^1\text{H}$ - $^{13}\text{C}$  HSQC of **3a** in  $\text{C}_6\text{D}_6$  exhibits a positive (blue) cross peak at 3.21 ppm ( $^1\text{H}$ ) and 34.51 ppm ( $^{13}\text{C}$ ) that is indicative of a  $-\text{CH}_2$  group. A negative (red) cross peak at 1.52 ppm ( $^1\text{H}$ ) and 22.95 ppm ( $^{13}\text{C}$ ) is a  $-\text{CH}_3$  group. The corresponding  $^1\text{H}$  NMR signals integrate to 2 and 6 protons, respectively, and are therefore assigned as carbons  $\eta$  and  $\alpha$ .

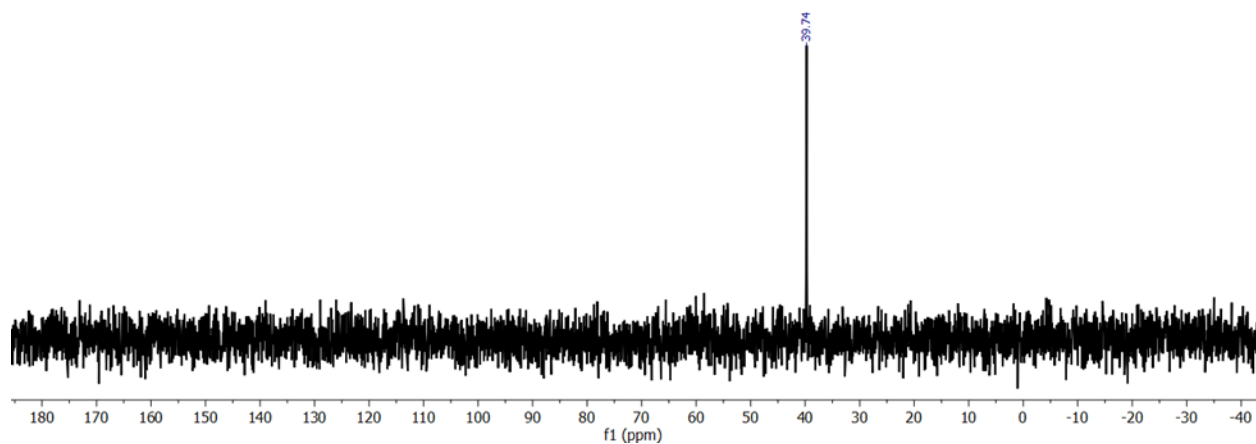


**Figure S6:**  $^{31}\text{P}$  NMR spectrum of isolated 3a in toluene- $d_8$

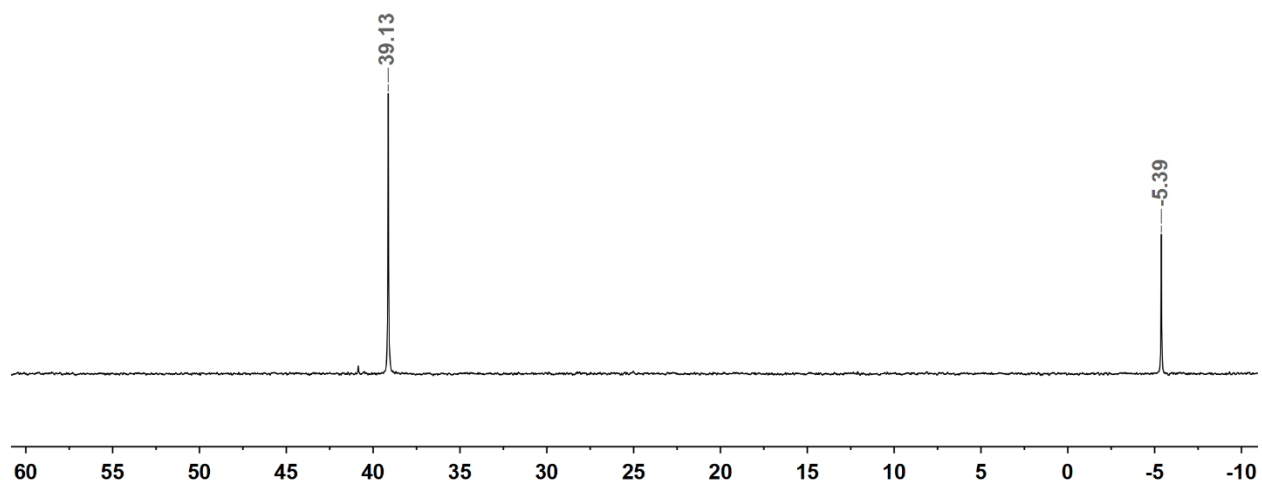


**Figure S7:**  $^{31}\text{P}$  NMR spectrum of 3a formed in situ in  $\text{C}_6\text{D}_6$ . Free  $\text{PPh}_3$  is present

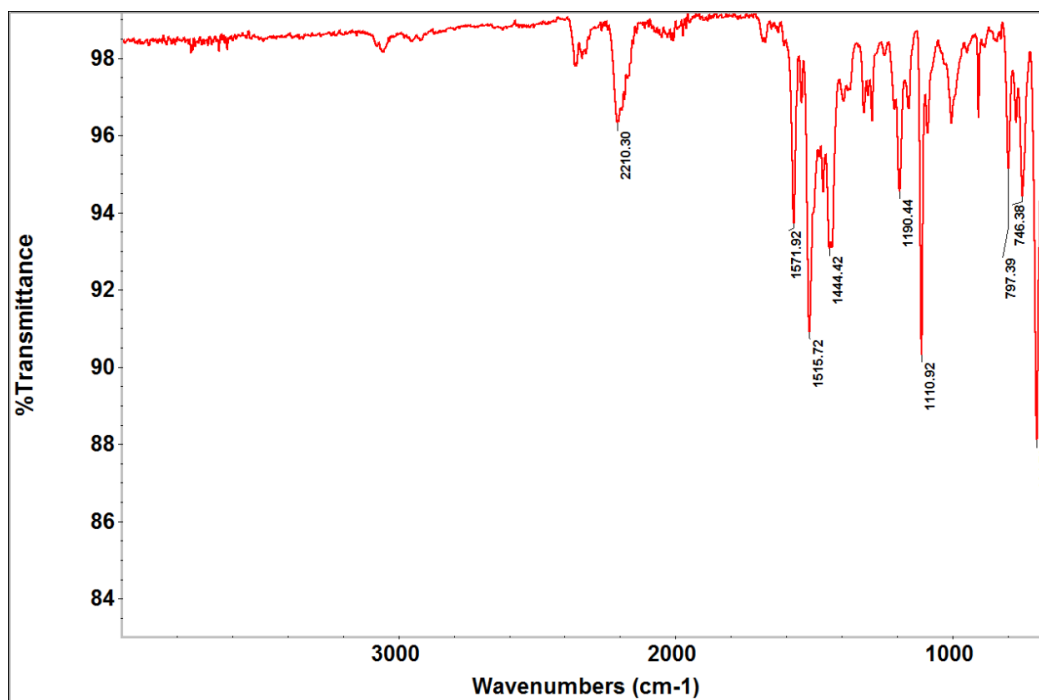


Figure S8: ATR IR of crystalline 3a. Trace CO<sub>2</sub> ~2400 cm<sup>-1</sup>

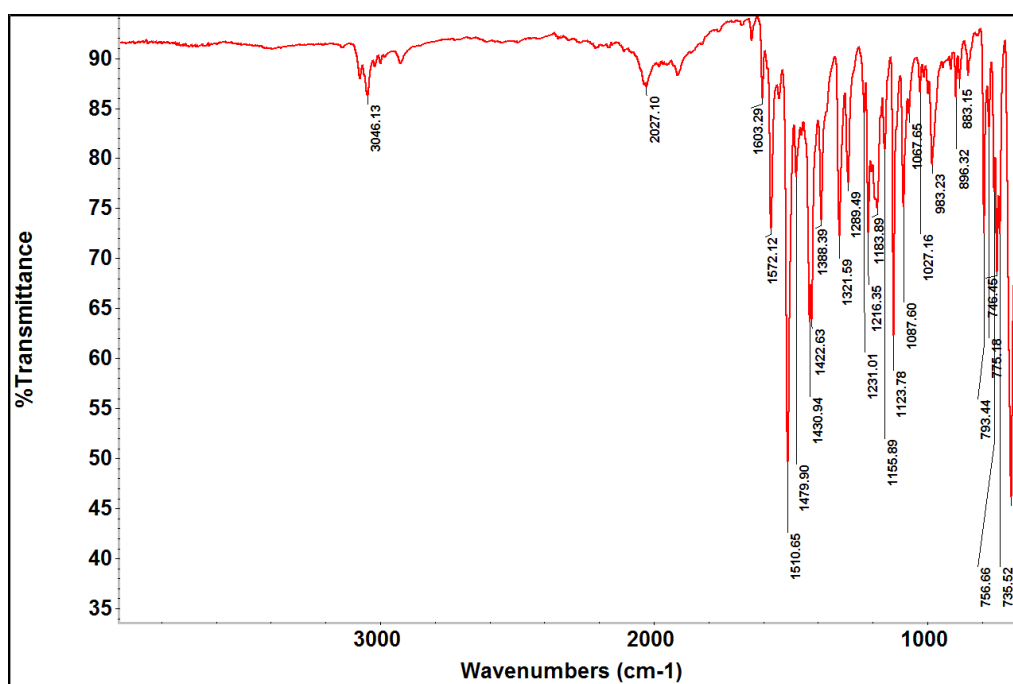


Figure S9: ATR IR of 3a prepared by precipitation with pentane from a solution of THF

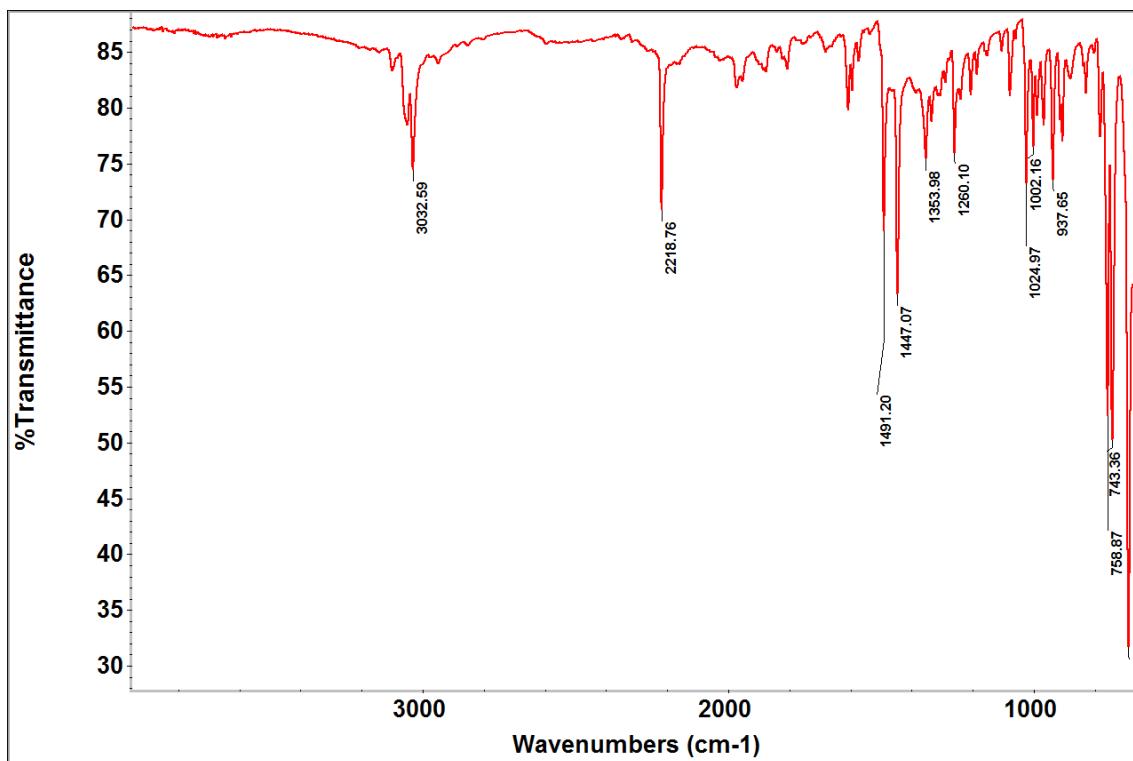


Figure S10: ATR IR of  $\alpha$ -phenylcinnamionitrile

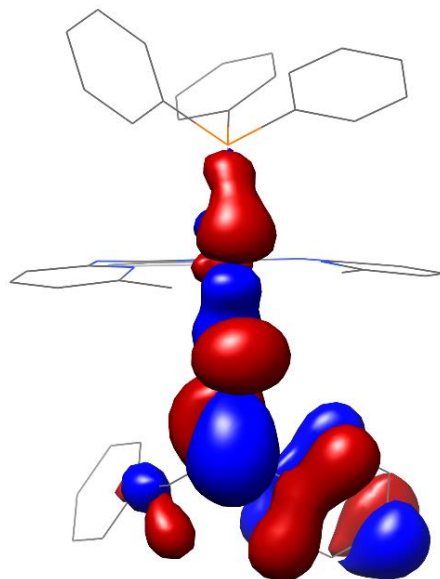
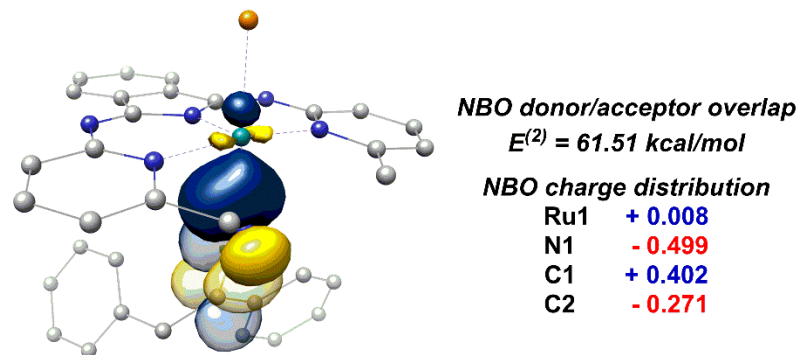


Figure S11: Depiction of the HOMO ( $-4.042$  eV) for 3a using rb3lyp/631-G(d,p)/SDD/PCM in benzene



**Figure S12: Optimized geometry and NBO analysis for **3a** using rb3lyp/631-G(d,p)/SDD level of theory**

To establish the electronic influence imparted by both Ru and the C2 substituents, **3a** was interrogated using Density Functional Theory (DFT; rb3lyp, 6-31G(d,p) for C, H, N, P/SDD for Ru/PCM in benzene). The highest occupied molecular orbital for **3a** (HOMO,  $-4.042 \text{ eV}$ ) is composed of a filled Ru *d*-orbital and the extended  $\pi$ -network between the C2=C1=N1 unit (Figure S11). Natural Bond Orbital (NBO) analysis provided insight into the thermodynamic stability of **3a**; a stabilization energy ( $E^2$ ) of  $61.51 \text{ kcal/mol}$  was calculated between the Ru–N donor NBO and C1–C2 acceptor NBO (Figure S12). Additionally, the filled *p*-orbitals of the keteniminate overlap with the acceptor orbitals of the  $\alpha$ -phenyl substituent, with  $E^2 = 19.49 \text{ kcal/mol}$ . The NBO analysis highlights the two significant interactions from the *N* and C2 substituents: Ru engages in  $\pi$ -bonding to the unsaturated unit, and the aromatic Ph group enables delocalization through the  $\text{sp}^2$  carbanion (C2). Additionally, the NBO analysis of **3a** established the charge distribution across the C2=C1=N1 unit. While C1 exhibits electrophilic character with an NBO charge of  $+0.402$ , C2 and N1 are nucleophilic with NBO charges of  $-0.271$  and  $-0.499$ , respectively.

### Solution stability of **3a** in C<sub>6</sub>D<sub>6</sub>

The solution stability of **3a** was assessed using variable temperature <sup>31</sup>P and <sup>1</sup>H NMR spectroscopy. **3a** was formed *in situ* following procedure II, using C<sub>6</sub>D<sub>6</sub> (2 mL) instead of THF, and PhTMS (1.2 x 10<sup>-2</sup> mmol) as an internal standard. 600 μL of the solution was transferred to a sealed NMR tube and analyzed by variable temperature NMR spectroscopy. <sup>1</sup>H and <sup>31</sup>P spectra were collected at 25, 40, 60, and 75 °C. The instrument was equilibrated to each temperature for 10 minutes. After equilibration, the sample remained at the indicated temperature for an additional 10 minutes. The <sup>1</sup>H integral ratio of PhTMS to **3a** (using the -CH<sub>2</sub> signal at 3.20 ppm) was used to quantify the extent of decomposition after 20 minutes at each temperature. The initial <sup>1</sup>H NMR spectrum in C<sub>6</sub>D<sub>6</sub> at 25 °C is shown in Figure S12 and shows that 1,4-hydride insertion from **1** to **2a** occurred quantitatively (>99 % NMR yield). At 60 °C, 99% **3a** remained after 20 minutes. At 70 °C, broadening of PPh<sub>3</sub> was observed in the <sup>31</sup>P spectrum, and less than 10% decomposition of **3a** occurred after 20 minutes. Upon returning to 25 °C, 89% **3a** remained, indicating that the decomposition of **3a** is irreversible. **3a** continued to decompose in solution at 25 °C, and after 17 h 68% of **3a** was observed.

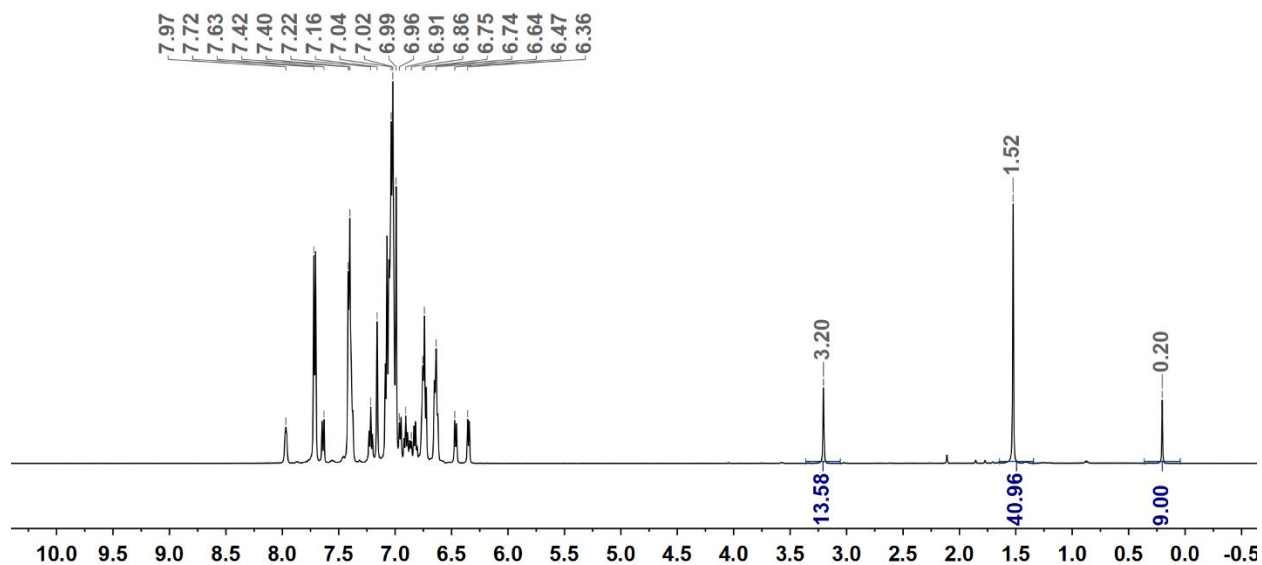


**Figure S13. Initial <sup>1</sup>H NMR spectrum of **3a** formed from **1** and **2a** in C<sub>6</sub>D<sub>6</sub>. Insertion occurs quantitatively (>99% NMR yield) based on PhTMS as the internal standard.**

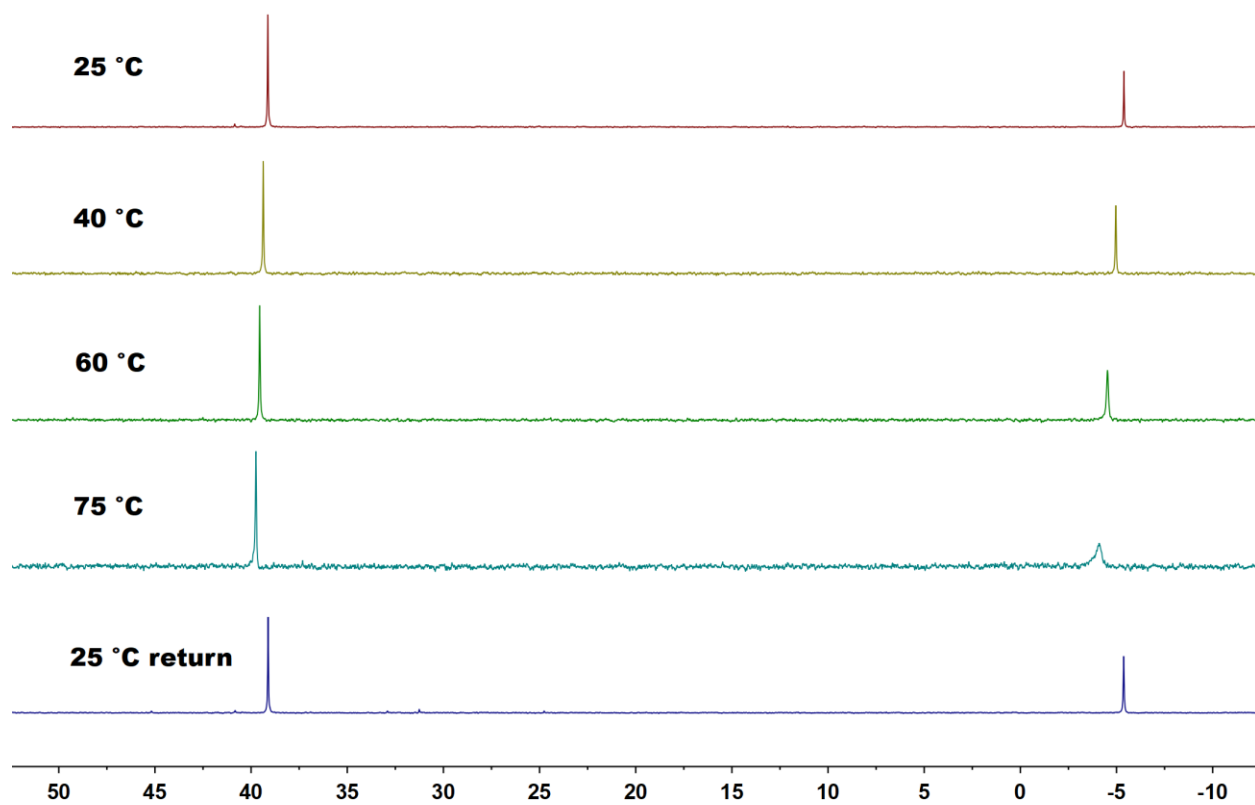


**Figure S14.**  $^{31}\text{P}$  NMR spectra of 3a after 20 minutes at 25, 40, 60, and 75 °C.



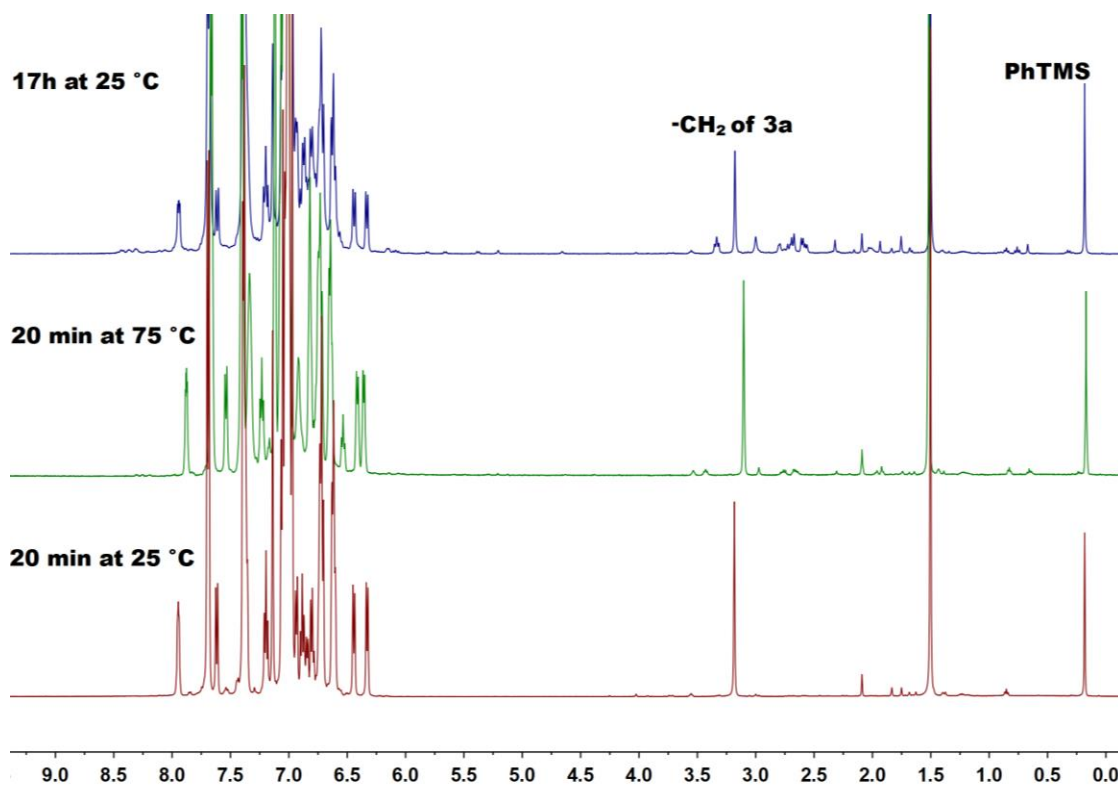


Figure S15.  $^1\text{H}$  NMR spectra of 3a after 20 minutes at 25 and 75  $^\circ\text{C}$ , and after 17h at 25  $^\circ\text{C}$ .

Table S2. Amount (mmol) of 3a remaining after 20 minutes at indicated temperature.

Temp ( $^\circ\text{C}$ )	3a (mmol)	% 3a
25	0.082	>99
40	0.082	>99
60	0.080	98
75	0.073	91
25	0.071	89
25 (after 17 h)	0.054	68

### III. *In situ* characterization of Ru-keteniminates **3b-3e**

A 20 mL vial was charged with **1** (10 mg, 0.01 mmol),  $\alpha,\beta$ -unsaturated nitrile (0.012 mmol), and 750  $\mu\text{L}$  toluene- $d_8$ . Once dissolved, the solution was transferred to a sealed NMR tube and analyzed by  $^1\text{H}$ ,  $^{31}\text{P}$ , and  $^{13}\text{C}$  NMR spectroscopy at 35  $^\circ\text{C}$ . The spectra for complexes **3b-3d** formed *in situ* are provided below. Additionally, samples of **3b-3d** were prepared for ATR-IR spectroscopic analysis by precipitating the Ru-keteniminates from a solution of THF with pentane.

#### In situ formation of **3b**

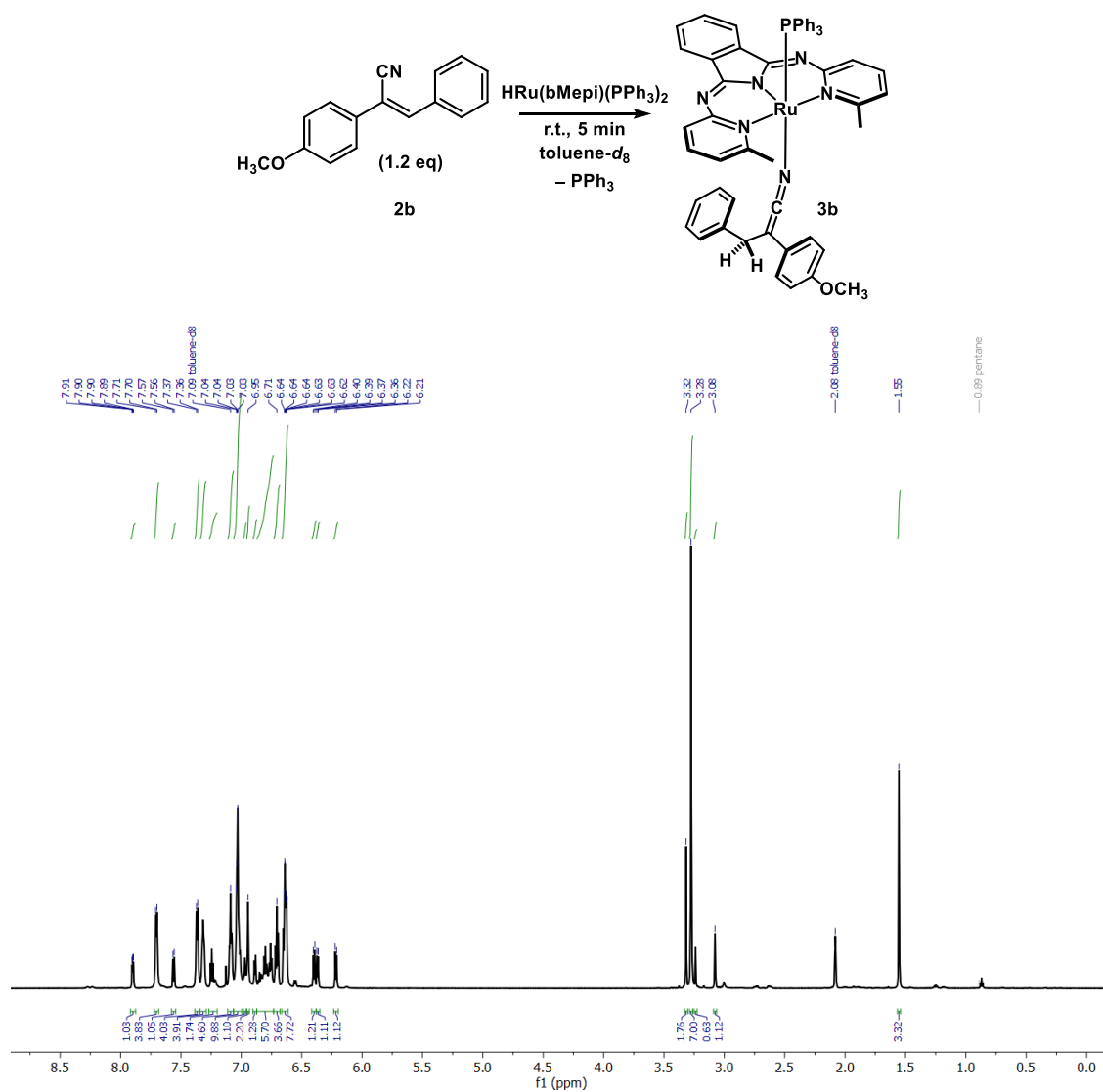


Figure S16:  $^1\text{H}$  NMR spectrum for **3b** prepared *in situ* in toluene- $d_8$

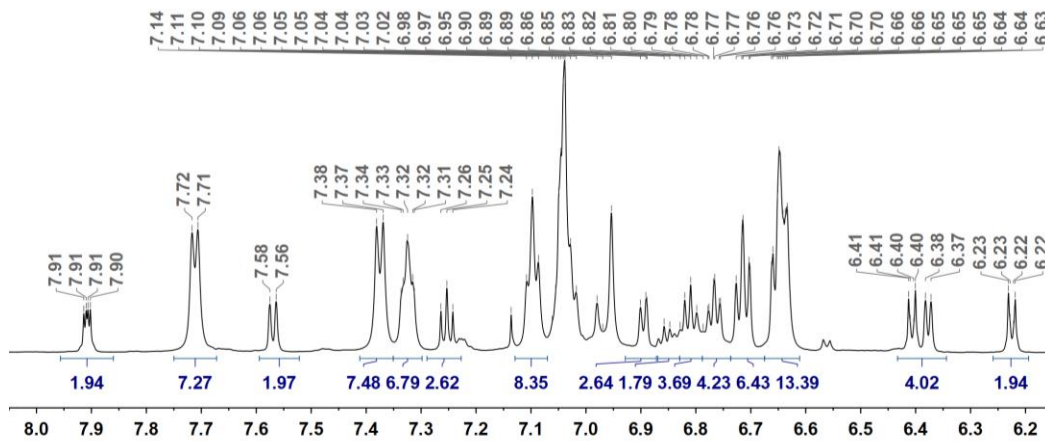


Figure S17: Aromatic region of the  $^1\text{H}$  NMR spectrum of 3b in  $\text{toluene-}d_8$

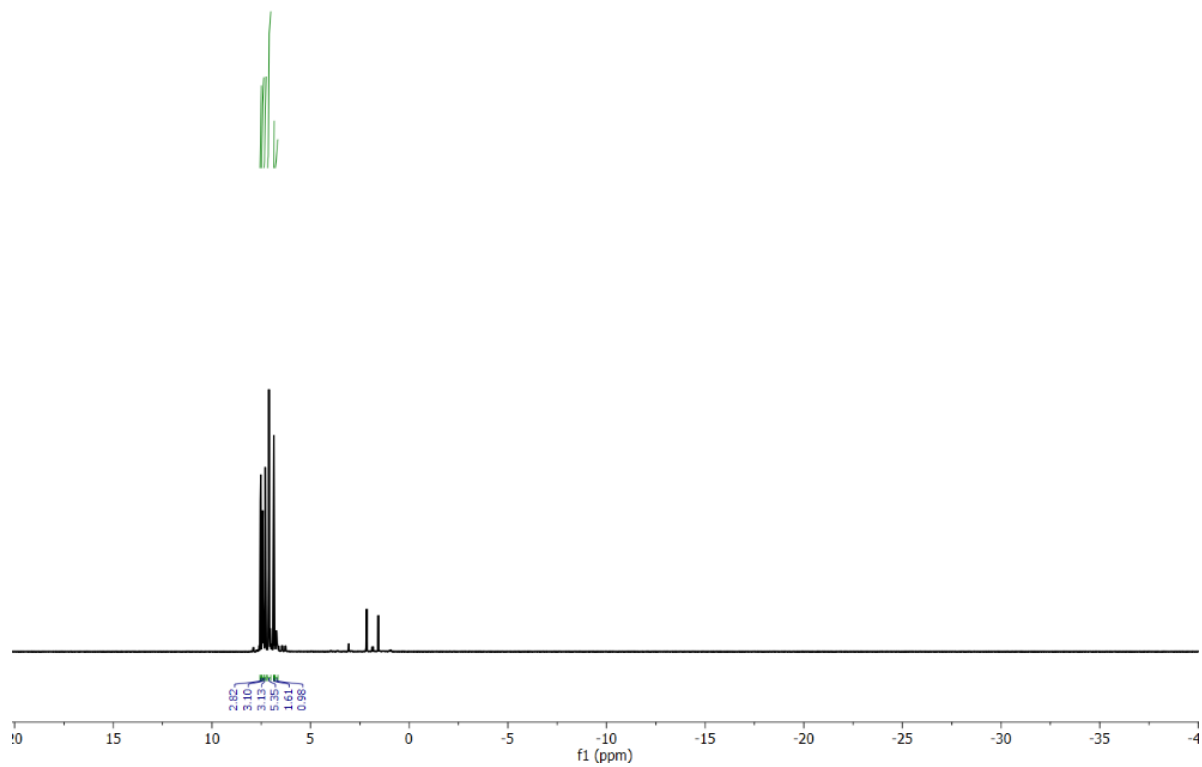


Figure S18: Expanded  $^1\text{H}$  NMR spectrum of 3b in  $\text{toluene-}d_8$  showing the hydride region

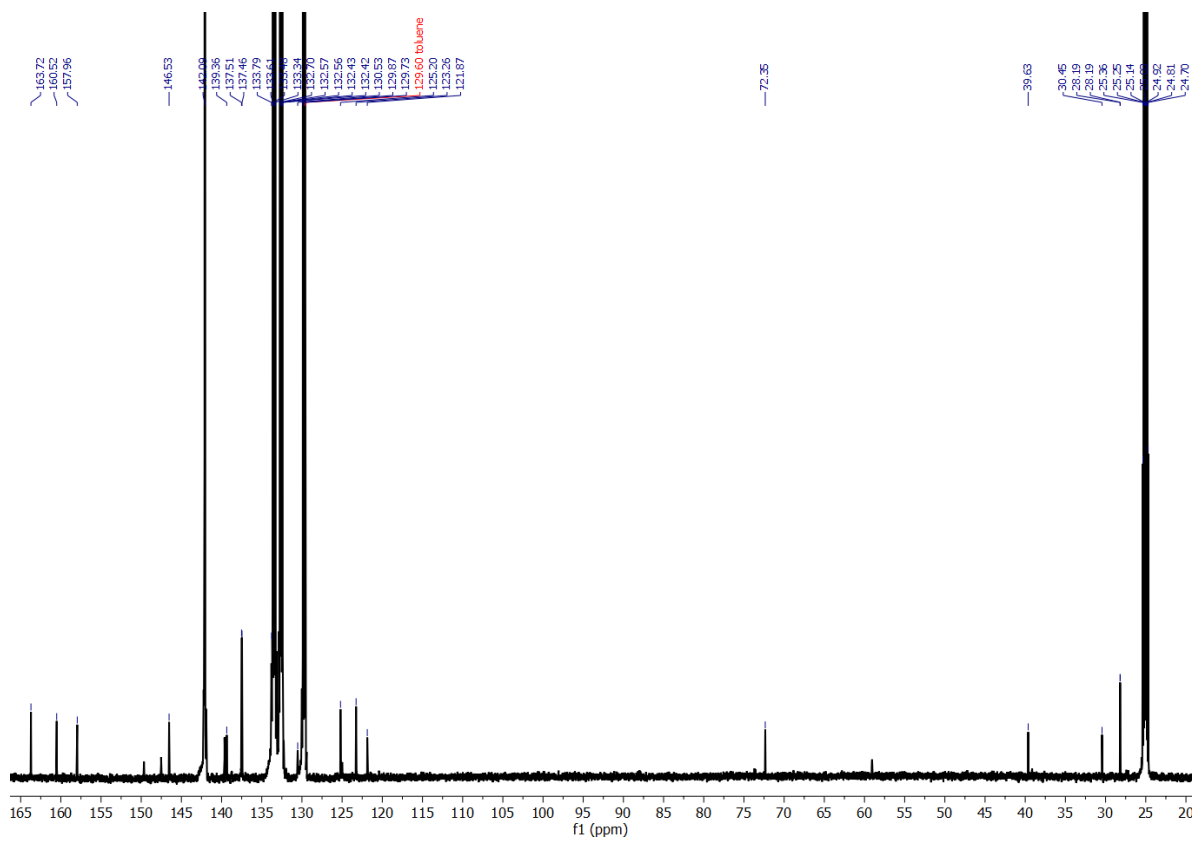


Figure S19:  $^{13}\text{C}$  NMR spectrum of 3b in toluene- $d_8$

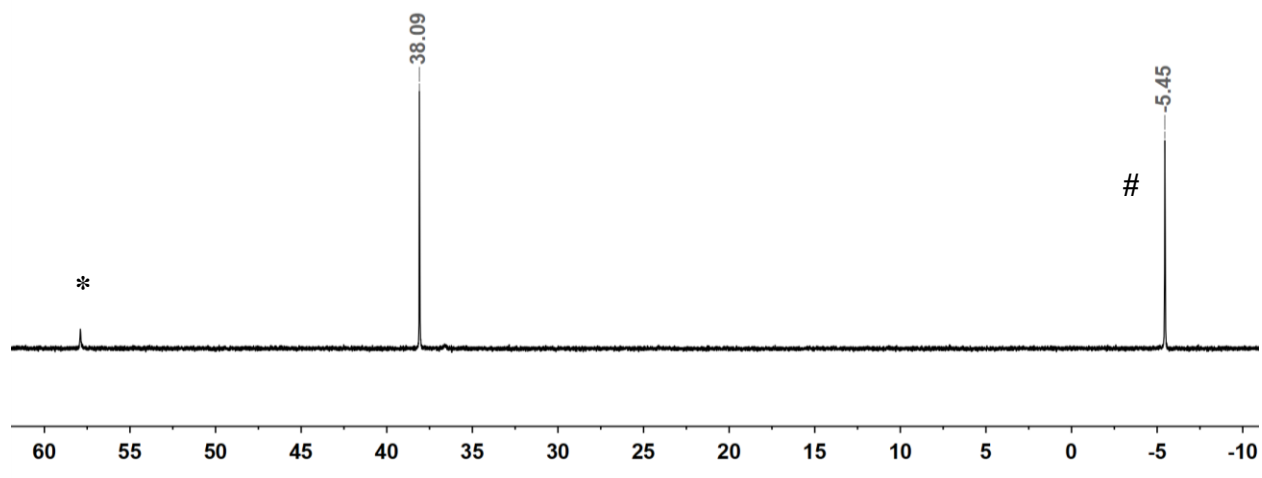


Figure S20:  $^{31}\text{P}$  NMR spectrum of 3b in toluene- $d_8$ . # =  $\text{PPh}_3$ ; \* = unknown byproduct

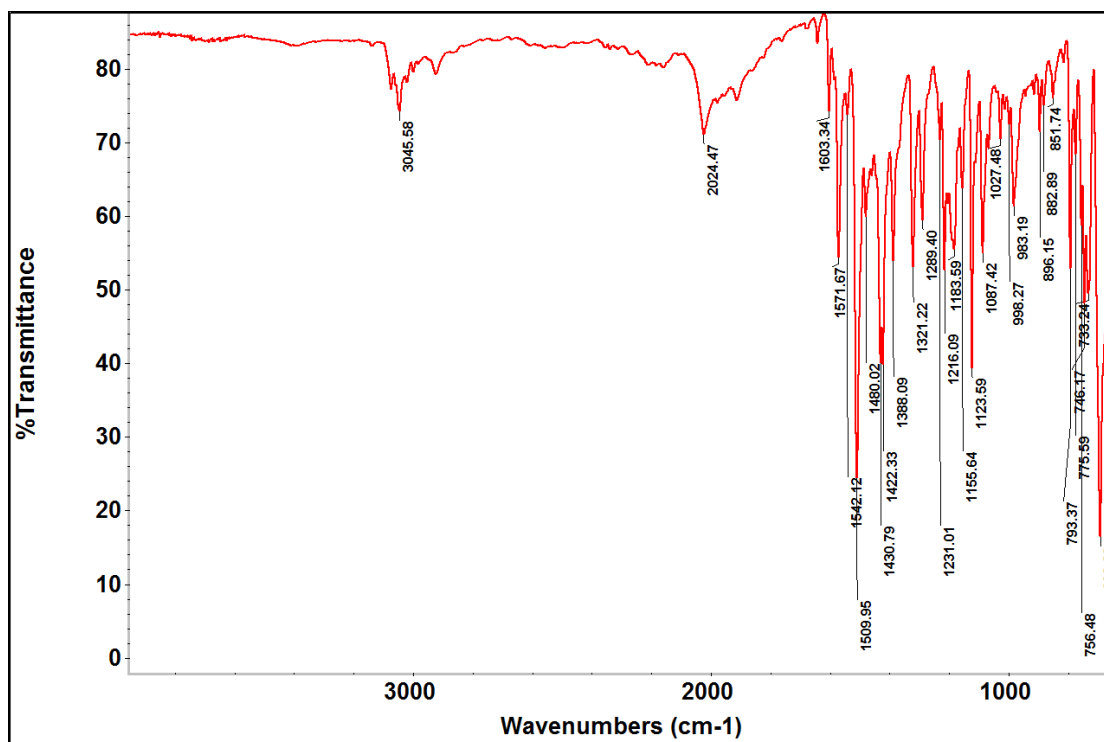
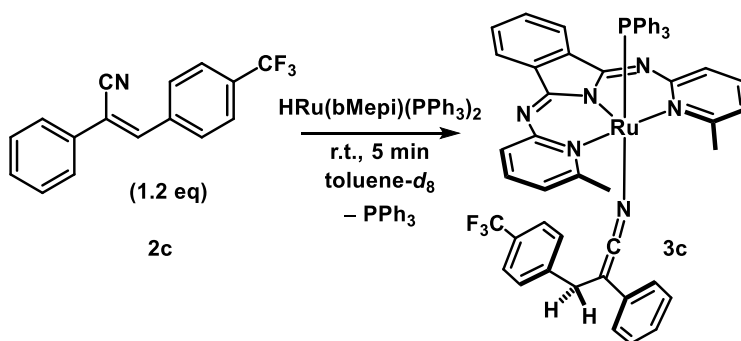


Figure S21: ATR IR spectrum of 3b precipitated with pentane from a solution of THF

### In situ formation of 3c



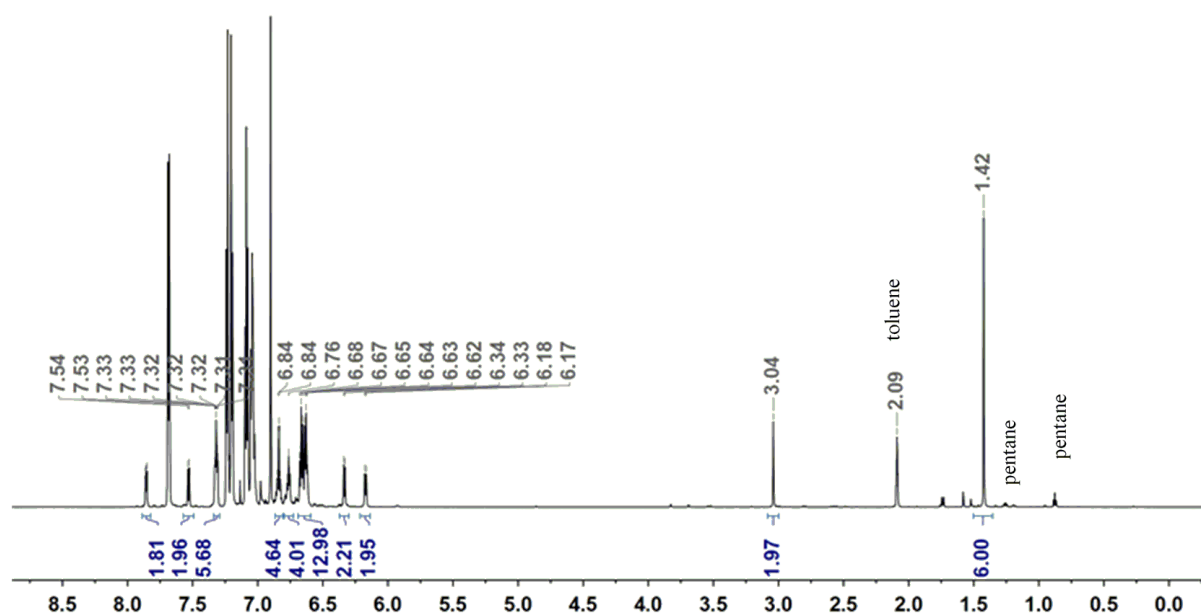


Figure S22:  $^1\text{H}$  NMR spectrum of **3c** prepared *in situ* in  $\text{toluene-}d_8$

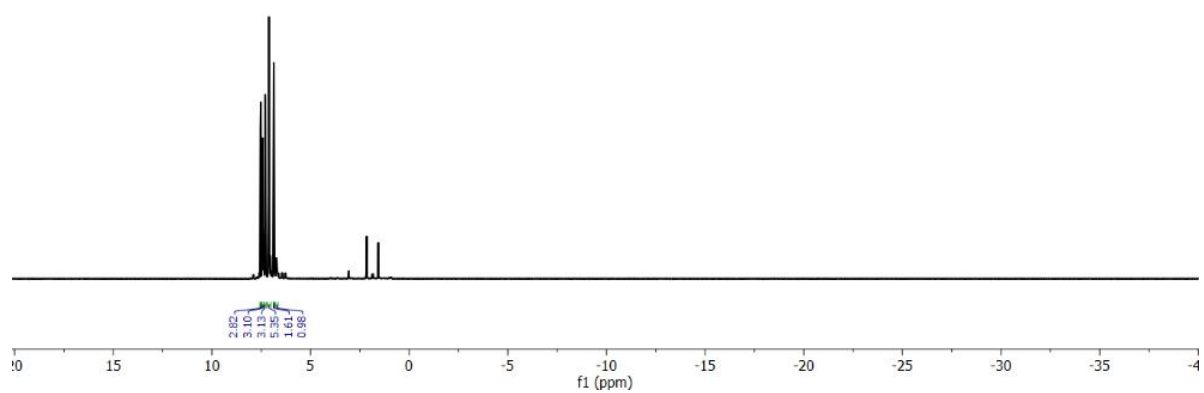


Figure S23: Expanded  $^1\text{H}$  NMR spectrum of **3c** in  $\text{toluene-}d_8$  showing the hydride region

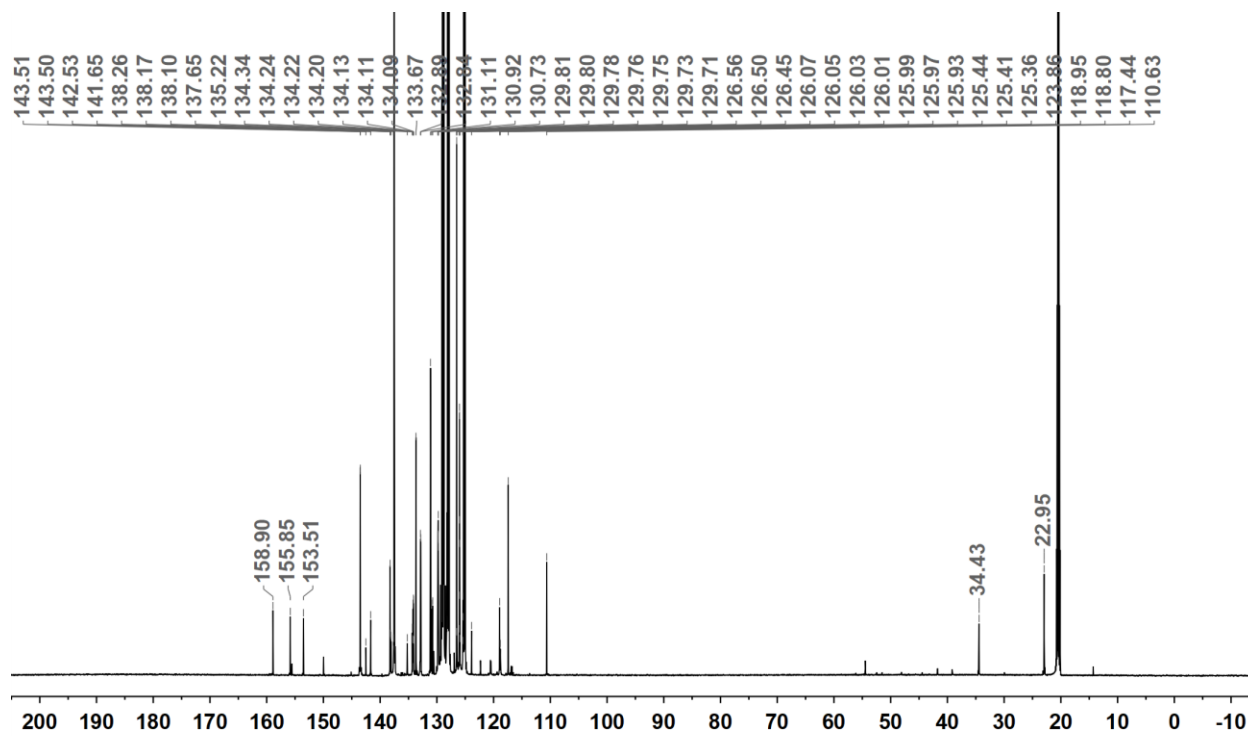


Figure S24:  $^{13}\text{C}$  NMR spectrum of 3c prepared *in situ* in toluene- $d_8$

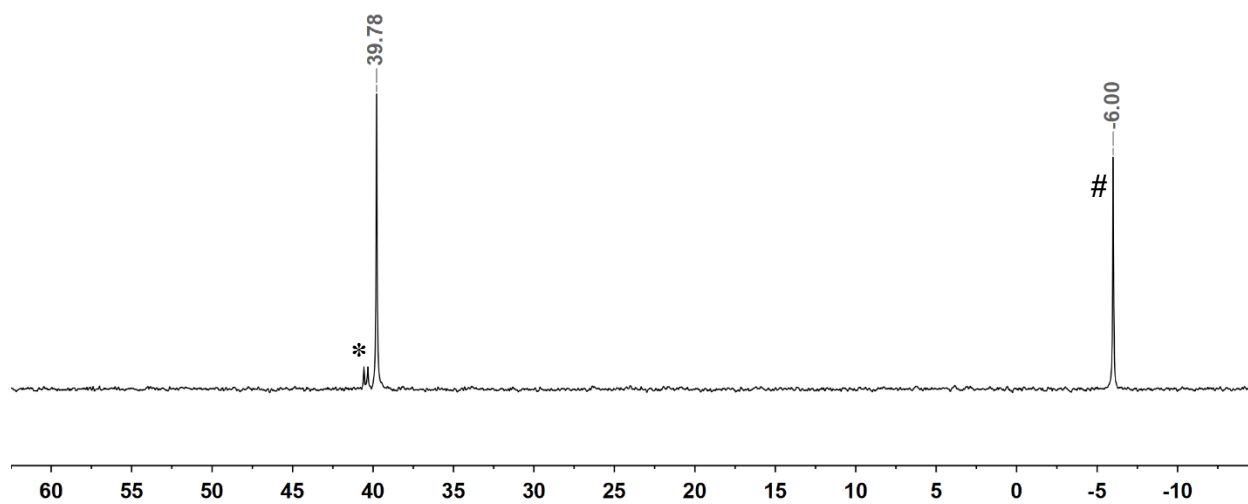
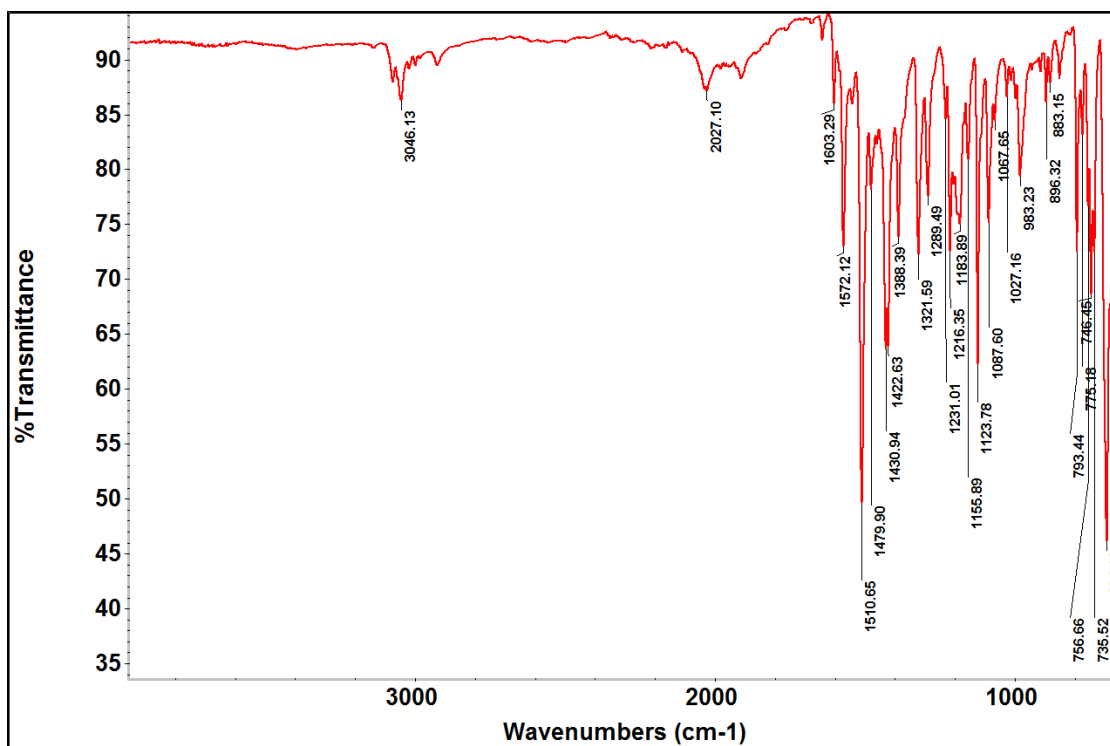
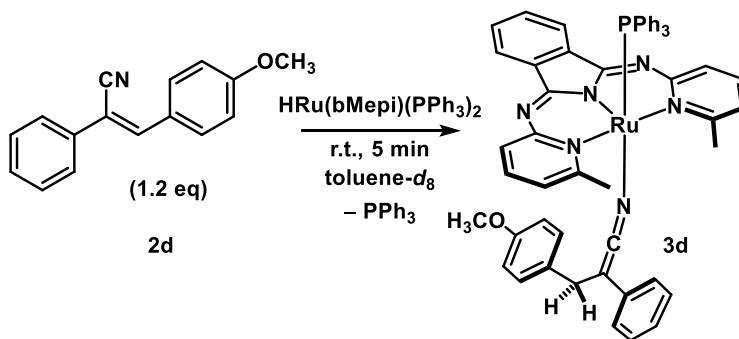


Figure S25:  $^{31}\text{P}$  NMR spectrum of 3c prepared *in situ* in toluene- $d_8$ . \* = unknown byproduct; # =  $\text{PPh}_3$



**Figure S26: ATR IR spectrum of 3c precipitated with pentane from a solution of THF  
In situ formation of 3d**





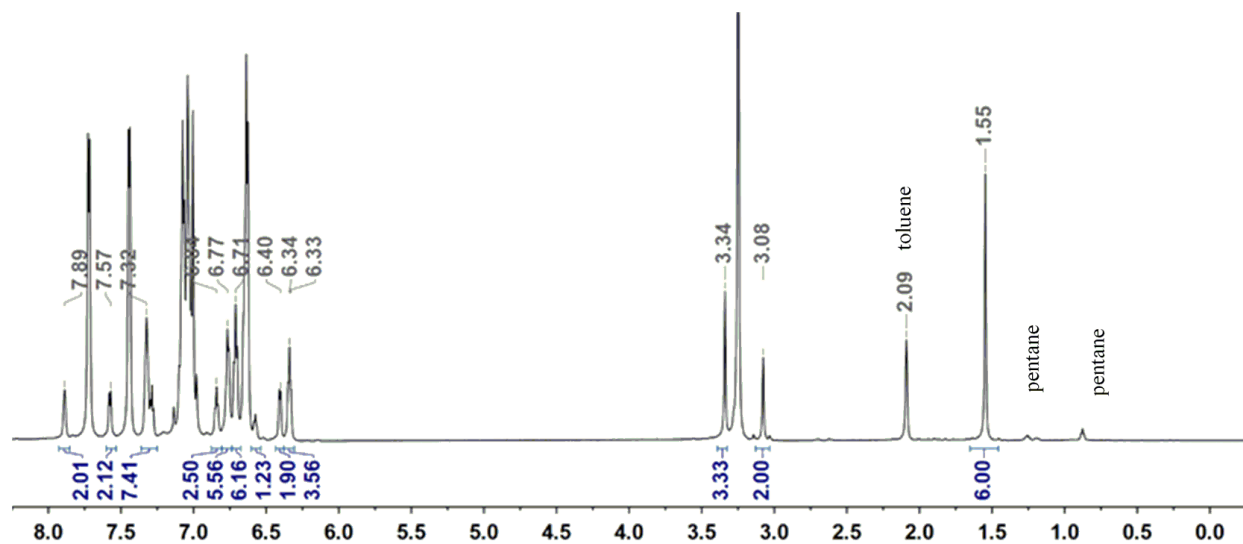


Figure S27:  $^1\text{H}$  NMR spectrum of 3d prepared in situ in  $\text{toluene-}d_8$

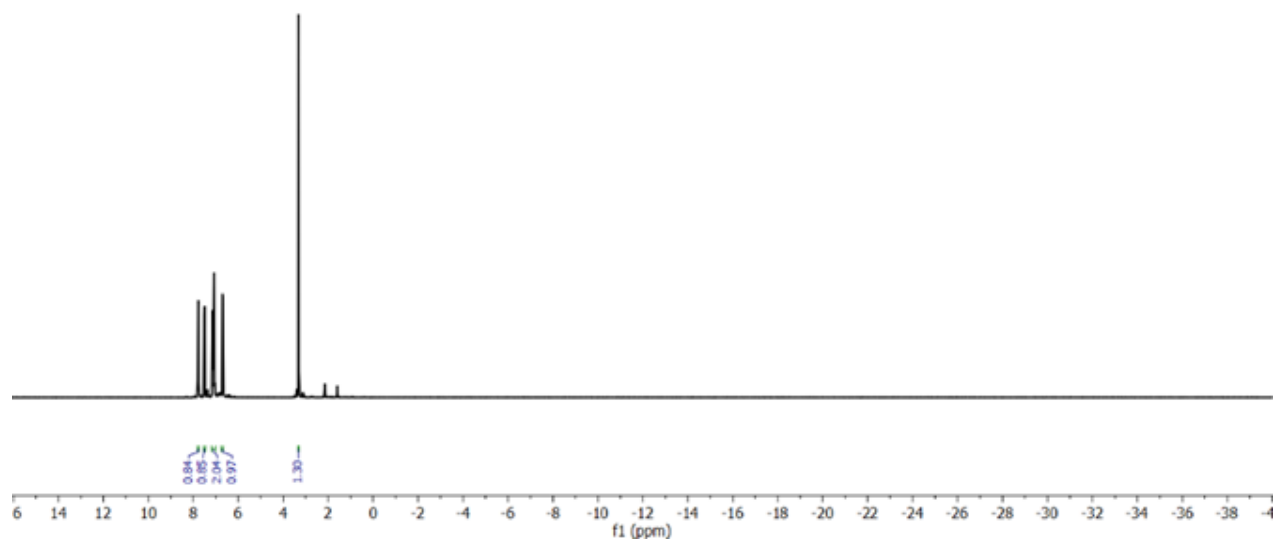


Figure S28: Expanded  $^1\text{H}$  NMR spectrum of 3d in  $\text{toluene-}d_8$  showing the hydride region

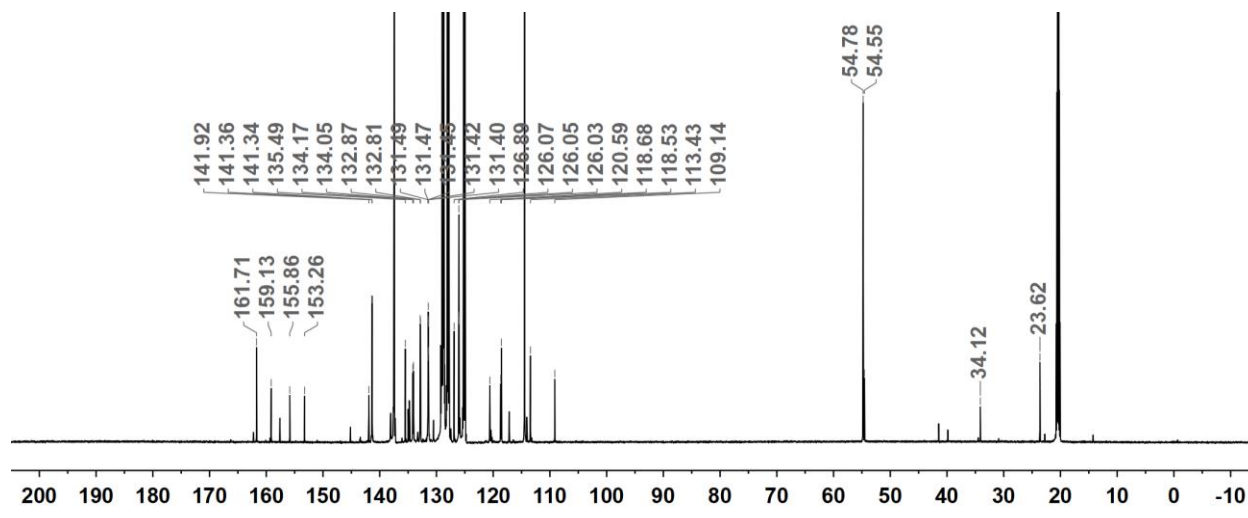


Figure S29: <sup>13</sup>C NMR spectrum of 3d prepared *in situ* in toluene-*d*<sub>8</sub>

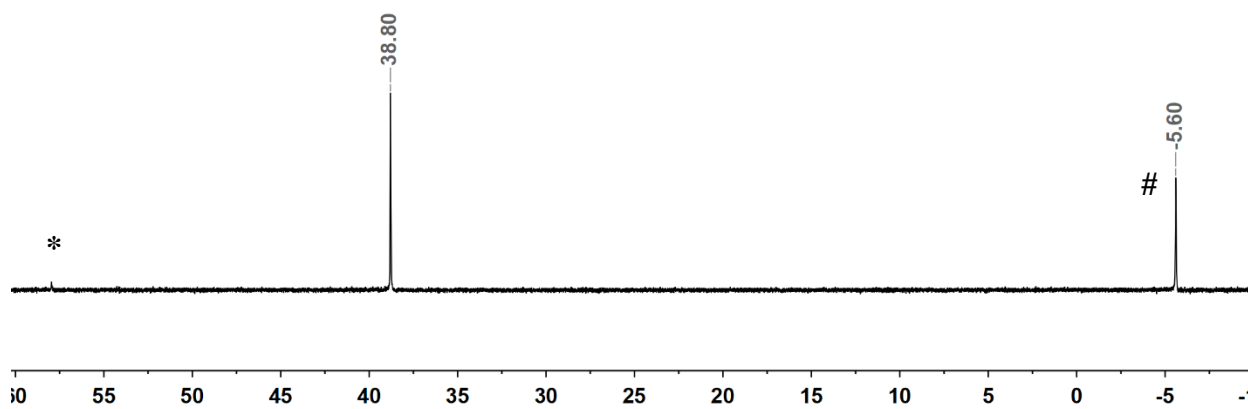


Figure S30: <sup>31</sup>P NMR spectrum of 3d in toluene-*d*<sub>8</sub>. # = PPh<sub>3</sub>; \* = unknown byproduct

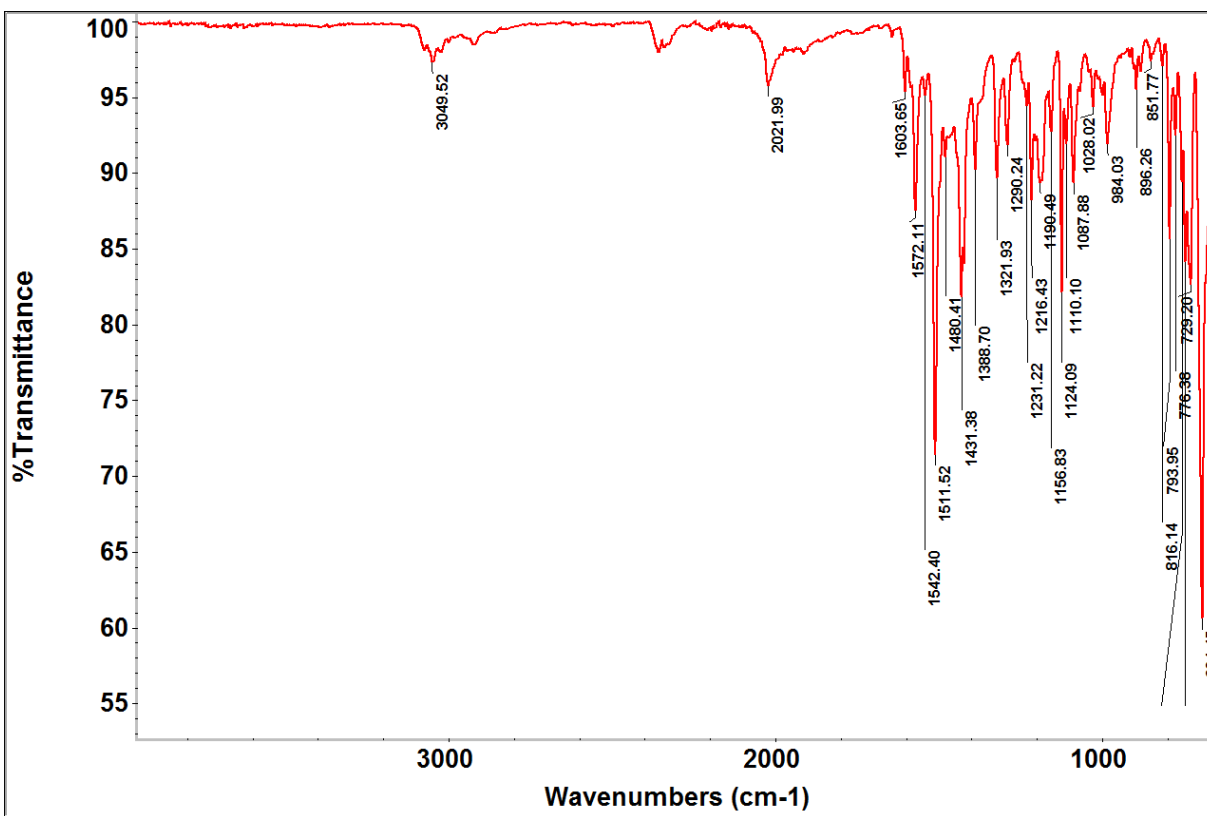
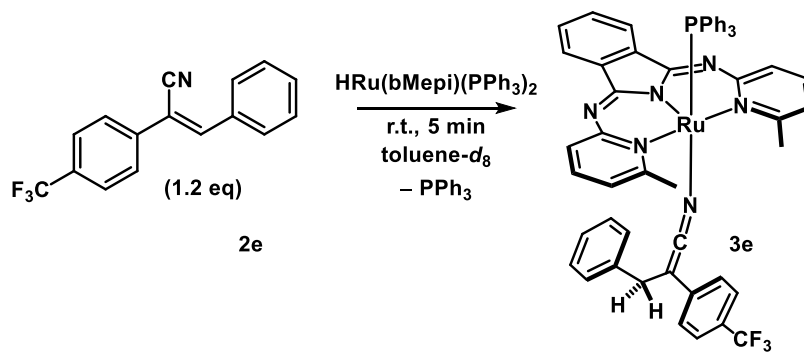


Figure S31: ATR IR spectrum of 3d precipitated with pentane from a solution of THF. Trace CO<sub>2</sub> ~2400 cm<sup>-1</sup>

### In situ formation of 3e



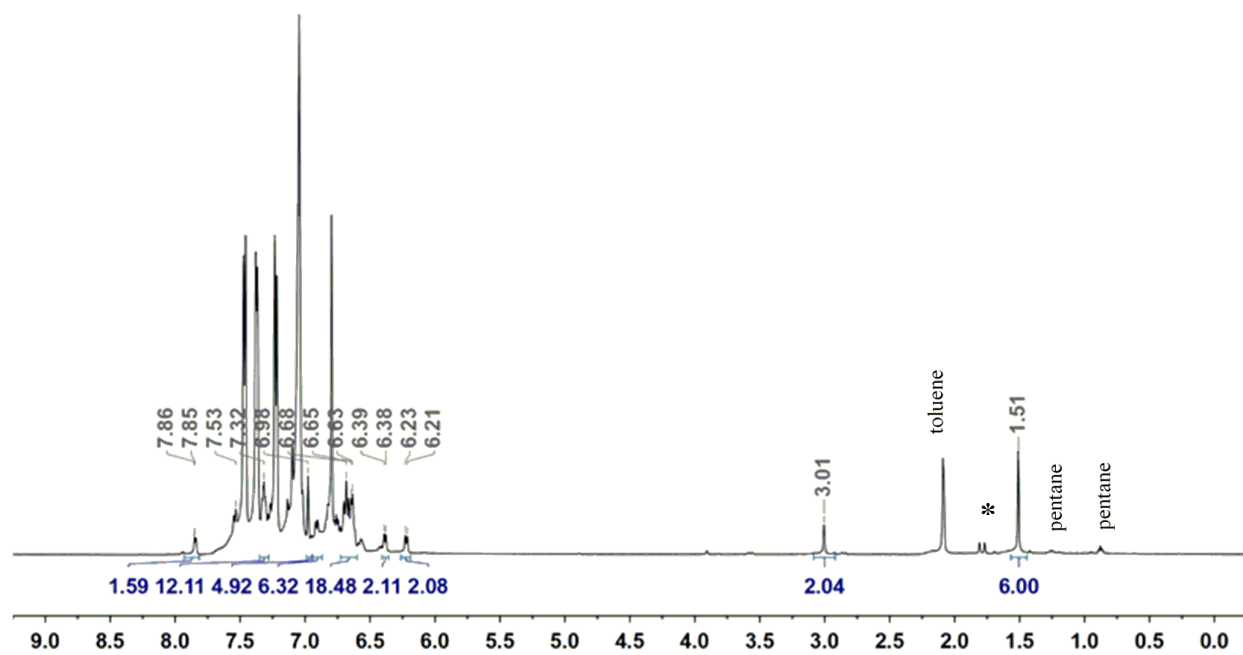


Figure S32:  $^1\text{H}$  NMR spectrum of **3e** prepared in situ in toluene- $d_8$ . \* = unknown byproduct

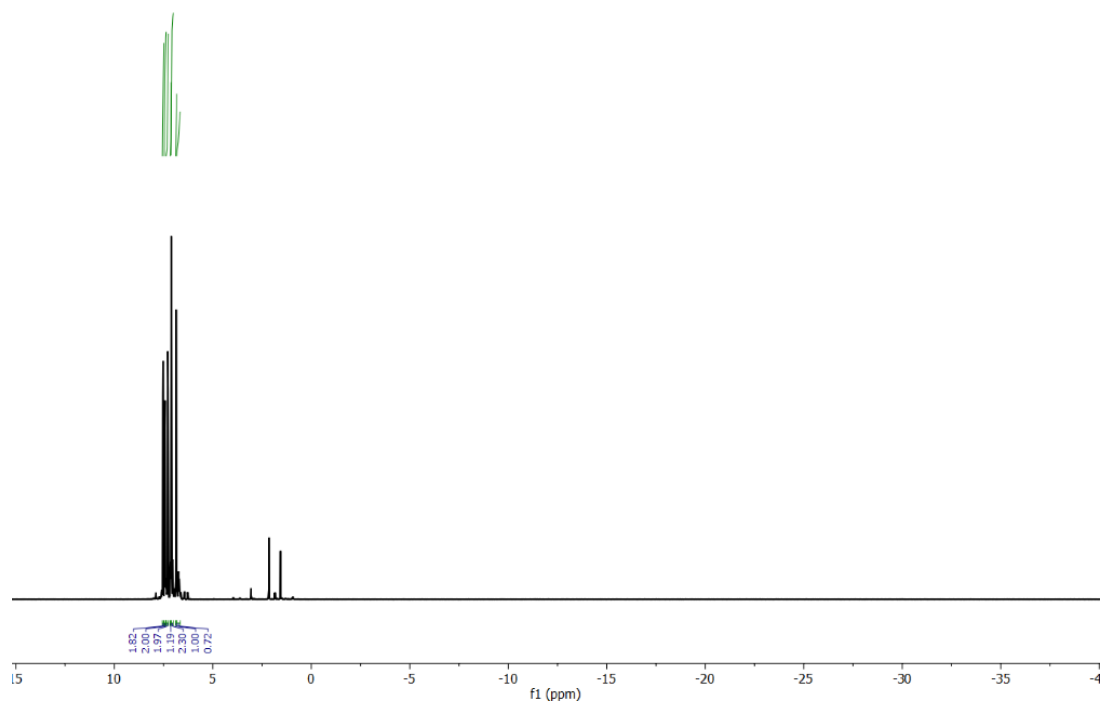


Figure S33: Expanded  $^1\text{H}$  NMR spectrum of **3e** in toluene- $d_8$  showing the hydride region

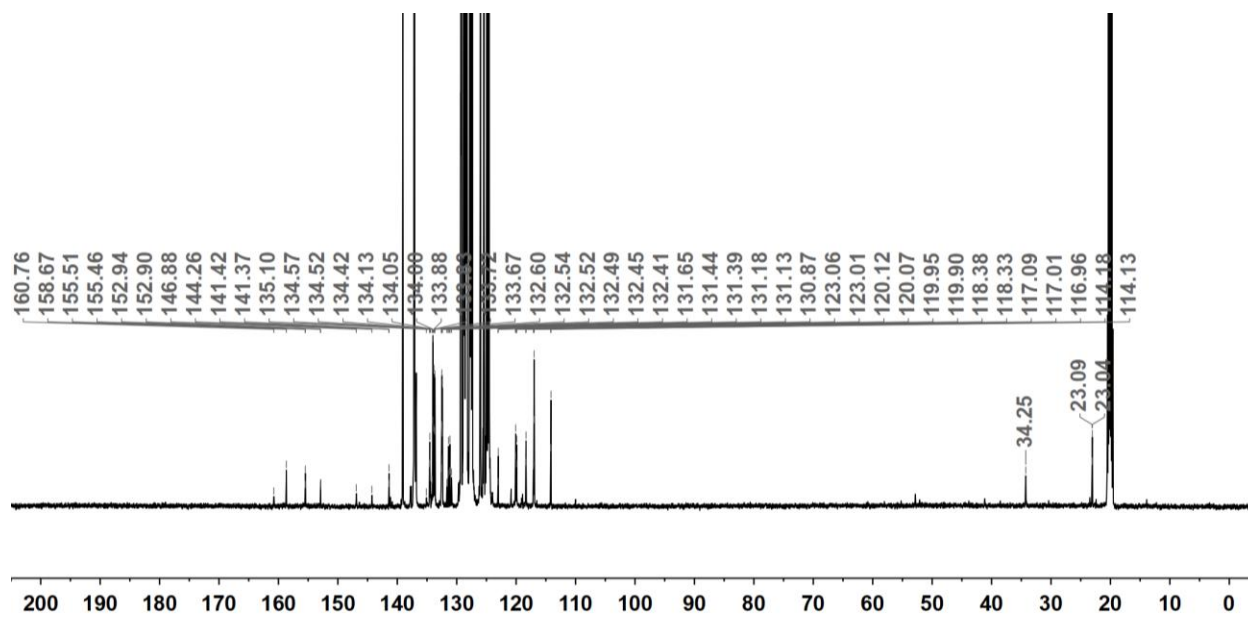


Figure S34:  $^{13}\text{C}$  NMR spectrum of 3e in toluene- $d_8$

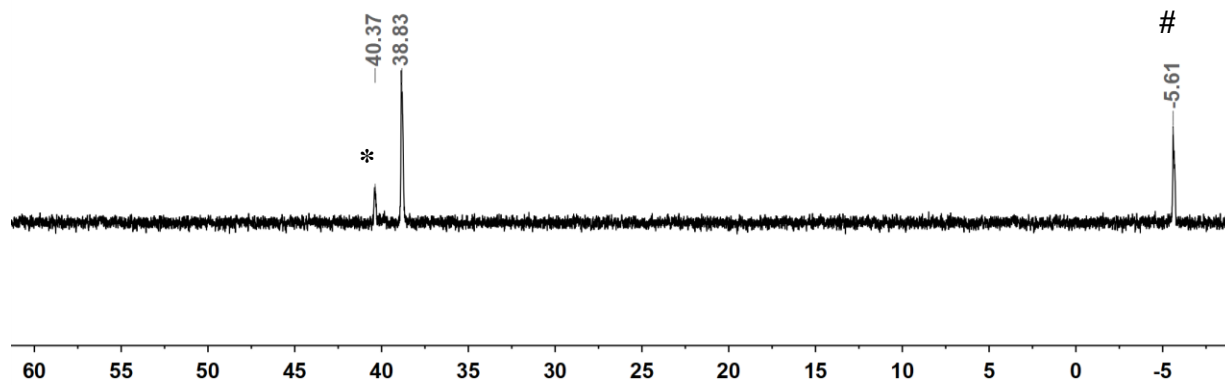


Figure S35:  $^{31}\text{P}$  NMR spectrum of 3e in toluene- $d_8$ . \* = unknown byproduct; # =  $\text{PPh}_3$

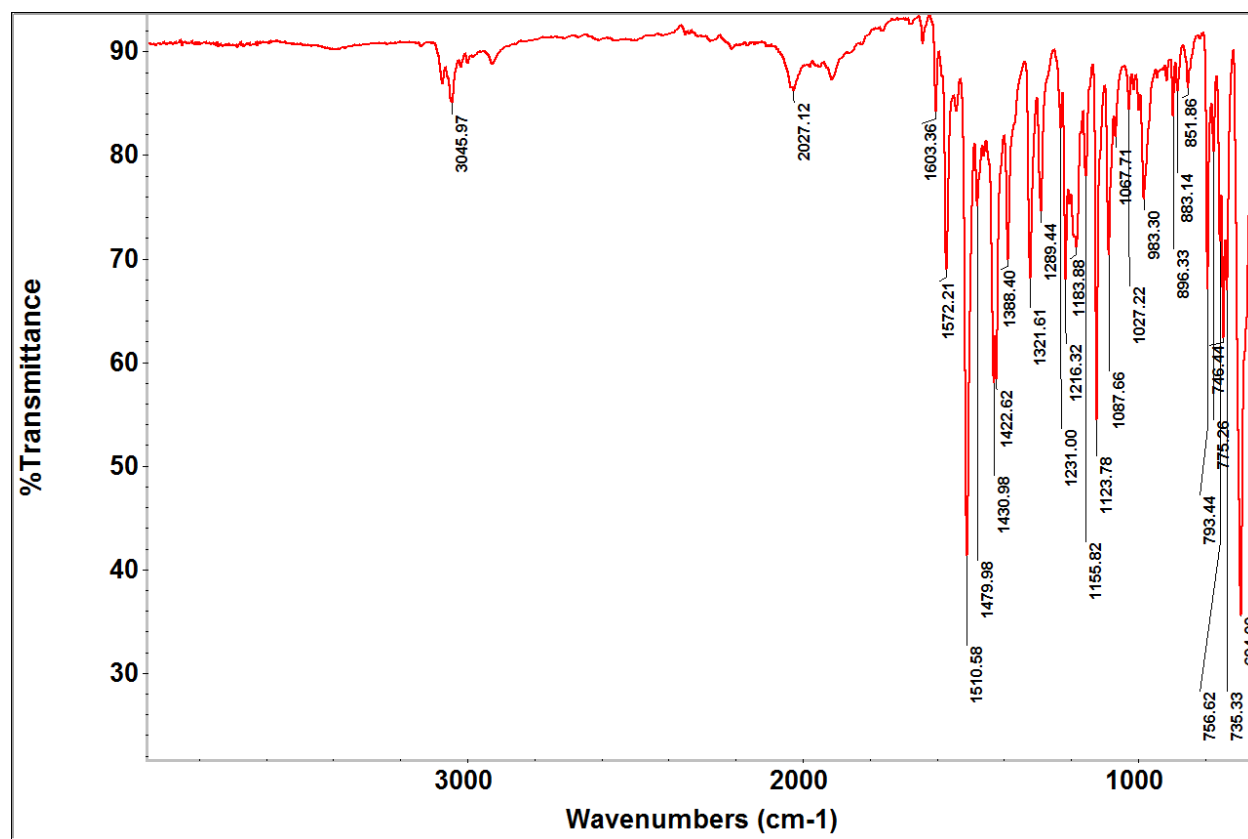


Figure S36: ATR IR spectrum of 3e precipitated with pentane from a solution of THF

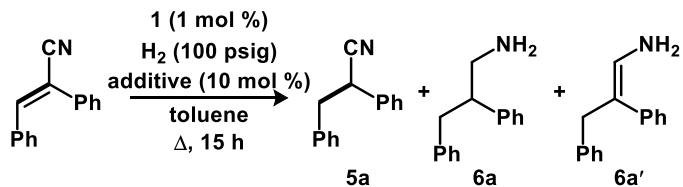
#### IV. General procedure for the hydrogenation and hydrogenative acylation of $\alpha,\beta$ -unsaturated nitriles using **1** and H<sub>2</sub>

All reactions involving H<sub>2</sub> were run in a 300 mL stainless steel Parr reactor equipped with a pressure gauge, burst disc, and inlet/outlet needle valve. Catalytic reactions were conducted in 8 mL scintillation vials that were loaded into an aluminum block machined to hold seven vials and fit into the 300 mL Parr reactor. Stock solutions of the  $\alpha,\beta$ -unsaturated nitrile (1M) were prepared in toluene and stored under N<sub>2</sub> at ambient temperature. A new stock solution of **1** (0.01 M) in toluene was prepared prior to each set of reactions. All catalytic reactions were prepared and sealed in the Parr bomb reactor in a glovebox under an N<sub>2</sub> atmosphere. The sealed Parr reactor was removed from the glovebox and pressurized with ultra-high purity H<sub>2</sub>. To exclude air from the reactions, the volume contained in the connection between the tank and the reactor was purged with H<sub>2</sub> for 10 minutes at 100 psig. All reactions were stirred at 1500 rpm.

##### A. Hydrogenation of $\alpha,\beta$ -unsaturated nitriles

An 8 mL vial containing a one-inch Teflon stir bar was charged with  $\alpha,\beta$ -unsaturated nitrile (0.25 mmol), and **1** (0.25 mL, 0.01 M,  $2.5 \times 10^{-3}$  mmol). The reaction mixture was diluted with toluene to a total volume of 2 mL, sealed with a PTFE septum lined cap, and pierced with a 27g needle. The reaction(s) were sealed in the Parr bomb reactor, removed from the glovebox, and placed in an aluminum heating block pre-heated to the corresponding reaction temperature. After purging the system with H<sub>2</sub>, the Parr bomb was charged with 100 psig H<sub>2</sub> and stirred at 1500 rpm. After 15 h, the reactor was cooled to ambient temperature and slowly vented to atmospheric pressure. After removing volatiles via rotary evaporation, the crude reactions were re-dissolved in CDCl<sub>3</sub> containing PhTMS as an internal standard. Product formation was assessed by <sup>1</sup>H NMR spectroscopy.

**Table S3. Hydrogenation of 2a using 1 (1 mol %) and H<sub>2</sub> (100 psi) in the presence of basic additives (10 mol %). <sup>a</sup>2 mol % 1, <sup>b</sup>The reaction was stopped after 1 h.**



Entry	Temp (°C)	Additive (10 mol%)	% conv. of 2a	5a	6a+6a'
1	30	None	7	7	0
2	30	KO <sup>t</sup> Bu	100	70	30
3	30	Cs <sub>2</sub> CO <sub>3</sub>	4	4	0
4	30	octNH <sub>2</sub>	99	99	0
5	70	None	99	51	44
6	70	Li <sub>2</sub> CO <sub>3</sub>	68	68	0
7	70	Na <sub>2</sub> CO <sub>3</sub>	44	44	0
8	70	K <sub>2</sub> CO <sub>3</sub>	43	43	0
9	80	None	99	0	99
10 <sup>a</sup>	100	DBU	93	93	0
11 <sup>b</sup>	110	None	55	55	0
12 <sup>b</sup>	110	KO <sup>t</sup> Bu	99	0	99
13 <sup>b</sup>	110	Cs <sub>2</sub> CO <sub>3</sub>	61	61	0



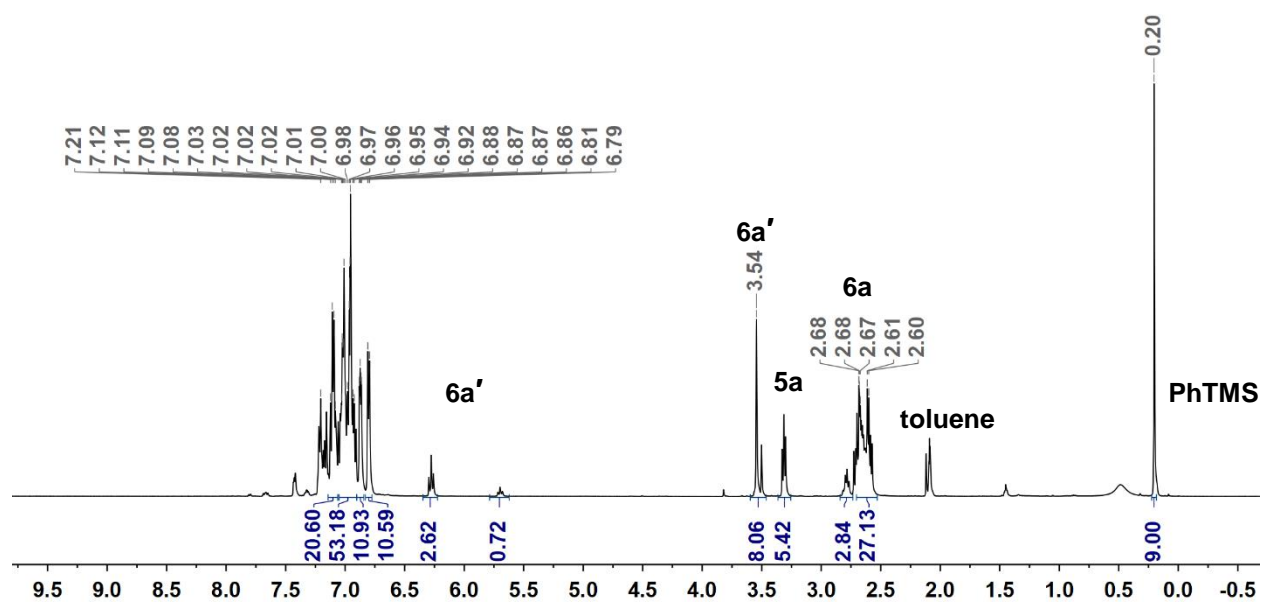
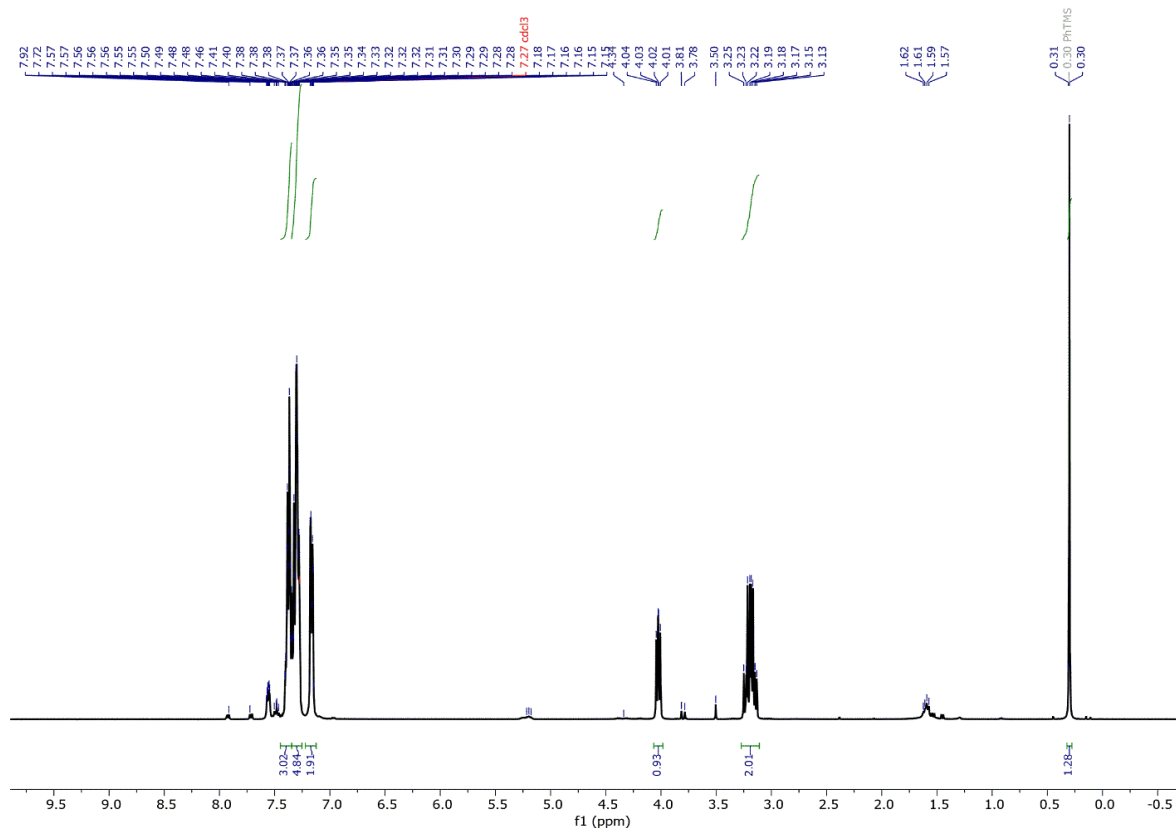


Figure S37.  $^1\text{H}$  NMR spectrum of the reaction mixture containing 5a, 6a, and 6a' resulting from the hydrogenation of 2a at 70 °C with 1 (1 mol %), and  $\text{H}_2$  (100 psig) (Table S3, entry 5)



**Figure S38.**  $^1\text{H}$  NMR spectrum showing only the formation of **5a** resulting from the hydrogenation of **2a** with DBU (10 mol %), **1** (2 mol %), and  $\text{H}_2$  (entry 10, Table S3)

### B. Hydrogenative acylation of $\alpha,\beta$ -unsaturated nitriles

An 8 mL vial containing a one-inch Teflon stir bar was charged with alkenyl nitrile (0.18-0.25 mmol), **1** (0.50 mL, 0.01 M,  $5.0 \times 10^{-3}$  mmol), DBU (3.7  $\mu\text{L}$ , 0.025 mmol) and anhydride (1.0 mmol). The reaction mixture was diluted with toluene to a total of 2 mL, sealed with a septum lined cap, and pierced with a 27g needle. The reaction(s) were sealed in the Parr bomb reactor, removed from the glovebox, and placed in an aluminum heating block pre-heated to the corresponding reaction temperature. After purging the system with  $\text{H}_2$ , the Parr bomb was charged with 100 psig  $\text{H}_2$  and stirred at 1500 rpm. After 15 h, the reactor was cooled to ambient temperature and slowly vented to atmospheric pressure. After removing volatiles via rotary evaporation, the crude reactions were redissolved in  $\text{CDCl}_3$  containing PhTMS as an internal standard. Product formation was assessed by  $^1\text{H}$  and  $^{13}\text{C}$  NMR spectroscopy. Reactions mixtures were purified by column chromatography. Column conditions: 0% to 5% ethyl acetate/hexanes over 20 column volumes, 10g  $\text{SiO}_2$ , flow rate: 25 ml/min.

### C. Hydrogenative acylation of $\alpha,\beta$ -unsaturated nitriles at reduced temperature and pressure.

To gain insight into the progress of product formation we monitored the reaction by  $^1\text{H}$  NMR spectroscopy under reduced temperatures and pressures. The reaction was performed with the standard quantities of reactants as describe in section IV, but at 50 psig  $\text{H}_2$  and 50 °C in a sealed J-Young NMR tube for 15 hours. These conditions afforded a different selectivity outcome (**4a** vs **5a**; see the table below). The acquired in situ NMR spectra indicated that the saturated nitrile **5a** is favored in comparison with the acylated product, **4a**. However, the appearance of **4a** did not track with the disappearance of **5a**. Moreover, once formed, **5a** did not convert to any another species.

**Table S4. Formation of 4a versus 5a with DBU (10 mol%), 1 (2 mol%), and  $\text{H}_2$  (50 psig), at 50 °C monitored by  $^1\text{H}$  NMR spectroscopy**

Time (hrs)	% <b>4a</b>	% <b>5a</b>
0	2.1	2
1	3.85	3.7
5	6.4	9.7
15	6.4	47.6

### V. Isolation and characterization of *tert*-butyl 2-cyano-2,3-diphenylpropanoate derivatives **4a-4k**

**tert-butyl 2-cyano-2,3-diphenylpropanoate (4a).** 0.25 mmol **2a**, 1.0 mmol  $\text{Boc}_2\text{O}$ . Column conditions: 0% to 5% ethyl acetate/hexanes over 20 column volumes, 10g  $\text{SiO}_2$ , flow rate: 25 ml/min. 52 mg, 95% yield.  $^1\text{H}$  NMR (500 MHz,  $\text{CDCl}_3$ )  $\delta$  7.66 (s, 4H), 7.31 – 7.20 (m, 4H), 7.16 (m, 2H), 3.67 (d,  $^2J_{\text{HH}} = 13.7$  Hz, 1H), 3.27 (d,  $^2J_{\text{HH}} = 13.6$  Hz, 1H), 1.40 (s, 9H).  $^{13}\text{C}$  NMR (126 MHz,  $\text{CDCl}_3$ )  $\delta$  165.44, 138.61, 133.66, 130.33, 128.35, 127.86, 126.84, 125.95, 125.92, 117.73, 85.19, 56.24, 44.06, 27.54. ESI-MS for  $\text{C}_{20}\text{H}_{21}\text{NO}_2$  [ $\text{M}+\text{Na}$ ]: Calc 330.1470; Found 330.1836.

**tert-butyl 2-cyano-3-(4-methoxyphenyl)-2-phenylpropanoate (4b).** 0.22 mmol **2b**, 1.0 mmol  $\text{Boc}_2\text{O}$ . Column conditions: 0% to 5% ethyl acetate/hexanes over 20 column volumes, 10g  $\text{SiO}_2$ , flow rate: 25 ml/min., 29 mg, 83 % yield.  $^1\text{H}$  NMR (500 MHz,  $\text{CDCl}_3$ )  $\delta$  7.55 – 7.47 (m, 3H),

7.42 – 7.34 (m, 3H), 7.27 (d,  $^3J_{\text{HH}} = 8.6$  Hz, 1H), 7.09 (d,  $^3J_{\text{HH}} = 8.7$  Hz, 2H), 6.78 (d,  $^3J_{\text{HH}} = 8.7$  Hz, 2H), 3.77 (s, 3H), 3.61 (d,  $^2J_{\text{HH}} = 13.7$  Hz, 1H), 3.21 (d,  $^2J_{\text{HH}} = 13.7$  Hz, 1H), 1.39 (s, 9H).  $^{13}\text{C}$  NMR (126 MHz,  $\text{CDCl}_3$ )  $\delta$  166.11, 159.03, 134.87, 131.48, 130.78, 128.92, 128.65, 126.21, 118.44, 113.57, 84.41, 56.62, 55.15, 43.19, 27.57. ESI-MS for  $\text{C}_{21}\text{H}_{23}\text{NO}_3$  [M+Na]: Calc 360.1578; Found 359.1578.

**tert-butyl-2-cyano-2-phenyl-3-(4-(trifluoromethyl)phenyl)propanoate (4c).** 0.18 mmol **2c**, 1 mmol  $\text{Boc}_2\text{O}$ . Column conditions: 0% to 5% ethyl acetate/hexanes over 20 column volumes, 10g  $\text{SiO}_2$ , flow rate: 25 ml/min. 42 mg, 74 % yield.  $^1\text{H}$  NMR (500 MHz,  $\text{CDCl}_3$ )  $\delta$  7.50 (d,  $^3J_{\text{HH}} = 9.2$  Hz, 4H), 7.40 (d,  $^3J_{\text{HH}} = 7.4$  Hz, 3H), 7.27 (d,  $^3J_{\text{HH}} = 7.4$  Hz, 2H), 3.69 (d,  $^2J_{\text{HH}} = 13.6$  Hz, 1H), 3.32 (d,  $^2J_{\text{HH}} = 13.6$  Hz, 1H), 1.39 (s, 9H).  $^{13}\text{C}$  NMR (126 MHz,  $\text{CDCl}_3$ )  $\delta$  165.72, 138.36, 134.31, 130.77, 130.28, 129.74, 129.11, 128.95, 126.07, 125.15, 125.12, 125.09, 125.06, 117.95, 113.95, 84.89, 55.90, 43.49, 27.53. ESI-MS for  $\text{C}_{21}\text{H}_{20}\text{F}_3\text{NO}_2$  [M+ H]: Calc 376.1524; Found 376.1309.

**tert-butyl-2-cyano-2-(4-methoxyphenyl)-3-phenylpropanoate (4d).** 0.22 mmol **2d**, 1 mmol  $\text{Boc}_2\text{O}$ . Column conditions: 0% to 5% ethyl acetate/hexanes over 20 column volumes, 10g  $\text{SiO}_2$ , flow rate: 25 ml/min. 24 mg, 78% yield.  $^1\text{H}$  NMR (500 MHz,  $\text{CDCl}_3$ )  $\delta$  7.44 (d,  $^3J_{\text{HH}} = 8.9$  Hz, 2H), 7.25 (s, 2H), 7.18 (d,  $^3J_{\text{HH}} = 9.5$  Hz, 2H), 6.90 (d,  $^3J_{\text{HH}} = 8.9$  Hz, 2H), 3.82 (s, 3H), 3.62 (d,  $^2J_{\text{HH}} = 13.6$  Hz, 1H), 3.24 (d,  $^2J_{\text{HH}} = 13.6$  Hz, 1H), 1.38 (s, 9H).  $^{13}\text{C}$  NMR (126 MHz,  $\text{CDCl}_3$ )  $\delta$  166.71, 160.11, 134.85, 130.81, 128.60, 127.90, 127.21, 118.95, 114.61, 84.77, 56.05, 55.73, 44.29, 32.00, 27.99, 23.06, 14.54. ESI-MS for  $\text{C}_{21}\text{H}_{23}\text{NO}_3$  [M+H]: Calc 338.1756; Found 338.1748.

**tert-butyl 2-cyano-3-phenyl-2-(4-(trifluoromethyl)phenyl)propanoate (4e).** 0.17 mmol **2e**, 1 mmol  $\text{Boc}_2\text{O}$ . Column conditions: 0% to 5% ethyl acetate/hexanes over 20 column volumes, 10g  $\text{SiO}_2$ , flow rate: 25 ml/min. 85 mg, 85% yield.  $^1\text{H}$  NMR (500 MHz,  $\text{CDCl}_3$ )  $\delta$  7.57 (s, 4H), 7.17 (s, 4H), 7.06 (d,  $^3J_{\text{HH}} = 5.0$  Hz, 2H), 3.58 (d,  $^2J_{\text{HH}} = 13.6$  Hz, 1H), 3.18 (d,  $^2J_{\text{HH}} = 13.7$  Hz, 1H), 1.31 (s, 9H).  $^{13}\text{C}$  NMR (126 MHz,  $\text{CDCl}_3$ )  $\delta$  165.44, 138.62, 133.79, 133.66, 130.32, 128.68, 128.49, 128.44, 128.35, 128.25, 127.86, 126.84, 125.95, 125.92, 117.73, 85.20, 56.24, 44.06, 27.54. ESI-MS for  $\text{C}_{20}\text{H}_{21}\text{F}_3\text{NO}_2$  [M+H]: Calc 376.1524; Found 376.1232.

**2-benzyl-3-oxo-3-phenylpropanenitrile (4f).** 0.25 mmol cinnamionitrile, 1 mmol benzyl anhydride. The reaction was done in mesitylene at 150 °C. Column conditions: 0% to 5% ethyl acetate/hexanes over 20 column volumes, 10g  $\text{SiO}_2$ , flow rate: 25 ml/min. 84% yield.  $^1\text{H}$  NMR

(500 MHz, CDCl<sub>3</sub>)  $\delta$  7.99-7.29 (m, 10H), 4.54 (dd,  $J$  = 8.8 Hz, 5.8 Hz, 1H), 3.42- 3.23 (m, 2H); <sup>13</sup>C NMR (126 MHz, CDCl<sub>3</sub>)  $\delta$  190.4, 136.4, 134.5, 129.5, 129.4, 129.3, 129.2, 128.0, 117.4, 88.5, 42.2, 35.9.

**2-benzoylbutanenitrile (4g).** 0.25 mmol 2-butenenitrile, 1 mmol benzyl anhydride. Column conditions: 0% to 5% ethyl acetate/hexanes over 20 column volumes, 10g SiO<sub>2</sub>, flow rate: 25 ml/min. 79% yield. <sup>1</sup>H NMR (500 MHz, CDCl<sub>3</sub>)  $\delta$  7.97 (d,  $J$  = 7.4 Hz, 2H), 7.66 (t,  $J$  = 7.4 Hz, 1H), 7.53 (t,  $J$  = 7.8 Hz, 2H), 4.30 (dd,  $J$  = 12.6, 5.6 Hz, 1H), 2.07 (ddd,  $J$  = 12.6, 7.5, 5.6 Hz, 2H), 1.17 (t,  $J$  = 7.5 Hz, 3H); <sup>13</sup>C NMR (126 MHz, CDCl<sub>3</sub>)  $\delta$  190.87, 134.60, 134.19, 129.26, 128.86, 117.36, 41.62, 23.70, 11.70.

**2-benzoyl-2-methylbutanenitrile (4h).** 0.25 mmol 2-methyl-2-butenenitrile, 1 mmol benzyl anhydride. Column conditions: 0% to 5% ethyl acetate/hexanes over 20 column volumes, 10g SiO<sub>2</sub>, flow rate: 25 ml/min. 81% yield. <sup>1</sup>H NMR (500 MHz, CDCl<sub>3</sub>)  $\delta$  7.97 (d,  $J$  = 7.4 Hz, 2H), 7.66 (t,  $J$  = 7.4 Hz, 1H), 7.53 (t,  $J$  = 7.8 Hz, 2H), 4.30 (dd,  $J$  = 12.6, 5.6 Hz, 1H), 2.07 (ddd,  $J$  = 12.6, 7.5, 5.6 Hz, 2H), 1.17 (t,  $J$  = 7.5 Hz, 3H); <sup>13</sup>C NMR (126 MHz, CDCl<sub>3</sub>)  $\delta$  190.87, 134.60, 134.19, 129.26, 128.86, 117.36, 41.62, 23.70, 11.70.

**2-benzyl-4,4,4-trifluoro-3-oxo-2-phenylbutanenitrile (4a').** 0.25 mmol **2a**, 1 mmol trifluoroacetic anhydride. Column conditions: 0% to 5% ethyl acetate/hexanes over 20 column volumes, 10g SiO<sub>2</sub>, flow rate: 25 ml/min. 93% yield. <sup>1</sup>H NMR (500 MHz, CDCl<sub>3</sub>)  $\delta$  7.66 (s, 4H), 7.31 – 7.20 (m, 4H), 7.16 (m, 2H), 3.67 (d, <sup>2</sup> $J_{\text{HH}}$  = 13.7 Hz, 1H), 3.27 (d, <sup>2</sup> $J_{\text{HH}}$  = 13.6 Hz, 1H). <sup>13</sup>C NMR (126 MHz, CDCl<sub>3</sub>)  $\delta$  165.44, 138.61, 133.66, 130.33, 128.35, 127.86, 126.84, 125.95, 125.92, 117.73, 85.19.

**2-benzyl-3-oxo-2,3-diphenylpropanenitrile (4a'').** 0.25 mmol **2a**, 1 mmol benzyl anhydride. Column conditions: 0% to 5% ethyl acetate/hexanes over 20 column volumes, 10g SiO<sub>2</sub>, flow rate: 25 ml/min. 92% yield. <sup>1</sup>H NMR (500 MHz, CDCl<sub>3</sub>)  $\delta$  7.66 (s, 4H), 7.31 – 7.20 (m, 4H), 7.16 (m, 2H), 3.67 (d, <sup>2</sup> $J_{\text{HH}}$  = 13.7 Hz, 1H), 3.27 (d, <sup>2</sup> $J_{\text{HH}}$  = 13.6 Hz, 1H). <sup>13</sup>C NMR (126 MHz, CDCl<sub>3</sub>)  $\delta$  165.44, 138.61, 133.66, 130.33, 128.35, 127.86, 126.84, 125.95, 125.92, 117.73, 85.19.

**2-benzyl-3-oxo-2-phenylbutanenitrile (4a''').** 0.25 mmol **2a**, 1 mmol acetic anhydride. Column conditions: 0% to 5% ethyl acetate/hexanes over 20 column volumes, 10g SiO<sub>2</sub>, flow rate: 25 ml/min. 89% yield. <sup>1</sup>H NMR (500 MHz, CDCl<sub>3</sub>)  $\delta$  7.66 (s, 4H), 7.31 – 7.20 (m, 4H), 7.16 (m, 2H), 3.67 (d, <sup>2</sup> $J_{\text{HH}}$  = 13.7 Hz, 1H), 3.27 (d, <sup>2</sup> $J_{\text{HH}}$  = 13.6 Hz, 1H), 1.40

(s, 9H).  $^{13}\text{C}$  NMR (126 MHz,  $\text{CDCl}_3$ )  $\delta$  165.44, 138.61, 133.66, 130.33, 128.35, 127.86, 126.84, 125.95, 125.92, 117.73, 85.19, 56.24, 44.06, 27.54.

### $^1\text{H}$ and $^{13}\text{C}$ NMR spectra of 4a-4h

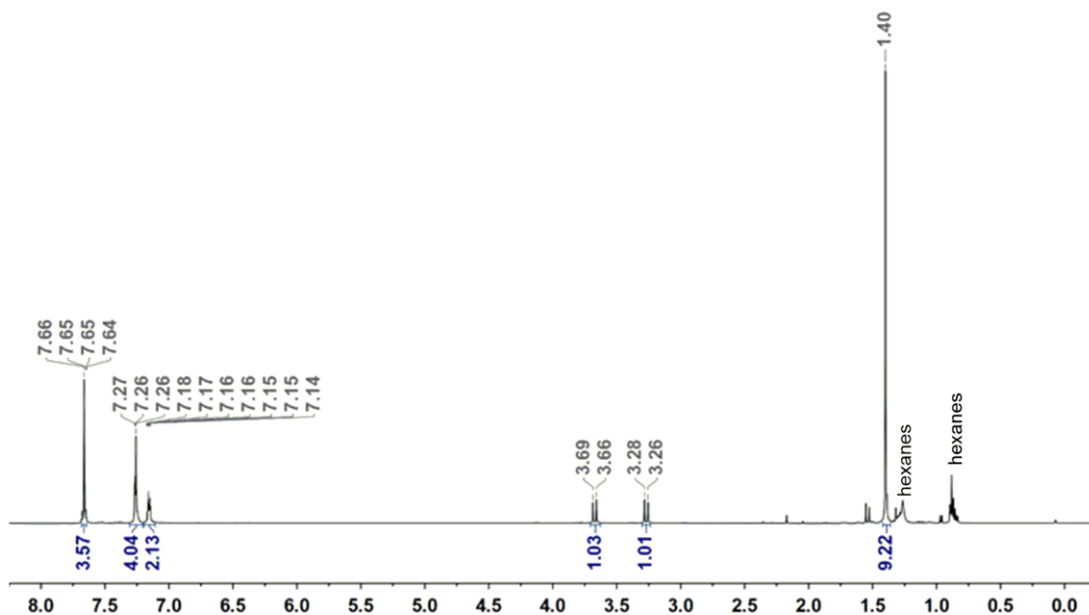


Figure S39.  $^1\text{H}$  NMR spectrum of 4a in  $\text{CDCl}_3$

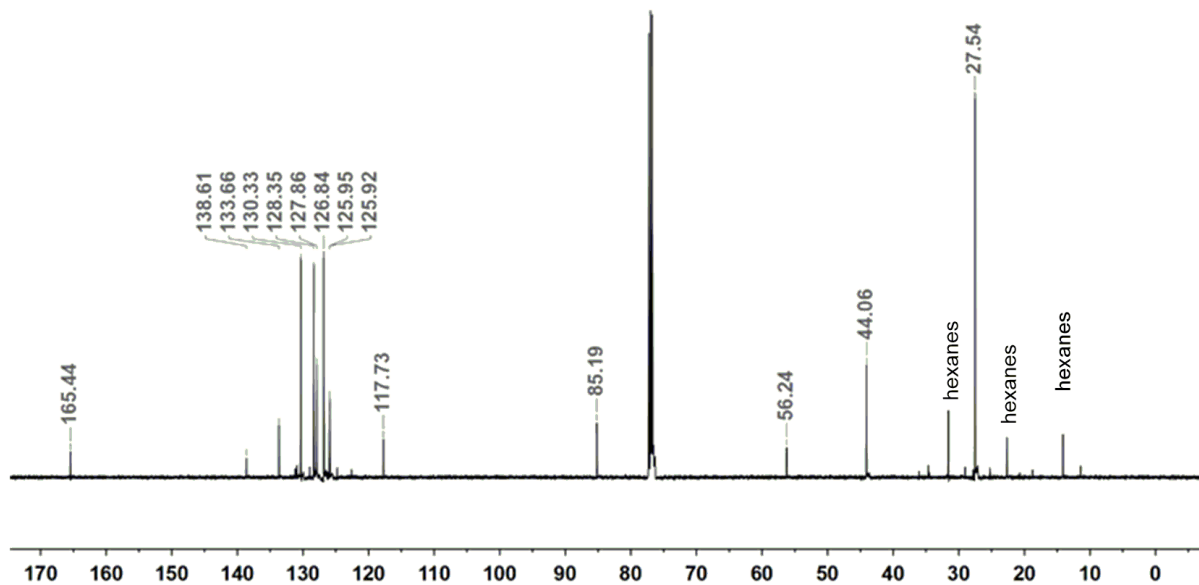


Figure S40.  $^{13}\text{C}$  NMR spectrum of 4a  $\text{CDCl}_3$

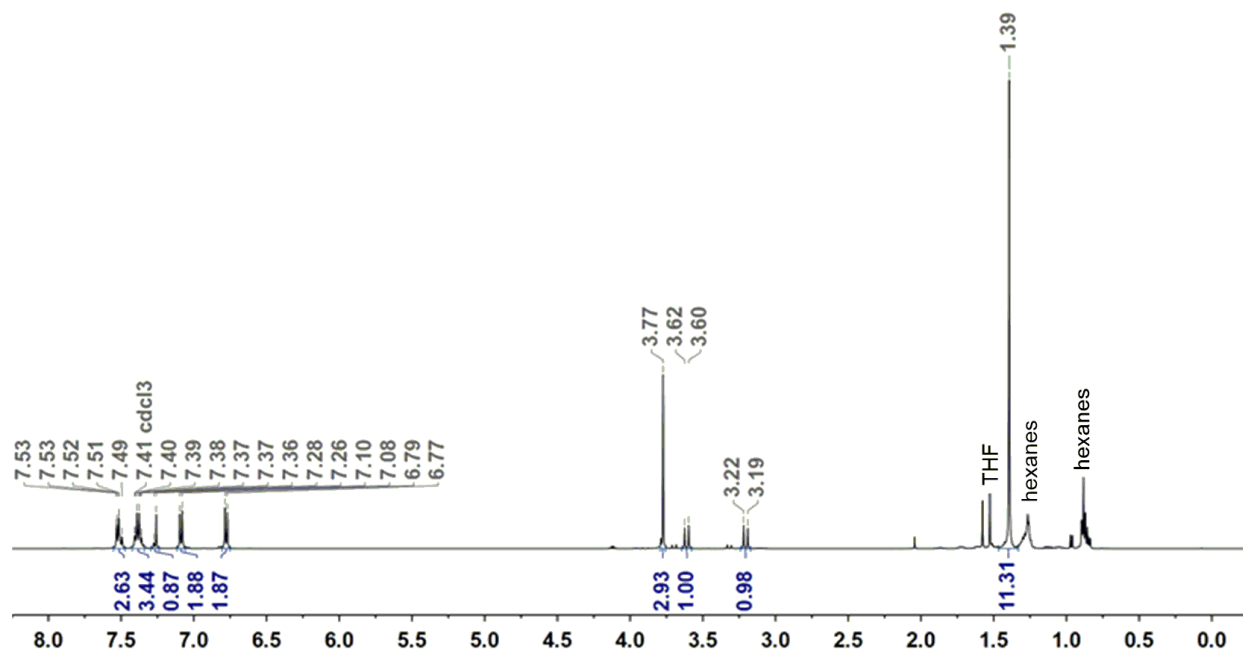


Figure S41.  $^1\text{H}$  NMR spectrum of 4b in  $\text{CDCl}_3$

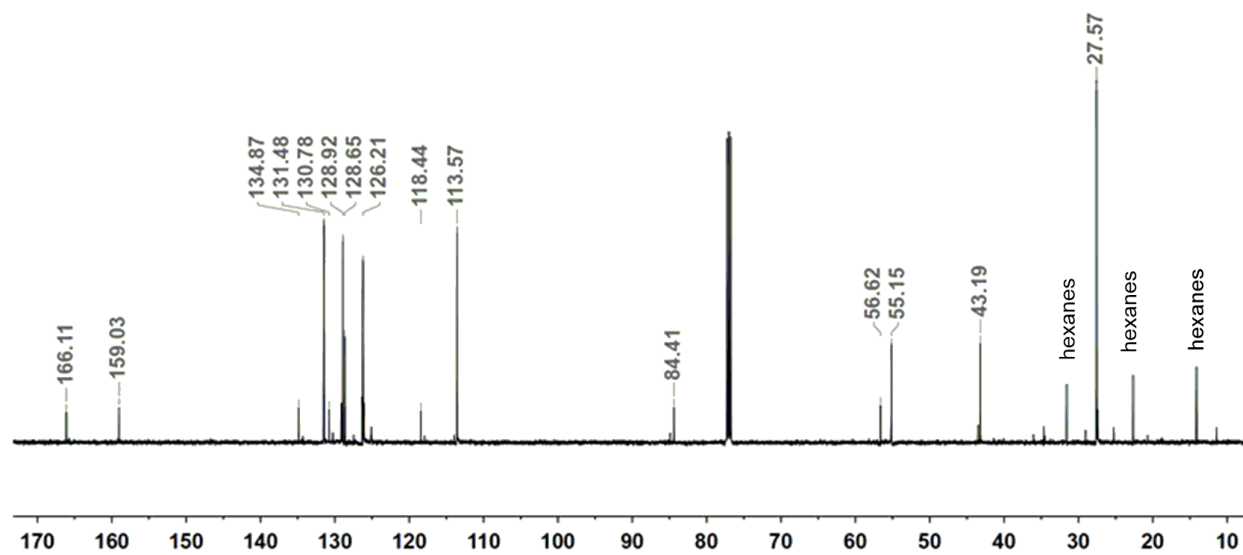


Figure S42.  $^{13}\text{C}$  NMR spectrum of 4b in  $\text{CDCl}_3$

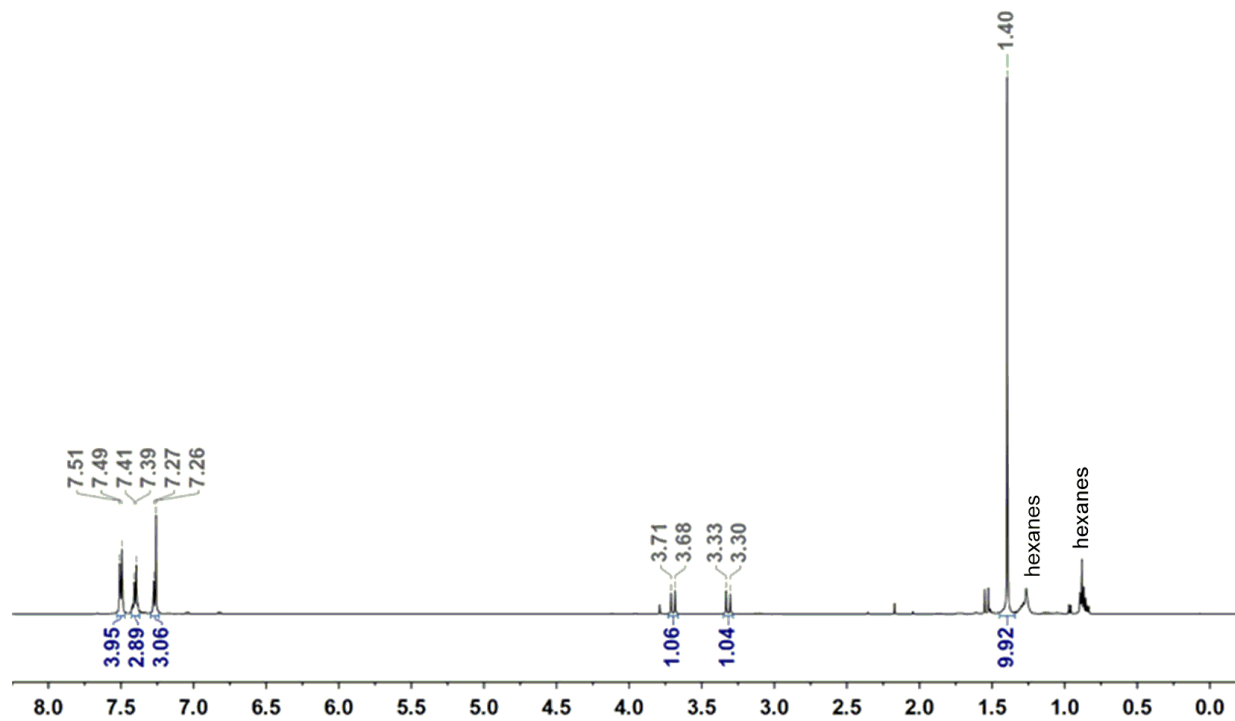


Figure S43.  $^1\text{H}$  NMR spectrum of 4c in  $\text{CDCl}_3$

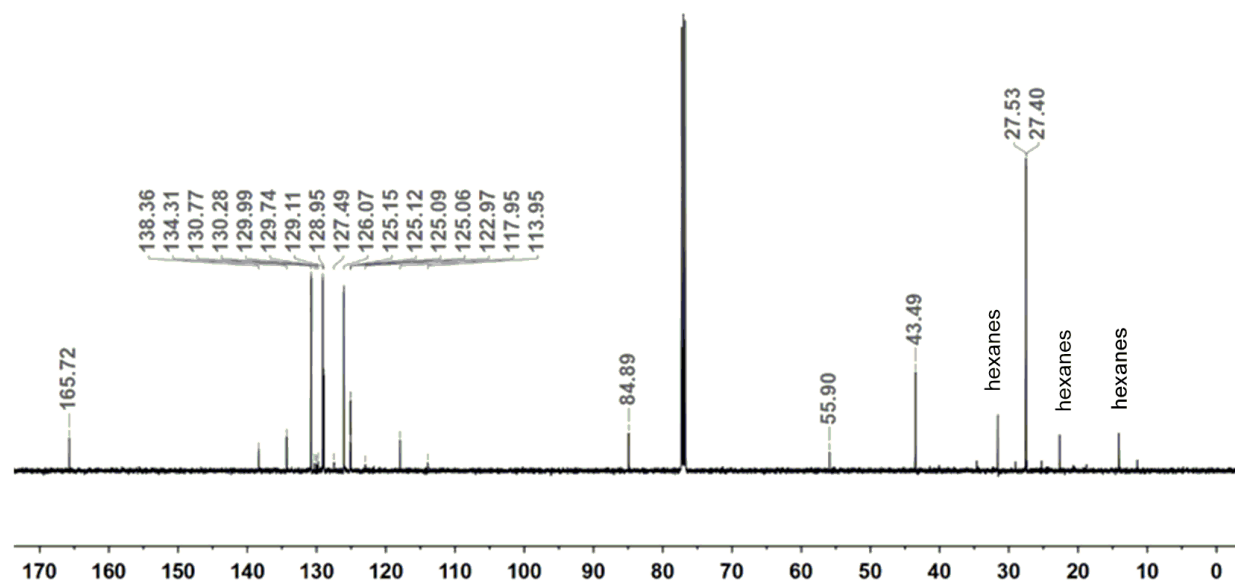


Figure S44.  $^{13}\text{C}$  NMR spectrum of 4c in  $\text{CDCl}_3$



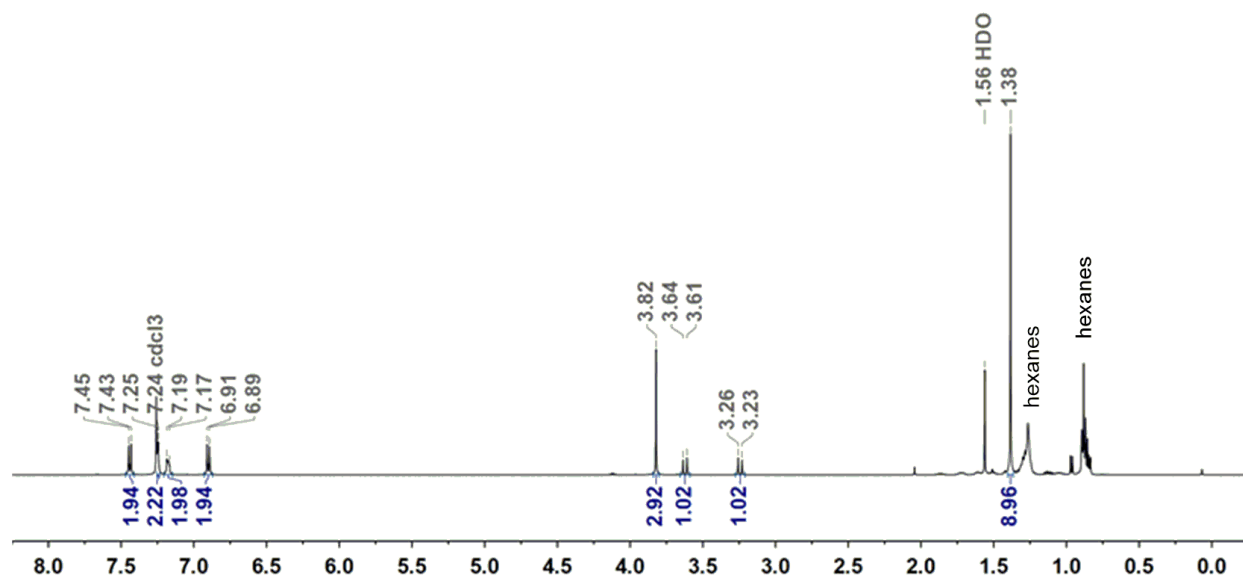


Figure S45.  $^1\text{H}$  NMR spectrum of 4d in  $\text{CDCl}_3$

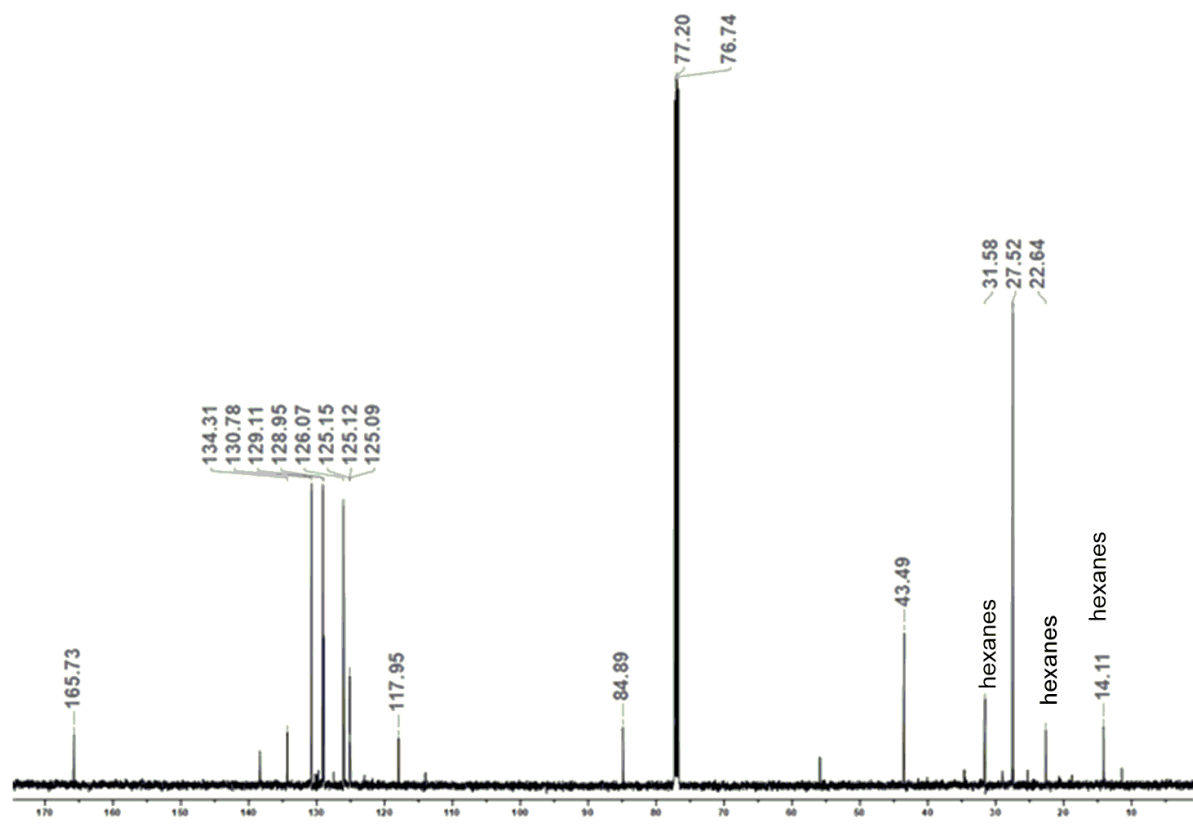


Figure S46.  $^{13}\text{C}$  NMR spectrum of 4d in  $\text{CDCl}_3$

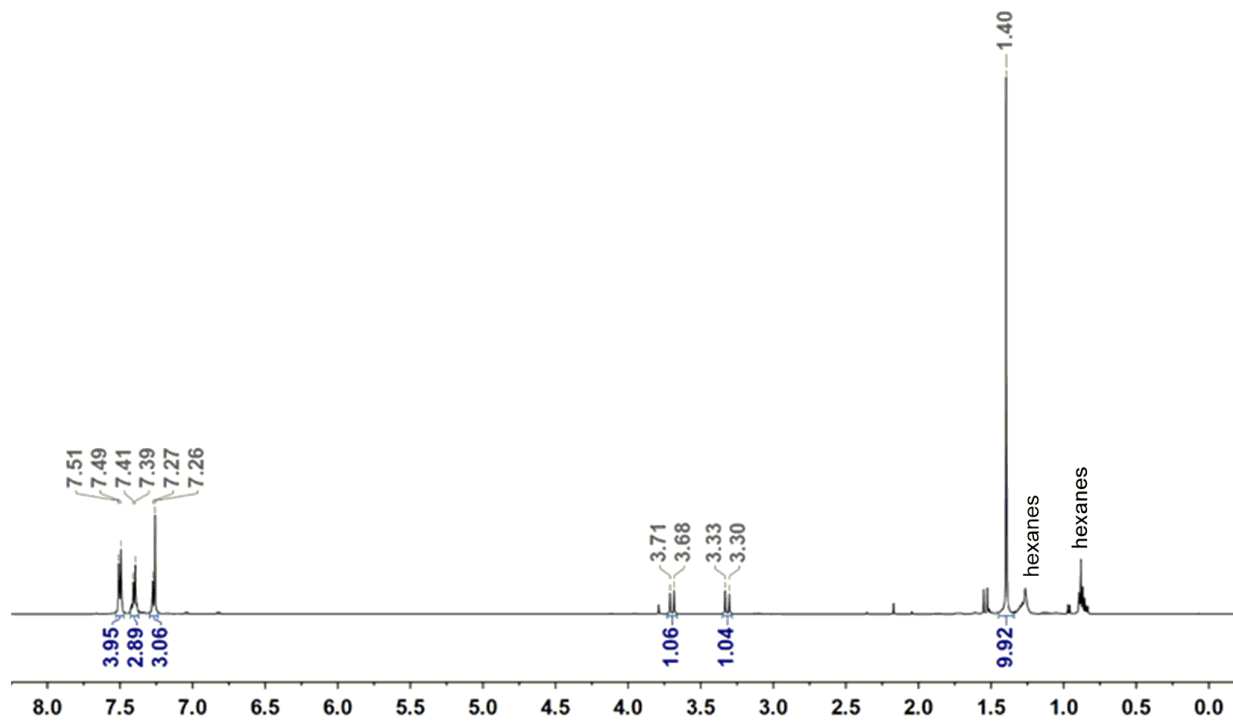


Figure S47.  $^1\text{H}$  NMR spectrum of 4e in  $\text{CDCl}_3$

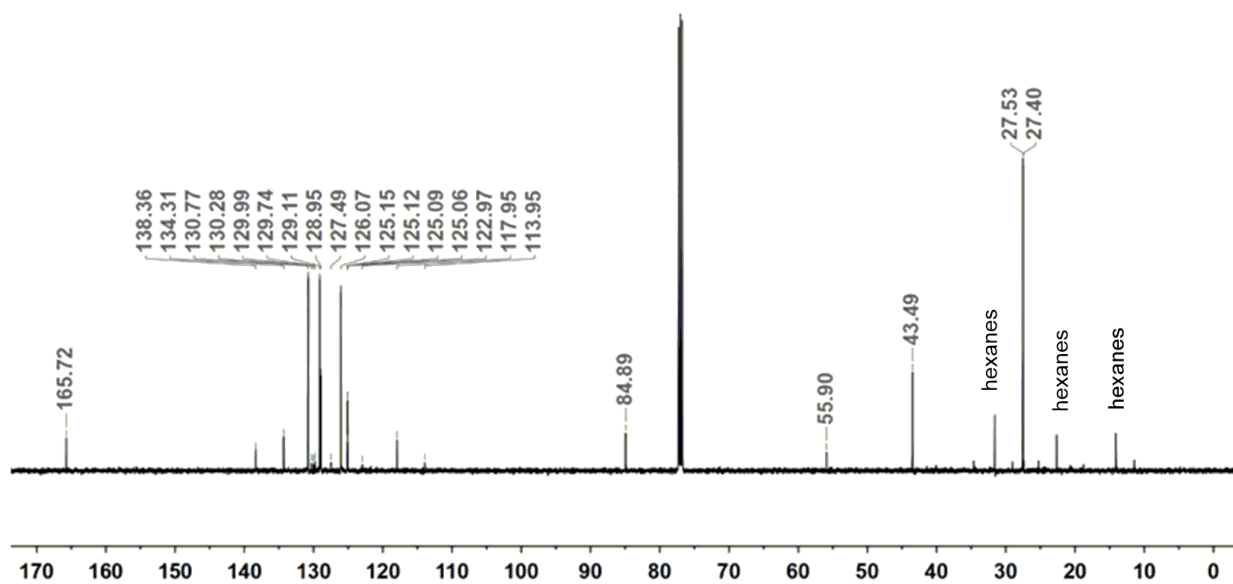
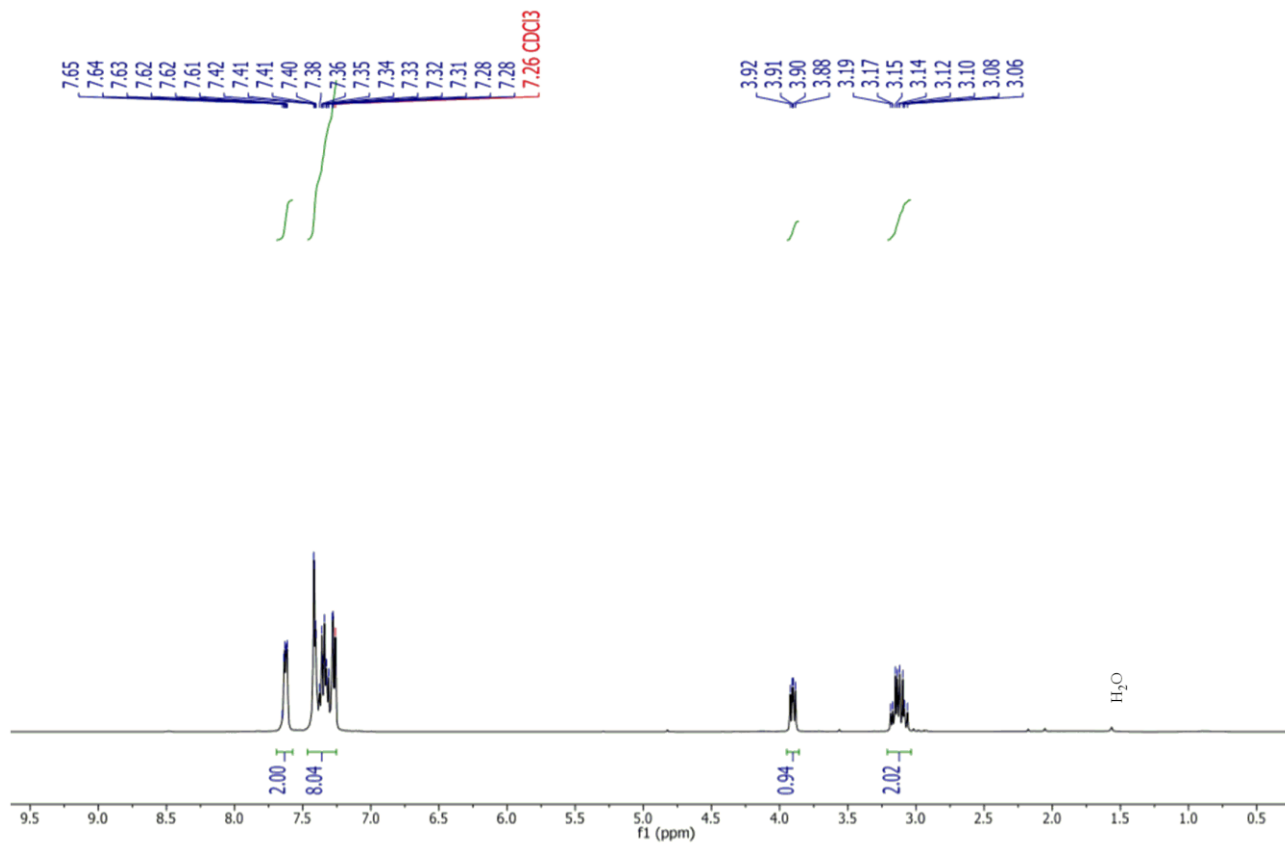


Figure S48.  $^{13}\text{C}$  NMR spectrum of 4e in  $\text{CDCl}_3$



**Figure S49.** <sup>1</sup>H NMR spectrum of 4f in CDCl<sub>3</sub>

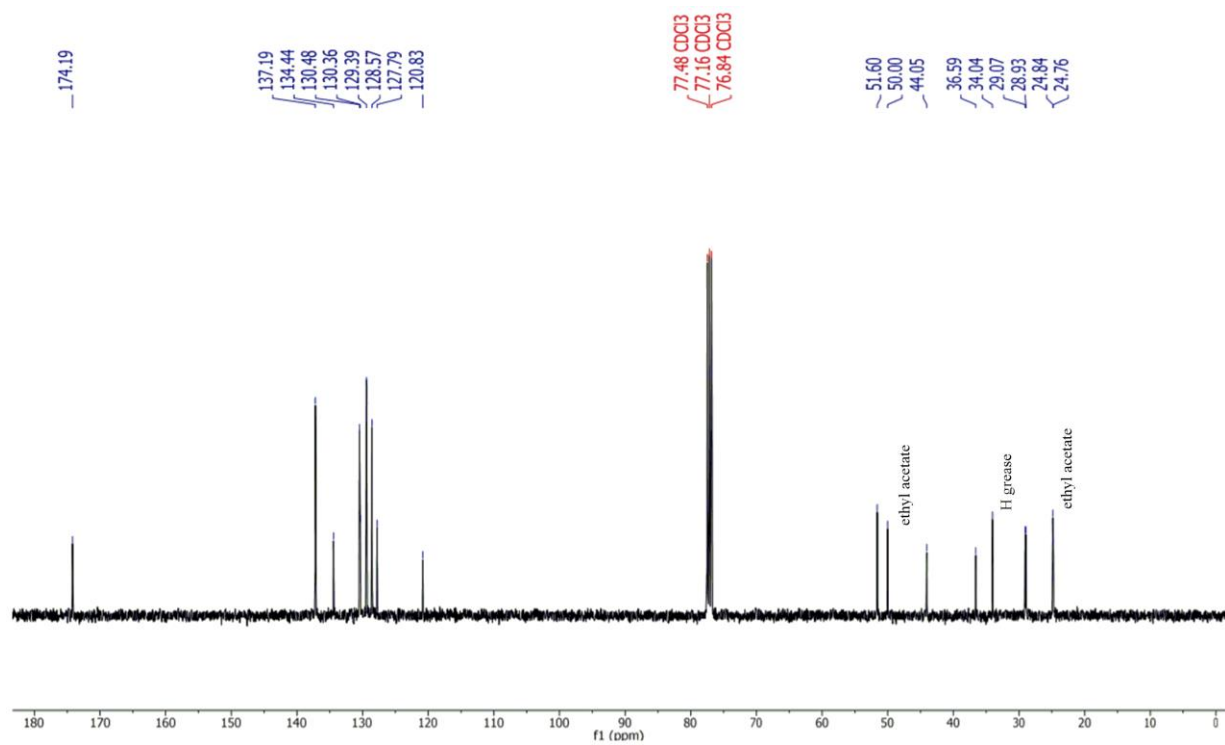


Figure S50.  $^{13}\text{C}$  NMR spectrum of 4f in  $\text{CDCl}_3$

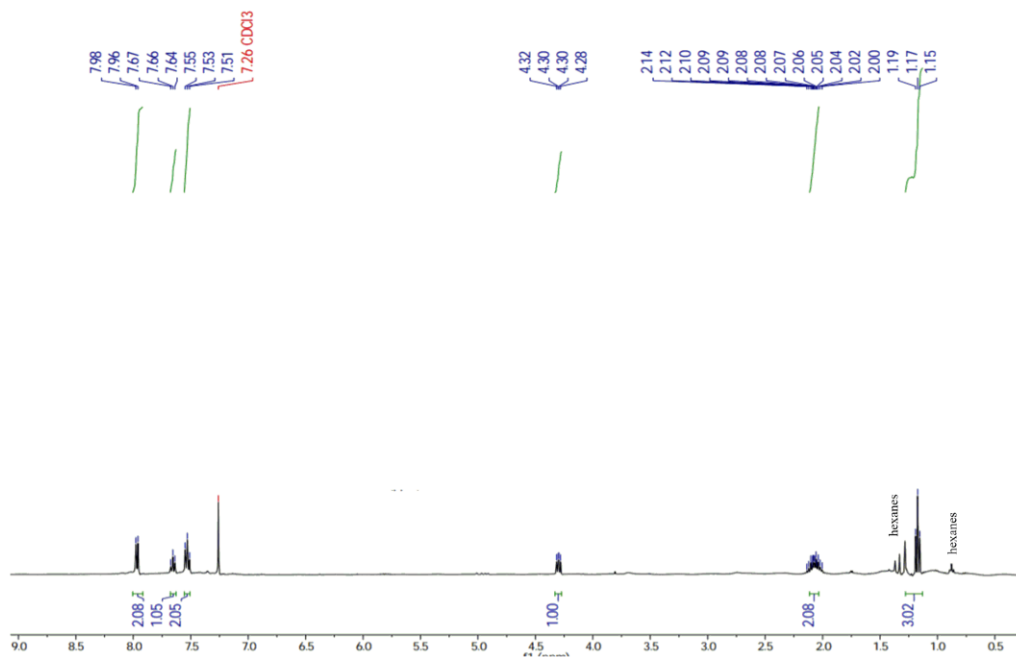


Figure S51:  $^1\text{H}$  NMR spectrum of 4g in  $\text{CDCl}_3$

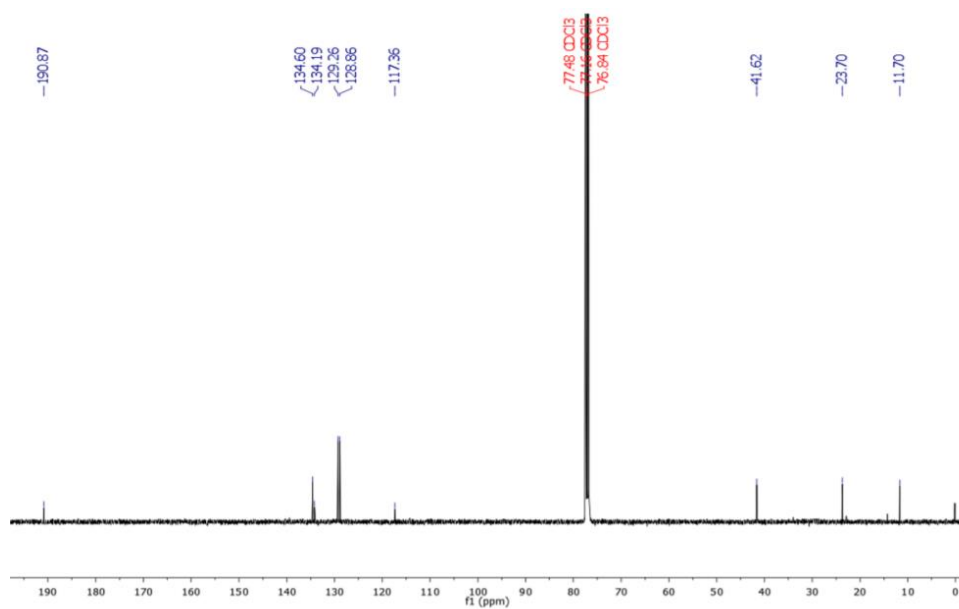


Figure S52: <sup>13</sup>C NMR spectrum of 4g in CDCl<sub>3</sub>

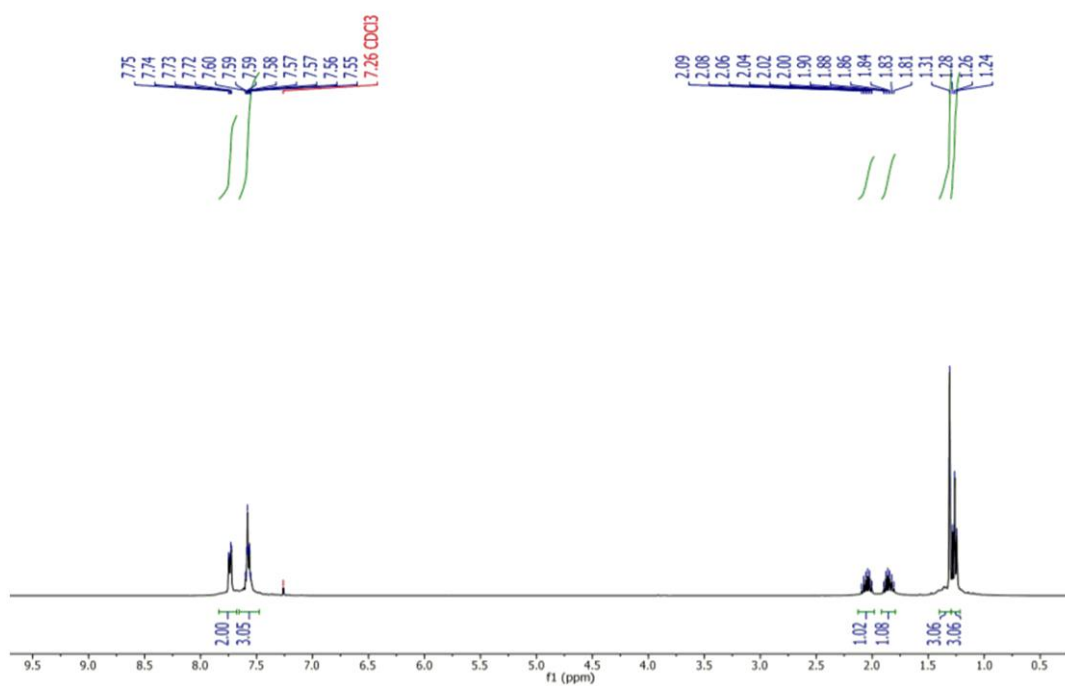
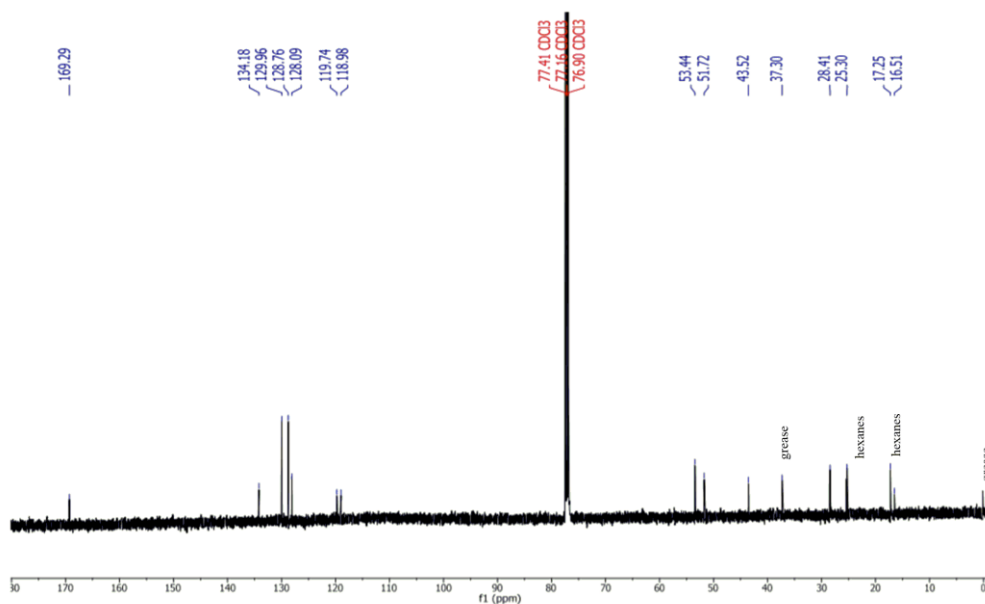


Figure S53: <sup>1</sup>H NMR spectrum of 4h in CDCl<sub>3</sub>



**Figure S54:**  $^{13}\text{C}$  NMR spectrum of **4h** in  $\text{CDCl}_3$

## VI. Control Reactions for hydrogenative acylation of $\alpha,\beta$ -unsaturated nitriles

### Reactivity of 2,3-diphenylpropanenitrile under hydrogenative acylation conditions

An 8 mL vial containing a one-inch Teflon stir bar was charged with 2,3-diphenylpropanenitrile (0.25 mmol), DBU (0.025 mmol),  $\text{Boc}_2\text{O}$  (1 mmol), and **1** ( $5 \times 10^{-3}$  mmol). The reaction mixture was diluted with toluene- $d_8$  to 2 mL and an  $^1\text{H}$  NMR spectrum was obtained. This sample was taken into a glovebox and transferred to an 8 mL vial, sealed with a septum lined cap, and pierced with a 27g needle. The reaction was sealed in a Parr bomb reactor, removed from the glovebox, and placed in an aluminum heating block pre-heated to  $100^\circ\text{C}$ . After purging the system with  $\text{H}_2$ , the Parr bomb was charged with 100 psig  $\text{H}_2$  and stirred at 1500 rpm. After 15 hours, the reactor was cooled to ambient temperature and slowly vented to atmospheric pressure. Product formation was assessed by  $^1\text{H}$  NMR spectroscopy. The  $^1\text{H}$  NMR spectrum obtained after 15 hours shows only 2,3-diphenylpropanenitrile and decomposition products of  $\text{Boc}_2\text{O}$  (tert-butyl alcohol). There was no trace of **4a**.

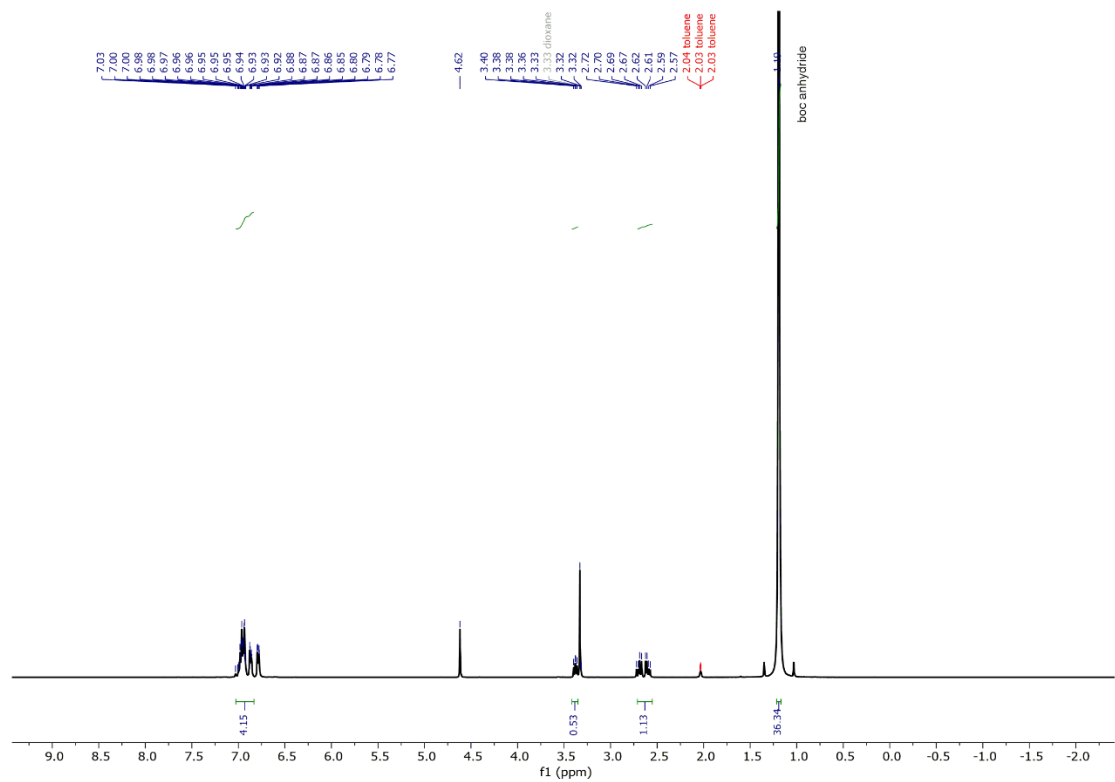


**Figure S55. Initial  $^1\text{H}$  NMR spectrum of 2,3-diphenylpropanenitrile under hydrogenative acylation conditions**

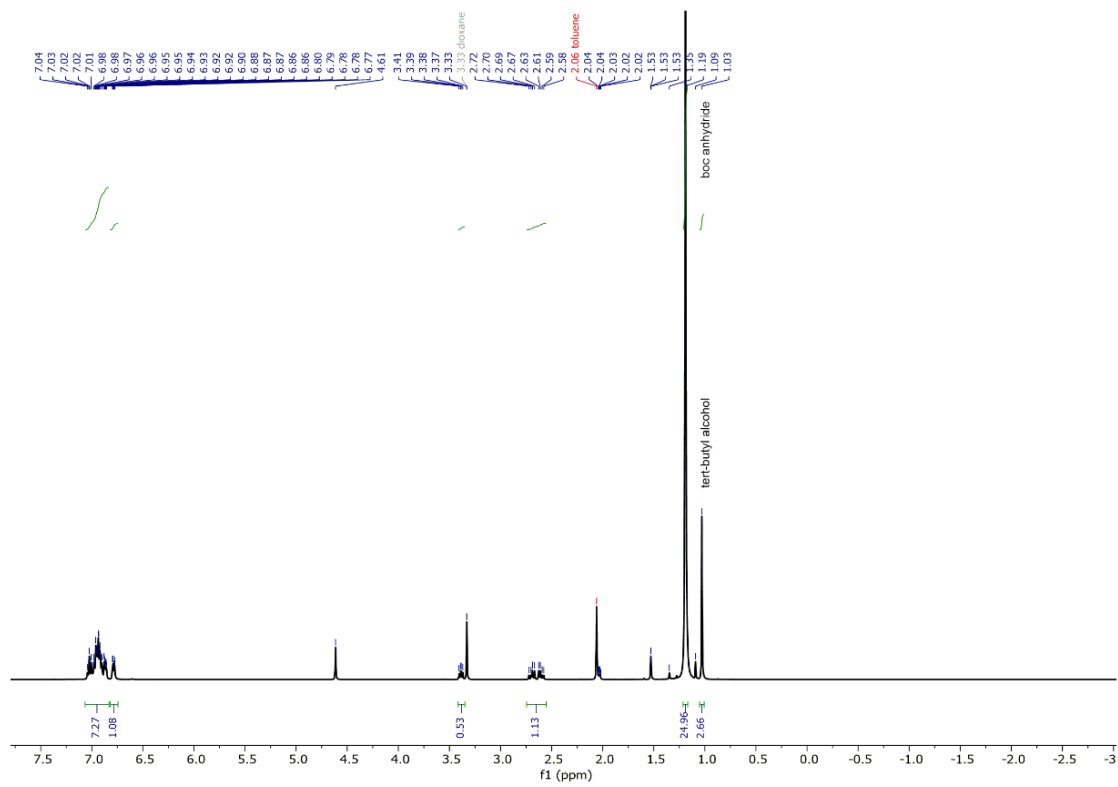
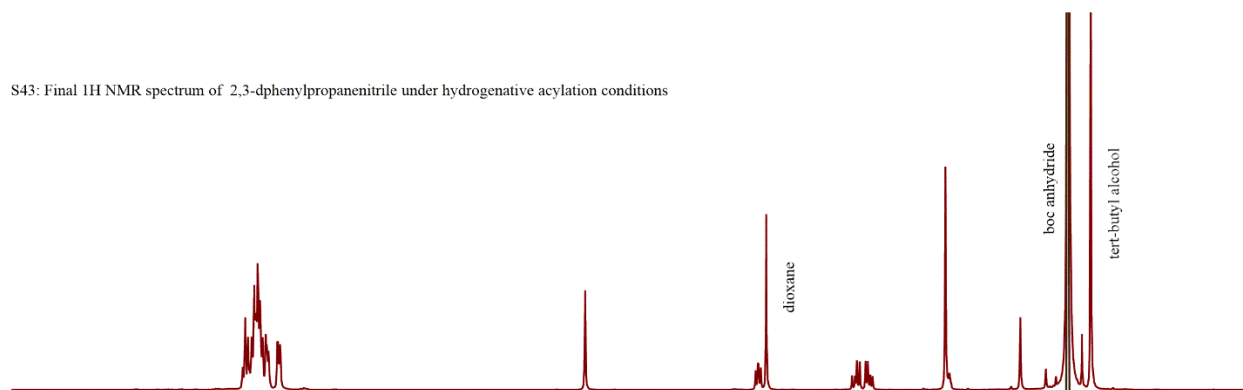


**Figure S56: Final  $^1\text{H}$  NMR spectrum of 2,3-diphenylpropanenitrile under hydrogenative acylation conditions**



S43: Final  $^1\text{H}$  NMR spectrum of 2,3-diphenylpropanenitrile under hydrogenative acylation conditions



S43: Initial  $^1\text{H}$  NMR spectrum of 2,3-diphenylpropanenitrile under hydrogenative acylation conditions

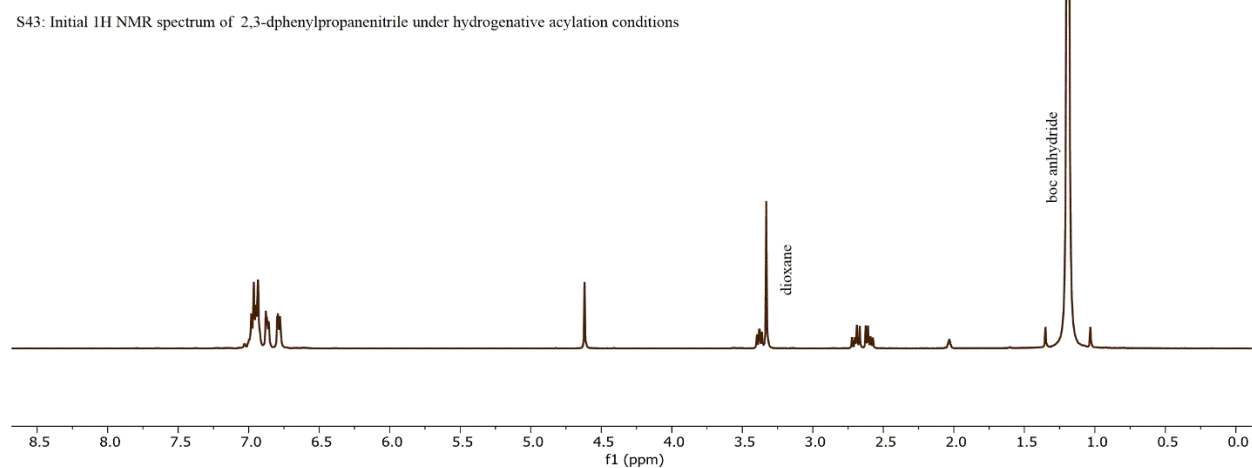


**Figure S57: Stacked  $^1\text{H}$  NMR spectra of initial and final timepoints for the reaction of 2,3-diphenylpropanenitrile under hydrogenative acylation conditions with 1.**

#### **Stoichiometric reactivity of 3a with $\text{Boc}_2\text{O}$ and DBU**

An 8 mL vial was charged **3a** (0.25 mmol), DBU (0.025 mmol),  $\text{Boc}_2\text{O}$  (1 mmol) and toluene- $d_8$  (0.60 mL). The solution was transferred to an NMR tube equipped with a Teflon cap, sealed, and placed in an aluminum block pre-heated to 100 °C. After 15 hours, the reaction was cooled to room temperature, PhTMS was added as an internal standard and product formation was assessed by  $^1\text{H}$  spectroscopy without further purification. The  $^1\text{H}$  NMR spectrum (Figure S51) shows **4a** formed in 95% NMR yield based on **3a** as the limiting reagent.

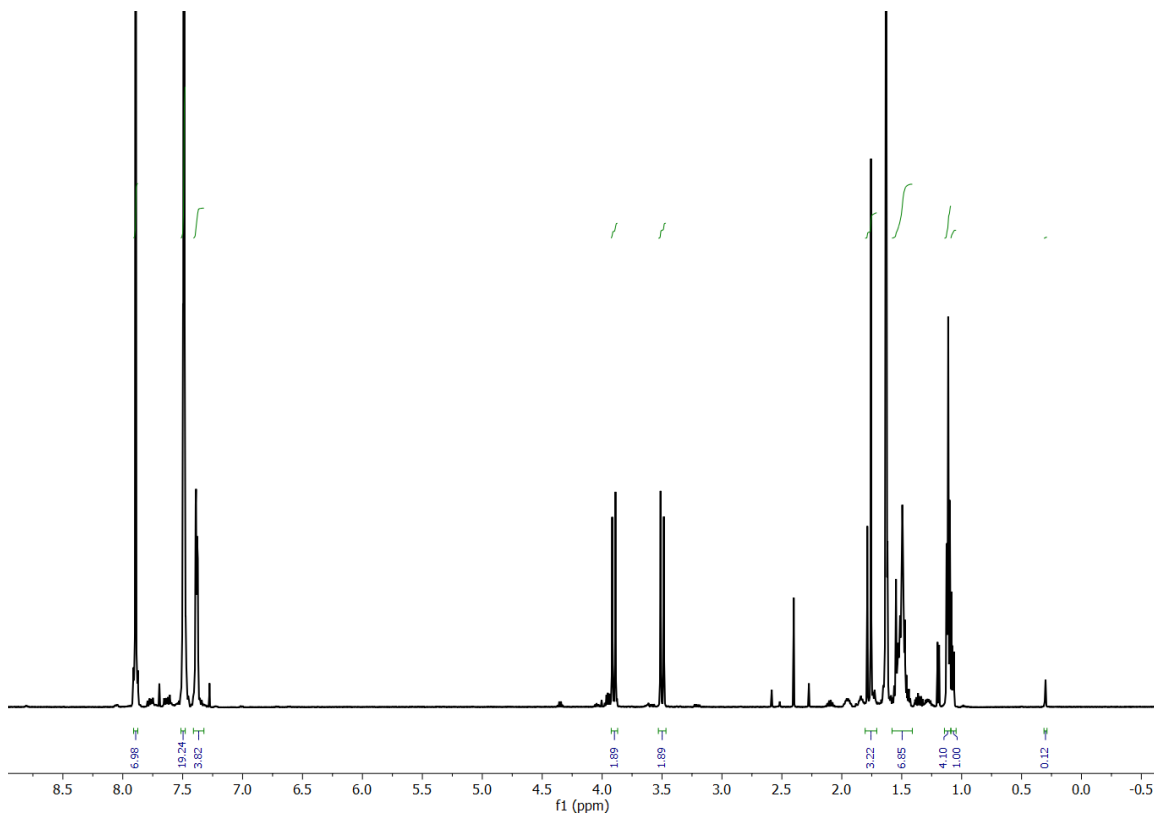


**Figure S58.**  $^1\text{H}$  NMR spectrum obtained from the stoichiometric reaction of **3a** with  $\text{Boc}_2\text{O}$  and DBU showing 95% conversion to **4a**

**Catalytic competence of 3a.** The reaction was set up according to procedure III with the modification that **3a** was used in place of **1**. An 8 mL vial containing a one-inch Teflon stir bar was charged with **2a** (0.25 mmol), **3a** ( $5.0 \times 10^{-3}$  mmol), DBU (0.025 mmol) and  $\text{Boc}_2\text{O}$  (1 mmol). The reaction mixture was diluted with toluene to a total of 2 mL, sealed with a septum lined cap, and pierced with a 27g needle. The reaction was sealed in the Parr bomb reactor, removed from the glovebox, and placed in an aluminum block pre-heated to  $100^\circ\text{C}$ . After purging the system with  $\text{H}_2$ , the Parr bomb was charged with 100 psig  $\text{H}_2$  and stirred at 1500 rpm. After 15 hours, the reactor was cooled to ambient temperature and slowly vented to atmospheric pressure. After removing volatiles via rotary evaporation, the crude reaction was re-dissolved in  $\text{CDCl}_3$  containing PhTMS as an internal standard. Product formation was assessed by  $^1\text{H}$  NMR spectroscopy. After 15 hours, the reaction with **3a** gave **4a** in 96% yield, compared to a 97% yield under identical reactions conditions with **1** as the catalyst.

### Reactivity of 2,3-diphenylpropanenitrile with Boc<sub>2</sub>O in the presence of 10% DBU

An 8 mL vial containing a one-inch Teflon stir bar was charged with 2,3-diphenylpropanenitrile (0.25 mmol), DBU (0.025 mmol), and Boc<sub>2</sub>O (1 mmol) in 2mL toluene-d<sub>8</sub>. The vial was heated to 100°C in a preheated aluminum block. After 15 hours, the reaction was cooled and product formation was assessed by <sup>1</sup>H NMR spectroscopy. The <sup>1</sup>H NMR spectrum obtained after 15 hours shows only 2,3-diphenylpropanenitrile and decomposition products of Boc<sub>2</sub>O (tert-butyl alcohol). There was no trace of **4a**.

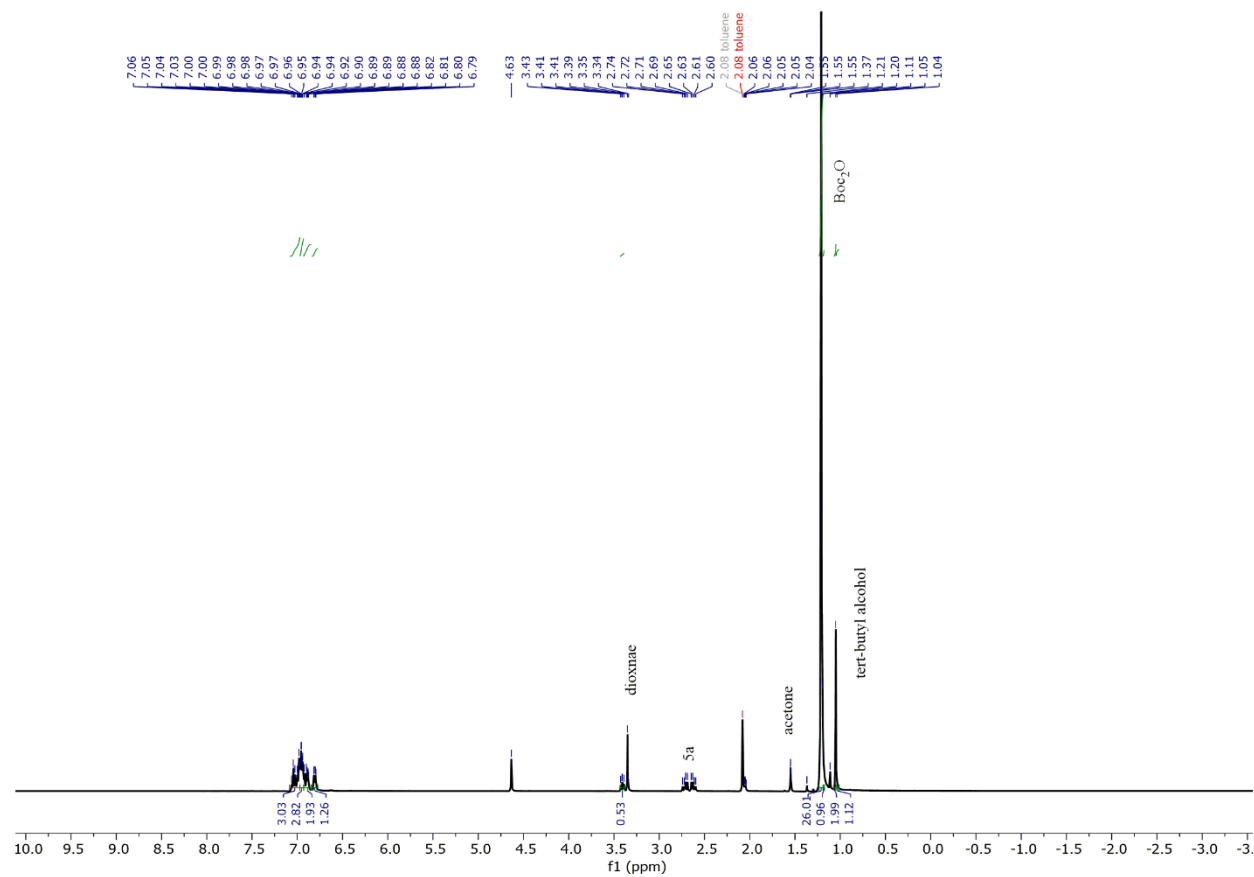


Figure S59. <sup>1</sup>H NMR spectrum of 2,3-diphenylpropanenitrile with Boc<sub>2</sub>O and 10% DBU

## VII. Proposed Catalytic Cycle

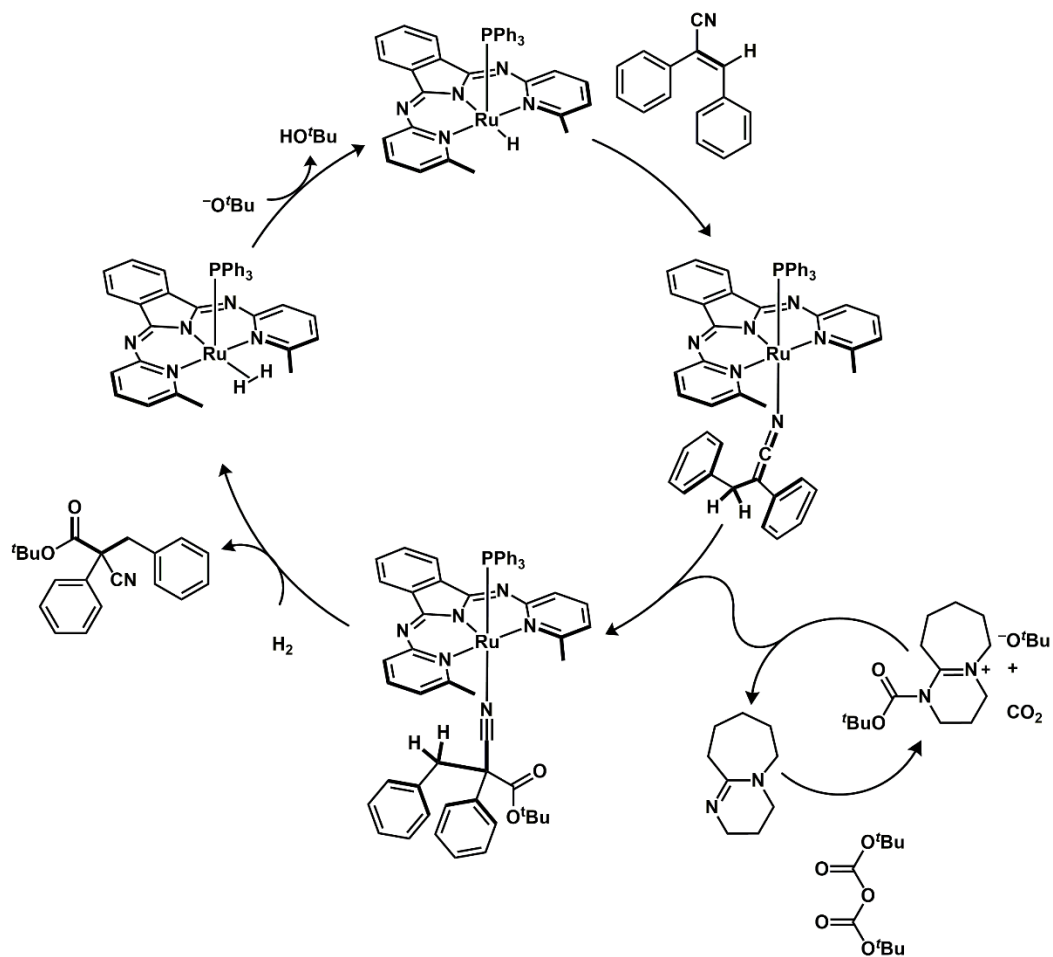


Figure S60. Proposed catalytic cycle

### VIII. Cation dependence of hydrogenation acylation in the presence of alkoxide bases

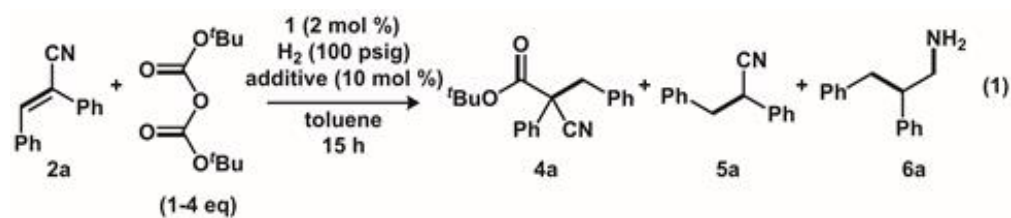


Table S5. Cation dependence of hydrogenative acylation in the presence of alkoxide bases

Entry	Temp (°C)	Additive	%conv.	% 4a	5a+6a
1	30	None	7	N/A	7
2	80	None	99	N/A	99
3	80	None	100	29	71
4	80	LiO <sup>t</sup> Bu	100	53	47
5	100	LiO <sup>t</sup> Bu	100	70	30
6	100	KO <sup>t</sup> Bu	100	40	60
7	100	NaO <sup>t</sup> Bu	100	40	60

### IX. Crystallographic Details for 3a

Crystal data	
Chemical formula	2(C <sub>53</sub> H <sub>43</sub> N <sub>6</sub> PRu)·5(C <sub>4</sub> H <sub>8</sub> O)
<i>M<sub>r</sub></i>	2152.47
Crystal system, space group	Monoclinic, C2/c
Temperature (K)	85
<i>a</i> , <i>b</i> , <i>c</i> (Å)	38.7102 (8), 17.6880 (3), 15.0126 (3)
β (°)	90.896 (2)
<i>V</i> (Å <sup>3</sup> )	10278.0 (3)
<i>Z</i>	4
Radiation type	Cu Kα
μ (mm <sup>-1</sup> )	3.18

Crystal size (mm)	0.06 × 0.06 × 0.04
Data collection	
Diffractometer	Dtrek-CrysAlis PRO-abstract goniometer imported rigaku-D*TREK images
Absorption correction	Multi-scan CrysAlis PRO 1.171.38.41 (Rigaku Oxford Diffraction, 2015) Empirical absorption correction using spherical harmonics, implemented in SCALE3 ABSPACK scaling algorithm.
$T_{\min}, T_{\max}$	0.606, 1.0
No. of measured, independent and observed [ $I > 2\sigma(I)$ ] reflections	78579, 9419, 7393
$R_{\text{int}}$	0.117
$(\sin \theta/\lambda)_{\text{max}}$ ( $\text{\AA}^{-1}$ )	0.608
Refinement	
$R[F^2 > 2\sigma(F^2)], wR(F^2), S$	0.065, 0.193, 1.06
No. of reflections	9419
No. of parameters	674
H-atom treatment	H atoms treated by a mixture of independent and constrained refinement
	$w = 1/[\sigma^2(F_o^2) + (0.1147P)^2 + 11.960P]$ where $P = (F_o^2 + 2F_c^2)/3$
$\Delta_{\text{max}}, \Delta_{\text{min}}$ ( $\text{e \AA}^{-3}$ )	1.10, -2.17

Computer programs: *SHELXS97* (Sheldrick, 2008), *XL* (Sheldrick, 2008), *Olex2* (Dolomanov *et al.*, 2009)

The -CH<sub>2</sub> methylene hydrogens on the ketinimate in **3a** were located in the difference density map and their positions were refined.

## X. Computational Details

### Cartesian coordinates (Å) based on 6-31g(d,p) and SDD optimized geometry of 3a

Ru	13.2144	4.8881	6.2194	H	10.4136	7.1371	13.5067
P	13.5391	6.1889	4.2904	C	10.6678	6.5428	11.5808
N	14.3422	3.2475	5.6155	H	10.0706	7.1477	11.204
N	16.4711	4.0718	6.4396	C	11.3441	5.6549	10.7642
N	14.7731	5.6531	7.1181	H	11.204	5.6867	9.8456
N	13.8041	7.6359	8.0908	C	13.82	2.6709	11.0344
N	12.0147	6.3977	7.0175	H	13.9618	1.9899	10.3589
N	12.6476	3.8135	7.9062	H	13.3478	2.2535	11.7714
C	12.1826	2.333	4.9701	C	15.1824	3.1255	11.5433
H	11.9501	3.1308	4.4882	C	15.7865	2.4746	12.615
H	11.8303	2.3879	5.8617	H	15.329	1.7953	13.0564
H	11.8114	1.5707	4.5182	C	17.0597	2.823	13.0338
C	13.6774	2.2022	5.0301	H	17.4499	2.3861	13.7559
C	14.3377	1.1214	4.5167	C	17.7462	3.8206	12.3809
H	13.8601	0.4334	4.1145	H	18.6064	4.047	12.6526
C	15.7231	1.0524	4.5948	C	17.1586	4.4857	11.3196
H	16.1878	0.3325	4.2345	H	17.6167	5.1684	10.8858
C	16.3872	2.0819	5.2237	C	15.8822	4.1301	10.9053
H	17.3148	2.0571	5.2883	H	15.4923	4.5759	10.1893
C	15.6893	3.1555	5.7611	C	14.4405	7.765	4.5242
C	16.0361	5.1313	7.0506	C	15.771	7.643	4.9205
C	16.9365	6.0263	7.7981	H	16.1264	6.7975	5.0691
C	18.3112	5.9732	8.0142	C	16.5711	8.7538	5.0962
H	18.8285	5.2746	7.684	H	17.4528	8.6565	5.3754
C	18.8723	7.0062	8.7453	C	16.0477	10.0167	4.8515
H	19.7901	7.0098	8.8954	H	16.578	10.7702	4.9791
C	18.0935	8.0392	9.2601	C	14.7468	10.1582	4.4237
H	18.5014	8.7113	9.7585	H	14.4073	11.0055	4.248
C	16.728	8.0905	9.0485	C	13.945	9.0474	4.2556
H	16.2084	8.7768	9.4012	H	13.069	9.1518	3.9598
C	16.1643	7.0734	8.2874	C	11.8882	6.5905	3.6206
C	14.7777	6.8258	7.8416	C	11.3493	5.7433	2.6299
C	12.4762	7.4396	7.7546	H	11.9011	5.1313	2.1976
C	11.586	8.4036	8.2409	C	10.0102	5.8105	2.2951
H	11.9153	9.1465	8.6927	H	9.6617	5.2339	1.6542
C	10.2367	8.2656	8.0608	C	9.177	6.748	2.9196
H	9.6437	8.8971	8.4	H	8.2718	6.7798	2.7094
C	9.7716	7.1548	7.3538	C	9.7014	7.6235	3.8473
H	8.8588	7.0292	7.2277	H	9.1565	8.2691	4.236
C	10.673	6.2456	6.8449	C	11.0421	7.5422	4.2045
C	10.21	5.0393	6.0794	H	11.3829	8.1294	4.841
H	10.4186	4.2451	6.5762	C	14.3852	5.6602	2.741
H	10.6564	5.0092	5.2282	C	14.9017	4.3795	2.5353
H	9.2614	5.0906	5.9443	H	14.8405	3.7375	3.2063
C	12.7983	3.7941	9.086	C	15.5139	4.0665	1.3119
C	12.9261	3.7357	10.4475	H	15.8663	3.2174	1.1768
C	12.2413	4.6997	11.2896	C	15.5969	5.0092	0.3107
C	12.4386	4.7315	12.6826	H	15.9986	4.7917	-0.4999
H	13.036	4.1337	13.0699	C	15.0789	6.2828	0.5119
C	11.7621	5.6354	13.4902	H	15.1197	6.916	-0.1681
H	11.9138	5.6301	14.4073	C	14.5037	6.6065	1.7262
C	10.87	6.541	12.9588	H	14.1902	7.4714	1.8673

### Summary of Natural Population Analysis for 3a:

		Natural				
Atom	No	Charge	Core	Valence	Rydberg	Total
Ru	1	0.00819	35.97817	7.95743	0.05620	43.99181
P	2	1.20086	9.99652	3.73879	0.06382	13.79914
N	3	-0.42344	1.99909	5.40763	0.01672	7.42344
N	4	-0.55105	1.99916	5.53637	0.01552	7.55105
N	5	-0.43957	1.99900	5.42336	0.01721	7.43957
N	6	-0.54210	1.99916	5.52720	0.01574	7.54210
N	7	-0.42801	1.99909	5.41269	0.01624	7.42801
N	8	-0.49907	1.99922	5.47441	0.02544	7.49907
C	9	-0.71755	1.99922	4.70836	0.00998	6.71755
H	10	0.24197	0.00000	0.75611	0.00192	0.75803
H	11	0.27998	0.00000	0.71811	0.00191	0.72002
H	12	0.25606	0.00000	0.74266	0.00128	0.74394
C	13	0.23750	1.99884	3.74438	0.01928	5.76250
C	14	-0.27964	1.99883	4.26803	0.01278	6.27964
H	15	0.25047	0.00000	0.74796	0.00156	0.74953
C	16	-0.19871	1.99892	4.18560	0.01420	6.19871
H	17	0.25230	0.00000	0.74613	0.00157	0.74770
C	18	-0.24984	1.99888	4.23676	0.01420	6.24984
H	19	0.26151	0.00000	0.73647	0.00202	0.73849
C	20	0.41160	1.99882	3.56332	0.02626	5.58840
C	21	0.47097	1.99886	3.50100	0.02917	5.52903
C	22	-0.07175	1.99877	4.05723	0.01575	6.07175
C	23	-0.20638	1.99887	4.19388	0.01362	6.20638
H	24	0.25689	0.00000	0.74096	0.00214	0.74311
C	25	-0.23613	1.99898	4.22349	0.01366	6.23613
H	26	0.24606	0.00000	0.75238	0.00156	0.75394
C	27	-0.23132	1.99898	4.21876	0.01358	6.23132
H	28	0.24610	0.00000	0.75234	0.00156	0.75390
C	29	-0.19948	1.99887	4.18710	0.01350	6.19948
H	30	0.25695	0.00000	0.74091	0.00214	0.74305
C	31	-0.06531	1.99877	4.05095	0.01559	6.06531
C	32	0.47975	1.99886	3.49233	0.02906	5.52025
C	33	0.40468	1.99882	3.56992	0.02658	5.59532



C	34	-0.25378	1.99888	4.24063	0.01428	6.25378
H	35	0.26332	0.00000	0.73466	0.00201	0.73668
C	36	-0.20237	1.99892	4.18923	0.01422	6.20237
H	37	0.25308	0.00000	0.74536	0.00156	0.74692
C	38	-0.27960	1.99883	4.26791	0.01286	6.27960
H	39	0.25224	0.00000	0.74621	0.00155	0.74776
C	40	0.25032	1.99883	3.73122	0.01963	5.74968
C	41	-0.71749	1.99921	4.70761	0.01068	6.71749
H	42	0.27228	0.00000	0.72572	0.00200	0.72772
H	43	0.25308	0.00000	0.74504	0.00188	0.74692
H	44	0.25753	0.00000	0.74122	0.00126	0.74247
C	45	0.40174	1.99883	3.57465	0.02478	5.59826
C	46	-0.27122	1.99878	4.25685	0.01558	6.27122
C	47	-0.03241	1.99887	4.01868	0.01487	6.03241
C	48	-0.25636	1.99893	4.24477	0.01266	6.25636
H	49	0.23469	0.00000	0.76315	0.00216	0.76531
C	50	-0.23468	1.99895	4.22180	0.01393	6.23468
H	51	0.23361	0.00000	0.76463	0.00175	0.76639
C	52	-0.27683	1.99894	4.26392	0.01397	6.27683
H	53	0.23201	0.00000	0.76630	0.00169	0.76799
C	54	-0.23845	1.99895	4.22553	0.01397	6.23845
H	55	0.23231	0.00000	0.76585	0.00184	0.76769
C	56	-0.24486	1.99892	4.23354	0.01239	6.24486
H	57	0.23452	0.00000	0.76346	0.00201	0.76548
C	58	-0.47134	1.99909	4.45956	0.01270	6.47134
H	59	0.26257	0.00000	0.73541	0.00202	0.73743
H	60	0.24182	0.00000	0.75531	0.00286	0.75818
C	61	-0.02760	1.99886	4.01313	0.01561	6.02760
C	62	-0.24389	1.99887	4.23235	0.01267	6.24389
H	63	0.23369	0.00000	0.76430	0.00201	0.76631
C	64	-0.23813	1.99895	4.22529	0.01390	6.23813
H	65	0.23684	0.00000	0.76142	0.00174	0.76316
C	66	-0.25287	1.99894	4.24034	0.01358	6.25287
H	67	0.23625	0.00000	0.76206	0.00169	0.76375
C	68	-0.23298	1.99895	4.22002	0.01401	6.23298
H	69	0.24037	0.00000	0.75768	0.00195	0.75963
C	70	-0.23090	1.99887	4.21902	0.01301	6.23090

H 71	0.24622	0.00000	0.75152	0.00226	0.75378
C 72	-0.35994	1.99879	4.33816	0.02299	6.35994
C 73	-0.22657	1.99887	4.21181	0.01588	6.22657
H 74	0.25182	0.00000	0.74578	0.00240	0.74818
C 75	-0.22895	1.99893	4.21570	0.01432	6.22895
H 76	0.24894	0.00000	0.74931	0.00175	0.75106
C 77	-0.22752	1.99894	4.21474	0.01385	6.22752
H 78	0.24494	0.00000	0.75342	0.00164	0.75506
C 79	-0.23266	1.99894	4.21964	0.01408	6.23266
H 80	0.24508	0.00000	0.75325	0.00167	0.75492
C 81	-0.22469	1.99884	4.21064	0.01520	6.22469
H 82	0.24749	0.00000	0.75026	0.00226	0.75251
C 83	-0.35610	1.99878	4.33444	0.02288	6.35610
C 84	-0.22493	1.99885	4.21121	0.01487	6.22493
H 85	0.25099	0.00000	0.74678	0.00223	0.74901
C 86	-0.23300	1.99894	4.21996	0.01410	6.23300
H 87	0.24644	0.00000	0.75190	0.00166	0.75356
C 88	-0.22952	1.99894	4.21666	0.01392	6.22952
H 89	0.24583	0.00000	0.75254	0.00163	0.75417
C 90	-0.23177	1.99892	4.21863	0.01422	6.23177
H 91	0.24792	0.00000	0.75036	0.00172	0.75208
C 92	-0.23900	1.99888	4.22423	0.01590	6.23900
H 93	0.25281	0.00000	0.74502	0.00218	0.74719
C 94	-0.36246	1.99879	4.34070	0.02298	6.36246
C 95	-0.21487	1.99886	4.20100	0.01500	6.21487
H 96	0.23986	0.00000	0.75797	0.00217	0.76014
C 97	-0.23493	1.99893	4.22172	0.01428	6.23493
H 98	0.24628	0.00000	0.75200	0.00173	0.75372
C 99	-0.22457	1.99894	4.21181	0.01382	6.22457
H 100	0.24597	0.00000	0.75240	0.00163	0.75403
C 101	-0.23306	1.99894	4.22008	0.01404	6.23306
H 102	0.24717	0.00000	0.75117	0.00166	0.75283
C 103	-0.21540	1.99885	4.20123	0.01532	6.21540
H 104	0.25317	0.00000	0.74458	0.00225	0.74683

===== \* Total \* 0.00000

163.91101 296.93749 1.15150 462.00000

## XI. References

- (1) Kulp, S. S. Knoevenagel Condensation to Alpha-Phenylcinnamitriles: NaBH<sub>4</sub> Reduction to Propanenitriles *Journal of Chemical Education* **1988**, *65*, 742.
- (2) Ladhar, F.; Gharbi, R. E. Direct Synthesis of  $\alpha,\beta$ -Unsaturated Nitriles in Solid/Liquid Heterogeneous Medium *Synthetic Communications* **1991**, *21*, 413-417.
- (3) D'Sa, B. A.; Kisanga, P.; Verkade, J. G. Direct Synthesis of  $\alpha,\beta$ -Unsaturated Nitriles Catalyzed by Nonionic Superbases *The Journal of Organic Chemistry* **1998**, *63*, 3961-3967.
- (4) Tseng, K.-N. T.; Kampf, J. W.; Szymczak, N. K. Base-Free, Acceptorless, and Chemoselective Alcohol Dehydrogenation Catalyzed by an Amide-Derived Nnn-Ruthenium(II) Hydride Complex *Organometallics* **2013**, *32*, 2046-2049.
- (5) Dolomanov, O. V.; Bourhis, L. J.; Gildea, R. J.; Howard, J. A. K.; Puschmann, H. *J. Appl. Crystallogr.* **2009**, *42*, 339.
- (6) Sheldrick, G. *Acta Crystallogr. Sect. A.* 2008, *64*, 112
- (7) Frisch, M. J.; Trucks, G. W.; Schlegel, H. B.; Scuseria, G. E.; Robb, M. A.; Cheeseman, J. R.; Scalmani, G.; Barone, V.; Mennucci, B.; Petersson, G. A.; Nakatsuji, H.; Caricato, M.; Li, X.; Hratchian, H. P.; Izmaylov, A. F.; Bloino, J.; Zheng, G.; Sonnenberg, J. L.; Hada, M.; Ehara, M.; Toyota, K.; Fukuda, R.; Hada, M.; Ehara, M.; Toyota, K.; Fukuda, R.; Hasegawa, J.; Ishida, M.; Nakajima, T.; Honda, Y.; Kitao, O.; Nakai, H.; Vreven, T.; Montgomery, J. A., Jr.; Peralta, J. E.; Ogliaro, F.; Bearpark, M.; Heyd, J. J.; Brothers, E.; Kudin, K. N.; Staroverov, V. N.; Kobayashi, R.; Normand, J.; Raghavachari, K.; Rendell, A.; Burant, J. C.; Iyengar, S. S.; Tomasi, J.; Cossi, M.; Rega, N.; Millam, J. M.; Klene, M.; Knox, J. E.; Cross, J. B.; Bakken, V.; Adamo, C.; Jaramillo, J.; Gomperts, R.; Stratmann, R. E.; Yazyev, O.; Austin, A. J.; Cammi, R.; Pomelli, C.; Ochterski, J. W.; Martin, R. L.; Morokuma, K.; Zakrzewski, V. G.; Voth, G. A.; Salvador, P.; Dannenberg, J. J.; Dapprich, S.; Daniels, A. D.; Farkas, O.; Foresman, J. B.; Ortiz, J. V.; Cioslowski, J.; Fox, D. J. Gaussian 09, revision A.02; Gaussian, Inc.: Wallingford, CT, 2009.
- (8) Chimera: <http://www.cgl.ucsf.edu/chimera>